Improving the Quality of Digital Surface Model Generated from Very High Resolution Satellite Stereo Imagery by Using Object Oriented Image Analysis Technique

Janak Raj Joshi

February, 2010

Improving the Quality of Digital Surface Model Generated from Very High Resolution Satellite Stereo Imagery by Using Object Oriented Image Analysis Technique

by

Janak Raj Joshi

Thesis submitted to the International Institute for Geo-information Science and Earth Observation in partial fulfilment of the requirements for the degree of Master of Science in Geo-information Science and Earth Observation, Specialisation: Geoinformatics

Thesis Assessment Board

Chairman:	Prof. Dr. M.G. Vosselman
External examiner:	Dr. Ing. S. Müller
Supervisor:	Dr. M. Gerke
Second Supervisor:	Dr. V.A. Tolpekin
Advisor:	Dr. N. Kerle

INTERNATIONAL INSTITUTE FOR GEO-INFORMATION SCIENCE AND EARTH OBSERVATION
ENSCHEDE, THE NETHERLANDS

Disclaimer

This document describes work undertaken as part of a programme of study at the International Institute for Geo-information Science and Earth Observation. All views and opinions expressed therein remain the sole responsibility of the author, and do not necessarily represent those of the institute.

Dedicated to My Parents,
Ultimate source of my inspiration!

Abstract

Digital Surface Models (DSMs) are widely used in many applications such as urban planning, disaster monitoring, surveying and mapping, construction and development. Very high resolution satellite (VHRS) image is one of many sources for DSM generation. Main advantage of VHRS image is its versatile application in geo information acquisition. Image matching techniques enable to extract digital surface models fully automatically, whereas high spatial resolution supports the extraction of urban features such as individual buildings. Many matching techniques in VHRS images are currently in use, but most of them do not produce anticipated result especially to preserve the building shape and outlines. Similarly (semi)automatic extraction of individual buildings, even in the highest resolution commercial data, is very difficult in a heterogeneous dense urban environment. Object-oriented analysis (OOA) methods have been used successfully in the image processing of some built-up area type, but success is highly dependent on settlement density, contrast and image characteristics.

In this research, a stereo pair of VHRS images (GeoEye-1) of Cairo is used. This research explores a possibility of using DSM generation and OOA technique together in such a way that one can benefit the other. To extract buildings accurately from VHRS images, a DSM can play an important role, whereas the building outlines extracted from the image by OOA can, in turn, help refine the quality of DSM. This mutual relationship between DSM and OOA can benefit each other and using these two techniques together can help optimally use the VHRS image.

The research was carried out in three main stages. Firstly, different aspects of DSM generation were explored to extract a DSM and produce an orthoimage. Then in a second step, the orthoimage was used in OOA for extracting building outline, in which the DSM was used as additional ancillary input data. Finally in the third step, the building outlines were used to improve the quality of DSM generated in the first step.

The result shows DSM generated from VHRS image by matching technique plays an important role in building extraction by OOA. In relatively open areas, 98% of the buildings are extracted within a positional accuracy of 1.1 m. The accuracy in terms of correctness and completeness of building extraction is more than 90% in sparse building areas and that around 85% in dense areas. Similarly, the quality of building DSM in urban area is also improved significantly. Most of the problems and artefacts in the photogrammetric DSMs like oversmoothing bell shape, spikes and streaking are removed. The output DSM, after improvement, models the narrow streets and gap between the buildings. The DSM preserves building outline and edges. This method also removes the bell shape and streaking effect in DSM. The accuracy of the improved DSM in terms of shape and position, however, depends upon the accuracy of the building outline and the height depends upon the accuracy of input DSM used.

Keywords: digital surface model, orthoimage, very high resolution satellite, object- oriented analysis, building extraction

Acknowledgements

I would like to take this opportunity to acknowledge the persons and organizations whose effort and contributions are valuable for me to accomplish my MSC degree.

First, I would like to thank the joint cooperation between Land Management Training Centre, LMTC (Government of Nepal), Kathmandu University, KU (Nepal) and ITC for creating this opportunity. My sincere gratitude to Mr. Babu Ram Acharya, Secretary, Government of Nepal and Mr. Rabin Kaji Sharma, the then Executive Director, LMTC, Dr. Arbind Tuladhar and Dr. Klaus Tempfli from ITC for their contribution to develop this programme and my inclusion in it. I would like to thank ITC for providing financial support to study this course here in the Netherlands.

Next, my heartfelt acknowledgement to my supervisor Dr. Markus Gerke; without his continuous help from the very beginning of the study, this research would not have completed. He supported me in shaping the ideas, developing the proposal, and carrying out the research. My sincere thanks go to my supervisors Dr. Valentyn Tolpekin and Dr. Norman Kerle for their suggestions and feedback which helped a lot to improve my research. I would like to express my sincere appreciation to Prof. Dr. George Vosselman for his comments and suggestion during my proposal and mid term defence for improvement of the research.

My special thanks go to Prof. Dr. Emmanual Baltasavias and Nusret Demir from ETH Zurich for their kind help in generating DSM in SAT-PP at ETH, Zurich. Similarly, Mr. Tarek Afifi, from Housing and Building Research Center, Cairo is acknowledged for his efforts in collecting and providing GCPs for this research.

I would also like to thank Ms. Muditha Heenkenda and Mr. Wan Bakx for their useful tips in software handling, and Mr. Sokhon Phem for his effort to manage 3D cluster for the research. I further extend my gratefulness to Ph.D students Mr. Adam Patrick Nyaruhuma for helping me in programming and Mr. Juan Pablo Ardila Lopez for his constructive comments after proof-reading of my research.

During my study, I got a lot of support from many people, specially, Mr. Gerrit Huurneman and Dr. Wietske Bijker and Dr. Rob Lemmens; some names could be missing because of the limitation of space, who helped me in one way or another. I would like to thank all of them.

My sincere thanks go to my friends Nawaraj, Melani and Hezron for their cooperation and willingness to help each other during the research. Similarly, I acknowledge the spirit of my friends Arun, Main, Mala, Mr. Oh and Leon to make the heavy cluster light and lively. Special thanks to my GFM Family for sharing 18 good months together.

My fellow Nepali friends Gopi, GRD, Diwakar, Jeny, Jay and Kehsav deserve my acknowledgement as they made me feel at home; special thanks to Ganesh for his guardianship and care. I am grateful to Nepali Community at Enschede for their hospitality.

Last but not least, how I can forget to express my emotional gratefulness for my family for their continuous support, help and patience throughout this period. They really faced a difficult time back home in my absence. Thank God! The hard time is over now, Sonu, Abhi…I am coming…

Table of contents

List of figures

List of tables

List of Annexes

List of Abbreviations

3D	Three dimensions
ALOS	Advance Land Observation Satellite
ALS	Airborne LASER Scanning
am	ante meridiem
ASCII	American Standard Code for Information Interchange
AT	Automated Triangulation
B	Blue
CAD	Computer Aided Drawing
CE	Circular error
cm	Centimetre
COTS	Commercial Off-the-Self
DEM	Digital Elevation Model
DLW	Dynamic Line Warping
DP	Dynamic Programming
DSM	Digital Surface Models
DTM	Digital Terrain Model
E	Easting
ETH	Swiss Federal Institute of Technology
FN	False Negative
FP	False Positive
G	Green
GCP	Ground Control Points
GIS	Geographic Information System
GMT	Greenwich Mean Time
GNSS	Global Navigation Satellite System
GPS	Global Positioning System
GSD	Ground Sample Distance
HRS	High Resolution satellite
InSAR	Interferometric Synthetic Aperture Radar
IRS	Indian Remote Sensing satellites
ITC	International Institute for Geoinformation Science and Earth Observation
km	Kilometre
LE	Linear Error
LIDAR	Light Detection and Ranging
LPS	Lieca Photogrammetry Suit
LSM	Least Square Matching
m	Meter
MF	Miss Factor
MPGC	Multi photo Geometrically Constrained
MPM	Multi Primitive Multi-image

MS	Multispectral
N	Northing
nDSM	Normalized digital Surface Model
NDVI	Normalised Difference of Vegetation Index
NIR	Near Infra Red
nm	Nanometer
NOAA	National Oceanic and Atmospheric Administration
OBIA	Object Based Image Analysis
OOA	Object-oriented (image) analysis
Pan	Panchromatic
PRISM	Panchromatic Remote-sensing Instrument for Stereo Mapping
R	Red
RMSE	Root Mean Square Error
RPC	Rational Polynomial Coefficient
SAT-PP	Satellite Image Precision Processing
SE	Structuring Element
SF	Split Factor
SGM	Semi Global Matching
sq	Square
SRTM	Suttle Radar Topographic Mission
SSI	Spectral Shape Index
TIN	Triangulated Irregular Network
TN	True Negative
TP	True Positive
URL	Uniform resource Locater
UTM	Universal Transverse Mercator
VHR	Very high resolution
VHRS	Very high resolution satellite
WGS	World Geodetic System
XLD	Extended Line Description

1. Introduction

1.1. Background

Information about the earth surface is becoming more and more important for many applications like urban planning, disaster monitoring, surveying and mapping, construction and development among others. Hence modelling the earth surface and extraction of topographic information is one of the most attractive research topics in Remote Sensing and Photogrammetry domain. Digital Elevation Model (DEM) is one of such important topographic data, which is being widely used for many applications (Maune, 2007).

There are many sources of DEM data such as traditional analogue contour map, aerial/satellite imagery, Light Detection and Ranging (LIDAR), Interferometric Synthetic Aperture Radar (InSAR). The resulting DEM may vary in quality. The selection of the data sources and technique for DEM generation generally follow the principle 'fitness for use' (Fu et al., 2008) and depend upon various factors like application, accuracy needed, topographic variation, available time and budget.

High Resolution Satellite (HRS) images are one of the sources for extracting various types of topographic information. Stereo capability in many HRS images makes extraction of DEM possible. With the emergence of Very High Resolution Satellite (VHRS) images by the end of the last decade, DEM extraction got a remarkable attention of the researchers. This trend is growing because of its very high potential in topographic information extraction (Fraser et al., 2002; Jacobsen, 2009). High spatial resolution, geometric quality, easy and timely image acquisition, independent of direct human interaction to the earth surface and no need to have the heavy and expensive instruments to the users end are some of the advantages of remotely sensed imagery over other methods (Kerle et al., 2004). These facts make VHRS data an efficient and economic option, very useful for applications such as large scale topographic mapping/updating (Holland et al., 2006). At the same time, increasing resolution and information volume, high feature density, and various problems caused by the terrain relief, object height, shadow and occlusion pose a challenge in processing of VHRS images to exploit their usability.

This research is carried out to explore some of the current issues in the field of extracting topographic information. Specifically, this research concentrates on methods of producing a DEM, extracting urban buildings, and improving the quality of produced DEM from VHRS image.

1.2. Definitions of the terms

As many researchers have used different terms for the same data, it creates confusion. Some terms are defined here in the context of this research.

1.2.1. Digital Elevation Model (DEM)

DEM refers to the digital representation of the topography of earth surface (Maune, 2007). DEM exists in many forms like a raster of a regularly spaced grid of elevation points, Triangulated Irregular Network (TIN) of elevation points and contour lines. DEM is a general term used to represent any

type of elevation data of the earth surface. For instance, DEM can be used to represent the actual terrain or bare surface of the earth without any natural or artificial object on it (the terrain model), actual surface of the earth with all types of object like buildings, trees, or any other artificial objects or natural vegetation on it (the surface model), and absolute elevation from ground level (the normalized surface model). But many researches do not agree with this explanation of DEM and use it synonymously for the actual terrain (bare earth) surface. In this research, the term DEM is used in generic sense to represent all elevation data.

1.2.1 Digital Surface Model (DSM)

DSM is specific type of DEM which represents the elevation of actual surface of the earth, which is seen by any sensor above the earth. It includes the elevation of every natural and/or artificial object like building, vegetation etc on the surface of the earth. The elevation data acquired directly from the remotely sensed images are always DSM.

1.2.2 Digital Terrain Model (DTM)

DTM is another specific term which refers the digital representation of actual terrain or bare ground elevation. It does not include the elevation of the objects above the ground surface like vegetation or buildings. For this research, DTM is used as a specific form of DEM, which represents only the bare earth surface. A DTM can be produced from a DSM by applying appropriate techniques like filtering or mathematical morphology.

1.2.3 Normalized Digital Surface Model (nDSM)

nDSM is the digital representation of the absolute elevation of the objects above the ground level. In other words, it can be understood as the digital representation of absolute height of the objects above the DTM. nDSM can be derived by subtracting a DTM from DSM (Krauß et al., 2008).

1.2.4 Very High Resolution Satellite (VHRS) image

Spatial Resolution of a satellite image refers to the measure of how closely lines can be resolved in an image. It can also be understood as the smallest size of the details that can be identified in the image. Spatial resolution of an image is measured by the ground sample distance (GSD) on the earth's surface (Reulke et al., 2006).

Satellites are continuously capturing images at different spatial resolutions. With the advancement of the technology, the spatial resolution of the satellite images is becoming higher and higher. In general, satellites can be categorised as low, medium, high, and very high resolution images. The images of spatial resolution lower (coarser) than 100 m can be termed as low, 10 – 100 m are medium, 2 - 10 m are high and images of resolution higher (finer) than 2 m can be termed as very high resolution (Kerle et al., 2004)

For this research, a VHRS image Geoeye-1 is used and VHR refers to the images of spatial resolution finer than 2 m.

1.2.5 Orthoimage

An orthoimage is an aerial/satellite image that has been geometrically corrected by the process of orthorectification, so that the image would have uniform geometry throughout the surface. Orthoimages are corrected to remove terrain relief effects and distortion, which is caused by the tilt

of camera's lens/sensor when the image was taken from the plane/satellite. A digital orthoimage has a geographic reference to the earth, a map like geometry and orthogonal projection which makes the distance measurements possible across the entire image (Schenk, 1999). In this research, orthoimage refers to an orthorectified and geo referenced image produced from a VHRS image.

1.2.6 Object Oriented Analysis (OOA) of VHRS images

Object oriented Analysis (OOA) of satellite images is a sub-discipline of GI Science, which deals with the partitioning of remotely sensed imagery into meaningful constituents called segments, and assessing their properties by using spatial, spectral and temporal scale (Blaschke, 2009). The most basic requirements of OOA are image segmentation, attribution, classification and the ability to query and link individual image objects in space and time. To achieve this, OOA incorporates knowledge from different disciplines involved in the generation and use of geographic information. Many researchers used the term Object Based Image Analysis (OBIA) synonymously (G.J.Hay and G.Castilla, 2008). In this research, we use the term OOA.

1.3 Application of VHRS image and DEM

DEM is being used widely for many applications and the demand is growing (Maune, 2007). The unprecedented growth in application and demand of DEM added challenge and responsibility in supply markets of DEM or source of DEM. The data producers would be looking for easier way to acquire the needed topographic information, which, in one hand, is easy to use without very specific knowledge and high level of expertise, instrument and accurate enough for required application, on the other hand, efficient and economic.

VHRS images are one of such option, which can be used for topographic information extraction. These images are easily available in archive or on demand from related vendors across the world. Users or providers do not need to depend on the administrative procedure to take permission for aerial flight and weather condition. They can cover any inaccessible and strategically restricted areas. They also do not need very high technology and expensive heavy equipments to the user's end. Moreover, the VHR images makes possible to capture small detail with sufficient accuracy for many of the above mentioned tasks and make this option viable and feasible to adopt.

VHRS images are not only used for DEM generation, but also for many other topographic information products. They can be used for orthoimage production, feature extractions for large scale topographic mapping (Holland et al., 2006), cadastral and property mapping (Prudhviraju et al., 2008), 3D building and city modelling (Sohn and Dowman, 2007), (Kocaman et al., 2006) and many others. This versatility of application makes VHRS images and information extraction from it as one of the most popular research topic in the last decade.

1.4 Motivation and problem statement

After the emergence of VHRS images, its use for DSM generation and automatic building extraction has remained an area of research interest in photogrammetry and remote sensing communities. Although topographic data can be acquired from many other methods like ground survey, aerial photogrammetry and laser scanning, VHRS image processing is becoming more popular as it is effective, efficient and fit for use for many applications (Konecny, 2003).

VHRS images are widely used in various geographic information acquisitions such as DSM generation and topographic feature extraction. Stereo viewing capability of satellite and sensor system from same orbital pass enables image matching more effective to extract DSM. High spatial resolution helps to extract small urban features. These improvements in satellite/sensor systems also add some challenges. The perspective viewing angle of sensor and height of building causes difference in geometric positioning, relief displacement and occlusion. Position of the sun and height of buildings causes shadow in the image. These problems affect image matching and result inaccurate DSM in urban areas.

Similarly, high spatial resolution enables to acquire a high density of detail with spectral heterogeneity which causes difficulty in automatic building extraction by pixel based classification. OOA can be a substitute for pixel based methods, as it relies not only on the spectral characteristics of pixels but also in the spatial and contextual information as well as the external information like DSM. Nevertheless, the success of OOA also depends upon urban structure, feature density and the image characteristics itself.

Researchers have presented several matching techniques for generating DSMs such as Least Square Matching (LSM), Dynamic Programming (DP) (Birchfield and Tomasi, 1999), Semi Global Matching (SGM) (Hirschmüller, 2005), Modified Multiple primitive multi image matching (Zhang and Gruen, 2006), and Dynamic Line Warping (DLW) (Krauß et al., 2005). These methods have been successfully implemented for DSM generation; however, they suffer from various problems in a dense urban environment and do not always give very accurate results. LSM has an effect of oversmoothing of DSM and cannot preserve the sharp edges or vertical wall of the building. The DP has an effect of streaking along the matching direction. Although SGM gives better result than LSM and DP, it is more time consuming and still not free from some unwanted artefacts and noise. Similarly, multiple primitive multi image matching and DLW method produce better result still not free from errors. The main problems in generating highly accurate DSM are discontinuous nature of urban environment, high density of features, sudden variations of height within small distance, significant occlusion and big shadows and repetitive similar pattern in the image.

Similarly, building extraction from VHRS image also faces many problems in dense urban areas. Main challenges in building extraction by OOA technique are dense urban environment, different spectral characteristics of the building due to different construction materials used, different shape size and height of buildings, variability within the similar object class, similarity among various object classes, occlusion, and shadows in images. OOA technique considers spatial and contextual information along with the spectral information. Further, additional ancillary input layers (e.g. DSM) can be used for image segmentation to create meaningful image object. OOA classifies these image objects by considering their various feature characteristics and formulating rulesets by using semantics and knowledge about the objects (Benz et al., 2004). LIDAR DSM has been widely used by many researchers for urban building extraction in OOA technique (Chen et al., 2009; Ebert et al., 2009; Kressler and Steinnocher, 2006; Shamaoma, 2005). However, application of photogrammetric DSM in OOA is not widely documented in literature so far.

Some of the problems mentioned above are illustrated in image in figure 1-1(a,b,c). Figure 1-1(d) simplifies the problem and shows schematic representation of DSM. Figure 1 -1(e) shows the spectral variability in same object, class and similarity among different class in VHRS image.

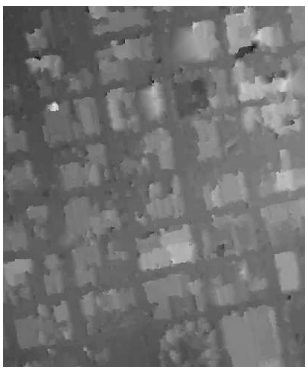

(a) Smoothing

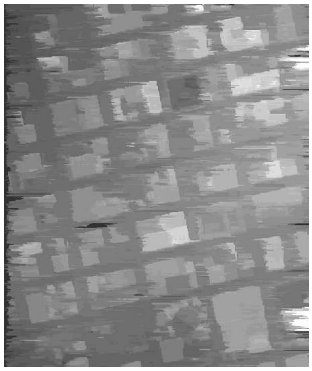

(b) Streaking

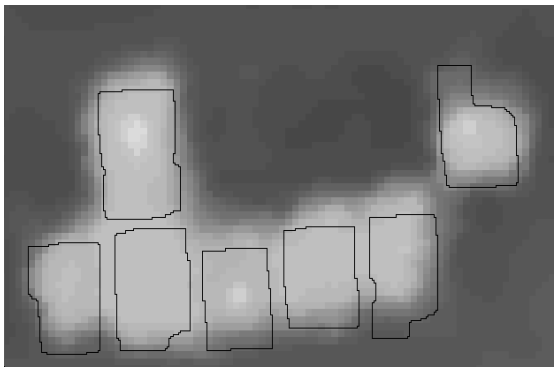

(c) Edges and gaps not modelled in DSM

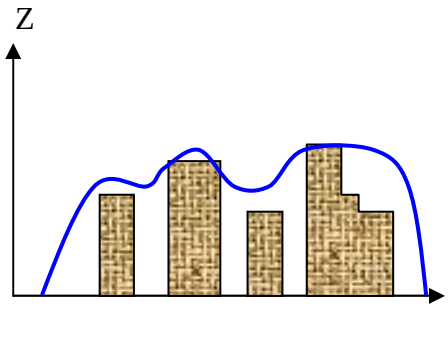

(d) Bell shaped DSM over building

(e) Spectral heterogeneity 1- within building, 2- among buildings, 3- among road, bare ground and buildings

Figure 1-1: Problem with DSM and building extraction

Literature review shows significant effort has been made for accurate DSM generation but this has not been always paid off. The generation of an accurate DSM, especially in urban areas, is still a big challenge. Similarly, there are many challenges in the OOA method used for urban building extraction. It is also seen that the DSM does not preserve sharp edges along the boundary of building roofs and hence the vertical walls cannot be modelled accurately. On the other hand, OOA method cannot extract accurate building outlines because of the similar spectral response of other objects like road and bare ground in the image. Therefore, it can be investigated whether the use of DSM generation and OOA together can improve the situation i.e. DSM generated from VHRS image can be used in OOA for accurate building outline extraction and extracted building outline by OOA can be used for improving the quality of photogrammetric DSM.

To extract building accurately from VHRS images by using OOA, DSM can play an important role whereas the building outline extracted by OOA can help to refine the quality of DSM. This mutual application of one on the other can benefit both techniques and their integration can help optimally use the VHRS images. Hence, this research explores the possibility of using DSM generation and OOA techniques together in such a way that one can benefit the other i.e. DSM extracted from VHRS stereo image can be used as auxiliary input data for OOA to extract accurate building outlines which, in turn, can be used for improving the quality of the DSM.

In this research, a VHRS image, GeoEye-1, of Cairo, Egypt is used. Cairo is a typical dense urban area with heterogeneous built up environment, dense features, and narrow streets having irregular

shape, size and height of buildings. Large shadow and occlusion, because of tall buildings, are other problems in the image. Furthermore, GeoEye-1 is a new VHRS image which has not been studied and documented widely yet. This research aims to tests the image against existing DSM generation and OOA techniques.

1.5 Research identification

This research is identified on the basis of the problem discussed in the section 1.4. A stereo pair of Geoeye-1 is used to carry out this research in order to explore the solution of above mentioned problems. It is intended to develop a new approach to integrate DSM generation and OOA techniques to improve the quality of DSM generated. The details of this research are as follows:

1.5.1 Research objectives

The main objective of this research is to develop a method for improving the quality of DSM generated from VHRS stereo images by using the OOA technique. Following sub objectives are defined to achieve the main objective:

1. To explore available image matching techniques for generation of DSM in a dense and heterogeneous urban area.
2. To extend the method of extracting the urban building from VHRS image by OOA technique, using photogrammetric DSM.
3. To develop an algorithm for improving the quality of DSM by using building outlines extracted by OOA technique.

1.5.2 Research questions

Following questions were formulated to achieve the objective of this research:

1. Which spectral band should be used for image matching in a VHRS stereo image to generate a DSM?
2. Are the shape and size of the buildings in urban area preserved in the resulting DSM?
3. Can the DSM, generated from VHRS stereo image by matching technique, be used (after filtering) to produce an accurate orthoimage?
4. Which information should be used to extract building in urban area by OOA technique:
    - What inputs/parameters should be used for segmentation?
    - What feature properties and knowledge are useful to extract the buildings?
    - How can a photogrammetric DSM support the extraction of the building outline?
5. What is the accuracy of extracted building outlines?
6. How to use building outlines to improve DSM?
7. What are the improvements in the final output DSM?

1.6 Innovation aimed at

The main innovation in the research is to use the digital photogrammetric workflow with OOA technique in such a way that both techniques can benefit each other. This research investigates how photogrammetric DSM can help to extract building in OOA and how these building outlines, in turn; help, to improve the quality of photogrammetric DSM. Moreover, this research tests the existing photogrammetric DSM generation techniques and OOA in a new VHRS image, GeoEye-1.

1.7 Scope of the Research

The scope of the research is mainly focussed on improving the quality of DSM, generated from VHRS stereo image by using the building outlines extracted by OOA technique. The task is limited to three main phases:

1. DSM generation from VHRS stereo images
2. Building outline extraction from VHRS image by OOA
3. Refining the DSM by using the extracted building outlines

1.8 Thesis outline

The thesis is presented in 7 chapters. The three main tasks related to three sub objectives: DSM generation, OOA of VHRS image, and refining DSM are dealt in three separate chapters. The reason behind this is each of these topics has its own big horizon. Each has its own literature, methods of implementation, and results. Including these all in a single chapter could result a big chapter and may lack proper connection with different included sections. Dealing a single specific technique in one chapter may be more relevant and information can be presented more effectively. Overall chapter plan is briefly described below:

Chapter 2: Study area and data

This chapter explains about the study area, its general extent and characteristics. It further gives information on various data used to carry out this research

Chapter 3: DSM generation and orthoimage production

This chapter gives an overview of different DSM generation methods. It also includes the methods of DSM generation adopted for this research and result obtained from it. It compares the result from two different methods and discusses the result. Further, this chapter also includes some aspects of orthoimage generation and its result.

Chapter 4: Building extraction by OOA

This chapter deals with the OOA technique. It presents the different aspects of building extraction by OOA: first, overviews the related techniques, followed by the method adopted for this research and presents the results. Finally, the accuracy of the extracted building by OOA technique is presented.

Chapter 5: DSM quality improvement

This chapter combines the results of chapter 3 and chapter 4. It first reviews the different quality aspects of DSM and then mentions about some method of improving DSM of urban building. Later, method of refining DSM adopted in this research is explained which is followed by the result obtained from it. Finally, the accuracy is assessed and discussed.

Chapter 6: Results synthesis and Discussion

This chapter discusses the overall results of the research. The results and findings are analysed and discussed against the research objective and questions and. At the same time, the limitation of the research and technique used are also mentioned.

Chapter 7: Conclusion and Recommendation

This chapter includes the concluding remarks on the research and recommendations for the future works.

The overall outline of the research and chapter plan is shown in figure 1-2.

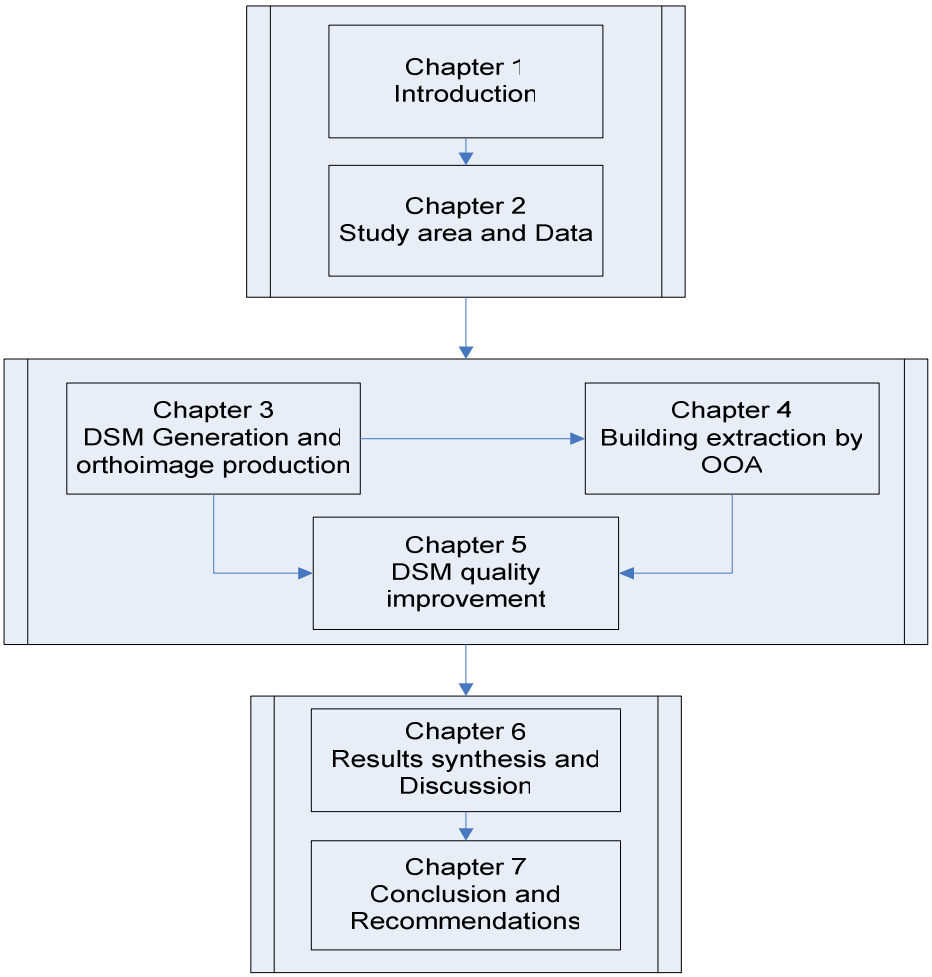

Figure 1-2: Outline of the thesis

2. Study Area and Data

2.1. Study Area: Cairo, Egypt

The study area for this research is Cairo, the capital and largest city of Egypt, located at 30°01'N 31°14'E. Cairo is a densely populated and crowded city having typical characteristics like heterogeneous built up areas with uneven settlements of irregular pattern, high rise and low buildings and narrow streets.

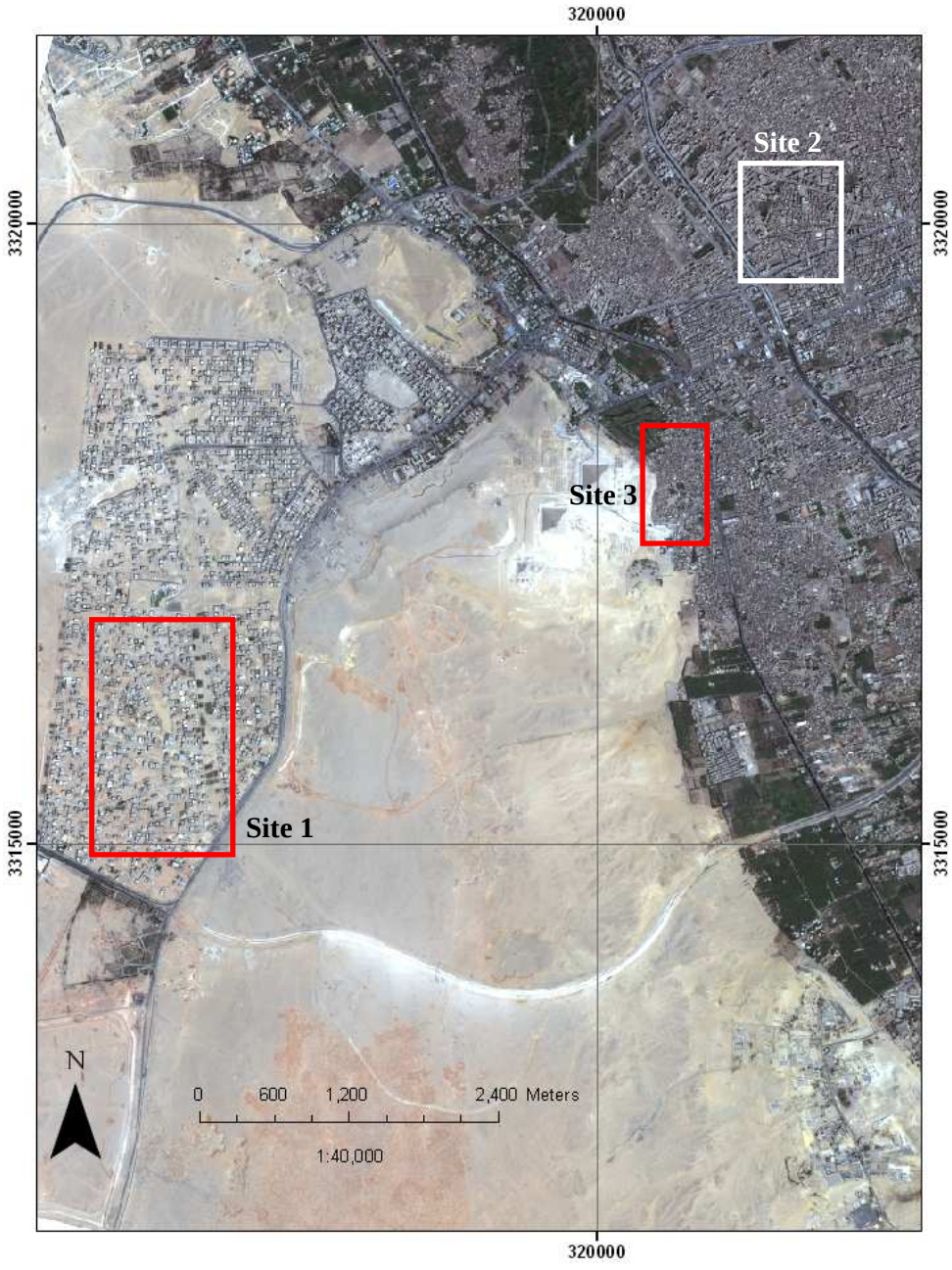

Figure 2-1: Location of the study area, south west part of Cairo, Giza

Keeping this diversity in mind, we choose the three different types of settlement areas for the study (see figure 2-2). Site 1 is a relatively open area with sparse buildings. The topography is fairly leveled with relatively higher ground elevation than the rest of the area. Site 2 is a dense urban area, with very crowded, clustered and mixed buildings of different height spread in a regular pattern. The topography is fairly leveled. Site 3 is a combination of open and crowded, very dense and highly populated area, with irregular buildings of different height, shape and size on a fairly level ground.

2.2. Data

A stereo pair of a VHRS image, Geoeye-1 is used for this research. In addition, different datasets produced from this stereo pair are used. The phases of implementation and specific datasets used are summarized in table 2-1.

Table 2-1: Task diveded in phases and data used

Phase	Task	Data Used
Phase 0	Orientation/preparation	Stereo image pair, ground control points
Phase 1	DSM generation	Stereo image pair
	Orthoimage production	Left/Right image, DTM
Phase 2	OOA	Orthoimage, nDSM
Phase 3	Refining DSM	Orthoimage, nDSM/DTM/nDSM, building outline layer

Some of the facts and technical specification of GeoEye-1 are mentioned in table 2-2 (GeoEye, 2009).

Table 2-2: Characteristics of GeoEye-1

Launch Date	September 6, 2008	
Camera Modes	• Simultaneous panchromatic and multispectral (pan- sharpened) • Panchromatic only • Multispectral only	
Resolution	• 0.41 m Pan, 1.65 m MS at Nadir • 0.5 m Pan, 2.0 m MS at off nadir (28° for commercial purpose)	
Band	Panchromatic	450 – 900 nm
	I. Blue	450 - 520 nm
	II. Green	520 - 600 nm
	III. Red	625 - 695 nm
	IV. NIR	760 - 900 nm
Metric Accuracy	Horizontal 2m (CE 90), Vertical 3m (LE 90) without GCP	
Swath and Scene area	• Nominal swath width - 15.2 km, • Scene area 15 km * 15 km	
Daily Monoscopic Area Collection Capacity	• Up to 700,000 sq km/day of pan • Up to 350,000 sq km/day of pan-sharpened multispectral	
Dynamic Range	11 bits per pixel per band	
Imaging Angle	Capable of imaging in any direction up to 60°	
Orbital Altitude	684 km	
Orbit type	Sun-synchronous	

2.2.1. Data used for DSM generation:

2.2.1.1. GeoStereo of western Cairo:

GeoEye-1 stereo pair of Western Cairo is provided. The approximate area covered by the image is about 225 sq km. Table 2-3 describes some more information about the provided image dataset.

Table 2-3: Detail specification of provided GeoEye stereo image

Product	GeoStereo	
Processing Level	Standard Geometrically Corrected	
Image Type	PAN/MS	
Interpolation Method	Cubic Convolution	
Algorithm	Projective	
Stereo	Stereo	
Datum	WGS84	
Reference Height	61.88 m	
File Format	TIFF	
Bits per Pixel per Band	11 bits per pixel	
Percent Cloud Cover	0	
Acquisition Date/Time	2009-07-02 08:47 GMT	
Image ID	000001	001000
Stereo Position	Right	Left
Nominal collection Azimuth	340	214
Nominal collection elevation	76.7 (incident angle 13.3)	72.6 (incident angle 17.3)

2.2.1.2. Ground Control Points

Eight ground control points (GCP) (WGS 84, UTM zone 36N) collected by differential GPS are used for accurate exterior orientation and correcting the bias in available RPC. Five of them are used as control points and three are used as check points. The summary accuracy is shown in table 2-4.

Table 2-4: Accuracy after AT and bias correction by using GCP

GCP	RMSE (pixel)	
	Control point (5)	Check points (3)
X	1.099	0.56
Y	0.98	1.30
Z	1.34	0.65
Total	0.87	

Final adjustment parameters:
Image ID 1 (right): a [0] = 18.898 and b [0] = 0.078
Image ID 2 (left): a [0] = 2.471 and b [0] = -0.547

2.2.2. Data used for orthoimage production

The datasets used for orthoimage production are Image (left and/or right) and DTM.

For orthoimage production, the left and right images are used. Additionally, for orthorectification and resampling process, the DTM generated from the stereo is used.

2.2.3. Data used for OOA

The datasets used to carry out OOA are orthoimage (right) and nDSM.
For OOA, the orthoimage generated from the right image in the first phase is used. To extract the elevated objects like building, the nDSM is used.

2.2.4. Data used for refining DSM

The datasets used for refining the DSM are nDSM and Vector layer of building outline.
To refine the DSM we use the building outline extracted as vector layer in the second phase.

2.2.5. Area of interest

As the image is too large and it is extremely time-consuming to analyse whole image, we have chosen three representative areas. The overview of these three study sites is shown in fig 2-2.

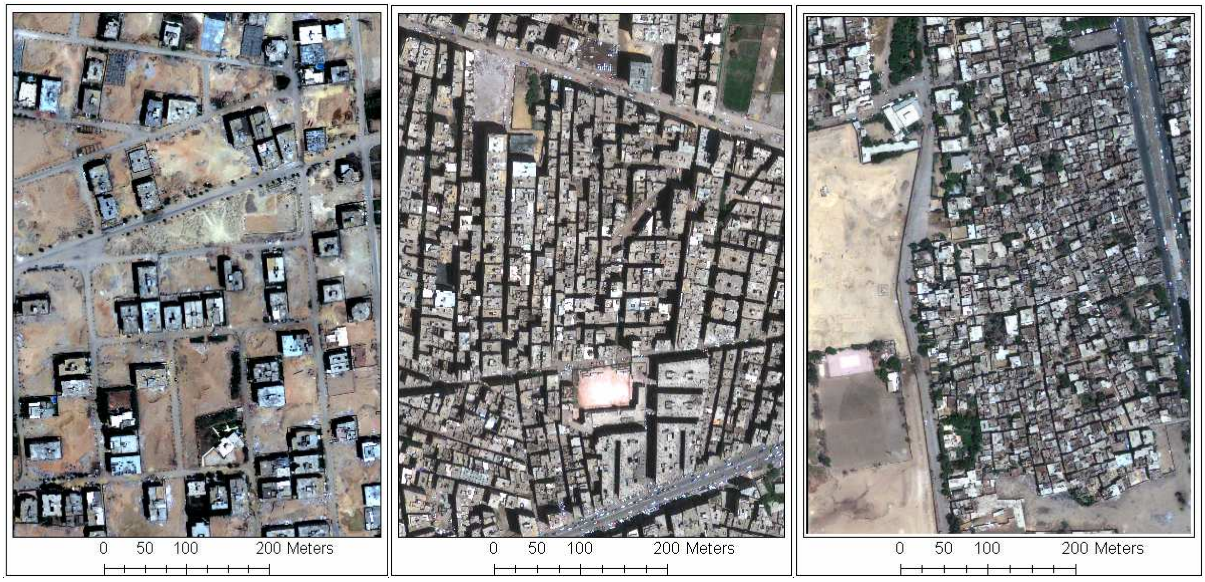

Figure 2-2: Study sites 1- sparse building (left), 2- dense regular buildings (middle) and 3- dense irregular buildings (right)

3. DSM and Orthoimage Production

3.1. Introduction

This chapter explores the available techniques of image matching for DSM generation and orthoimage production in a dense and heterogeneous urban area (sub objective 1). The chapter starts with a review on the DSM generation and orthoimage production techniques (section 3.2) followed by the methods adopted for the task (section 3.3). The results obtained from the implementation of the methods are presented with a brief discussion in section 3.4 and finally ends with a concluding remark (section 3.5).

3.2. Review on DSM generation and Orthoimage production techniques

3.2.1. DSM generation: data sources and techniques

Traditionally, the elevation data on the earth surface has been collected by conventional ground surveying and analogue photogrammetric methods, for instance theodolite traverse, tacheometry, levelling, or photogrammetric stereo plotting. Nowadays, the conventional ground surveying methods are largely replaced by Global Navigation Satellite System (GNSS) and analogue photogrammetric methods are replaced by the modern techniques like digital photogrammetric image matching, Light Detection and Ranging (LIDAR) and Interferofetric Synthetic Aperture Radar (INSAR) (Maune, 2007). This wide range of technology aids the availability of several types of elevation data in several formats. A brief overview of the different methods of extracting elevation data is given in table 3-2.

3.2.2. High Resolution Satellite (HRS) image

Resolution of a satellite image refers to the ground sampling distance. There are many operational satellites in the space, which are producing the images of different spatial resolution. A general categorisation of the satellite and sensor systems on the basis of the spatial resolution is shown in table 3-1 (Kerle et al., 2004).

After the emergence of Ikonos system in 1999, satellite images of spatial resolution of 1 m are made available. This is further followed by Quickbird system having spatial resolution or 0.61m in 2002 and now, since September 2008 Geoeye-1 with spatial resolution finer than 0.5 m is available in the market.

Table 3-1: Resolution of satellite images

Classification	Resolution	Examples satellite systems
Low resolution	Coarser than 100 m	Meteosat-8, NOAA-17,
Medium resolution	10 m to 100 m	Landsat-7, Terra
High resolution	2 m to 10 m	SPOT-5, Resourcesat-1, ALOS PRISM
Very High Resolution	finer than 2 m	Ikonos, Quickbird, GeoEye-1

Table 3-2: Overview of data sources and production techniques of DSM

	Aerial Photogrammetry	Satellite Photogrammetry	LIDAR	InSAR
Platform/ Sensor	Aerial, Passive optical sensor	Satellite, Passive optical sensor, line scanners	Aerial, NIR sensor	Aerial or spaceborne, active microwave sensor
Geometry	Overlapping images	Overlapping images	Near vertical laser scanning with narrow incident angle	Side looking Radar with wide incident angle
Technique	Image matching in stereo	Image matching in stereo	Distance calculation by measuring time	Phase difference in SAR images
Accuracy (possible)	1 m or better	Up to 2 m	Up to 10 cm	0.5-5m (aerial), 6m SRTM
Resolution	DSM grid points by automatic image matching and interpolation algorithm, depends upon various factors	DSM grid points by automatic image matching and interpolation algorithm, depends upon various factors	Irregular mass point, regular grid is generated by interpolation, 0.5-5m	Regular grid, 1-30 m, SRTM 1-3 arc second
Advantage	Can be in large scale, Highly accurate, near vertical geometry, low flying height yields clear and sharp images, user controlled,	Easy availability, large area coverage, frequent revisit time, easily capture inaccessible area, no need to bother administrative procedure, comparatively easier processing, no need of highly expensive equipments in user's end	Active sensor, anytime data collection, high point density, can penetrate vegetation in some degree, fast, accurate	Active sensor, any time data collection, weather independent, fast, large coverage, penetrate vegetation
Disadvantage	Flight planning and administration, highly expensive equipment, weather dependent, restricted areas, more complex processing	Weather dependent, especially cloud and fog, difficult for water or sand surface, off nadir perspective geometry, low(er) resolution and less accurate than aerial images	No data for water surface, expensive, limited use in rain, effected by multipath	Complicated process, multipath, noisy result, specular reflection, unreliable in shadows, buildings or mountains, limited in rainy condition
Influencing factors	Scale, flying height, focal length of camera or sensor used, topography, image matching algorithm	Image resolution, contrast, image geometry, topography, matching algorithm	Flying height, speed, scan angle, point density, topography, interpolation algorithm	Flying height, speed, incident angle, distance between antennas, wavelength, processing technique

3.2.3. HRS Images and stereo viewing capability

In human vision system, sensation of depth can only be felt if the same object is viewed from two different positions separated by certain distance called baseline. This process of viewing to see the third dimension of object is known as stereo viewing. In Photogrammetric measurements, the extraction of elevation information from any image is possible only if the same image is taken from two different viewing positions with certain overlap. Such image pairs are called stereo pairs. Nowadays, many satellite systems have the capability to capture images in stereo mode. Some of the VHR satellite/sensor systems with stereo viewing capability are listed in table 3-3.

Table 3-3: HRS with stereo viewing capabilities

Satellite/ Sensor	Swath width	Spatial Resolution	Temporal Resolution
Ikonos	11.3x11.3	Pan 1 m, MS 4 m	3 days
Quickbird	16.5x16.5	Pan 0.72, MS 2.88	1-3.5 days
GeoEye-1	15.2x15.2	Pan 0.5, MS 2.0	3 days

3.2.4. Methods of DSM generation from HRS image: Image Matching

Image matching technique has been used successfully to extract DEM from VHRS stereo images. It is the process of finding matching points (more generally, matching entities) in the corresponding stereo image pairs. The conjugate point (or entity) in the corresponding image is determined by comparing the certain characteristics of the entity on the basis of a similarity measure, generally the cost functions like correlation coefficient. Theoretically, the main tasks in image matching are: select a matching point in one image, finding its conjugate point in the other (stereomate) image, computing 3D position of the matched point in object space and finally, assess the quality of the matching (Schenk, 1999).

Basically, there are three types of matching algorithms, area based, feature based and relational matching. Out of these three, area based and feature based matching are two widely used methods of image matching (Vosselman et al., 2004). In area based matching, the gray level of a small area of one image, normally known as the template is compared with the corresponding matching entity in the other image. The template in the first image remains fixed and that is in the second image moves over the image to find the conjugate entity, and hence called as the search window. The comparison of gray value is made by the similarity measures like correlation coefficient. During the matching, the correlation coefficient is normally chosen as high as 0.8, but it depends upon surface type and hence it is chosen carefully. Because of the sudden and abrupt height variation among the buildings and occlusion, the matching task is challenging in urban areas. Smaller window size may be highly influenced by noise and the larger window may cause over smoothing of the resulting DSM. The area based matching can be performed by applying many different algorithms such as Cross Correlation and Least Square Matching (LSM) (Vosselman et al., 2004). In cross correlation matching, the template window is moved over search window to find a properly matching area. The matching is done on the basis of gray value intensity and only considers the translation of gray value pixels in corresponding images. LSM is more advanced method which considers the geometric transformation in the corresponding images also. The template not only looks for gray value change and translation, but also the rotational parameters and scale change between the image patch and calculates the correlation coefficient to determine the proper matching. LSM is based on the principle of least square i.e. the sum of the squared difference of the corresponding intensity value is minimized. It

also determines the accurate estimation of affine parameters which corrects the perspective geometry of the images.

In feature based matching, distinct features like points, edges and patches are independently extracted in all images first and then they are matched with the corresponding feature entities of the other image by comparing feature attributes and consistency in location of corresponding feature. Feature based matching can also be performed by applying different algorithms. Least square feature based matching method identifies distinct points as features to be matched in images, then these points are extracted in corresponding images, an initial correspondence is established by calculating correlation coefficient and finally, affine transformation parameters are calculated for robust least square adjustment. Dynamic programming, in contrast, does not calculate the transformation parameter, but simply finds corresponding features, mainly the edge features. It handles effectively the large depth discontinuity to perform a match in the epipolar images (Vosselman et al., 2004).

Researchers have used different matching techniques and their combinations for DEM generation from VHRS stereo images. An image matching technique discussed in Li and Gruen (2004) uses a combination of different matching algorithm. In this technique, image pyramid layers are generated and a coarse-to-fine hierarchical matching solution is used to reduce the matching space in the image. Feature points, edges and grid points are matched and the matching result of the feature points, grid points and edges is combined effectively to generate coarse DSM, which is later, refined by applying a so called modified Multi photo Geometrically Constrained (MPGC) matching algorithm (Developed by A. Gruen, in 1985) to give sub-pixel accuracy. This technique was further extended for automatic DSM generation by using multiple Ikonos images (Zhang and Gruen, 2006). Further experiments with this method are done by many other researchers in some other HRS images like Quickbird and ALOS/PRISM image in different terrain conditions (Baltsavias et al., 2008; Wolff and Gruen, 2007; Wolff and Gruen, 2008; Zhang and Fraser, 2008; Zhang and Fraser, 2007). The accuracy of matching is found within the range of 1-3 pixels depending upon the different terrain topography, landcover type, quality of ground control point used etc (Poon et al., 2005).

Another matching method - Dynamic Programming (DP) is preseted in Birchfield and Tomasi (1999). In this method, each pixel in the epipolar line of the left image is compared to all pixels of conjugate epipolar line in the right image. No windows are needed for matching. To find a matching point, a cost function is used. The minimal cost function determines the best match. It is calculated by combining three factors, sum of dissimilarity function of pixels matched in the epipolar line, reward function for correctly matched pixels and penalty function for occlusion (Alobeid et al., 2009).

This method works well for terrain with discontinuous height and sacrificed accuracy in smooth terrain surfaces but also strong streaking effect observed in the generated DSM. This streaking effect, because of one directional matching along epipolar line, can be neutralized by using the median filter (Alobeid et al., 2009). A method called dynamic line warping (DLW) is discussed in Krauss et al (2005) for DSM generation. This method can be used in the epipolar images. In this method, the similarity measure is a cost function calculated on the basis of intensity value and disparity measurement along the epipolar line. Because of the processing only along the epipolar line, it also yields streaking effect in the resulting DSM. This effect is neutralized in a method proposed by Hirschmuller (2005), a so called semi global matching (SGM). In this method, the matching is done along the epipolar line but the cost function for similarity measurement is

calculated along all possible neighbouring direction, which overcomes the streaking problem caused by one directional matching in DLW. Later, SGM method is extended by incorporating two factors in calculating the global cost functions: first , the dissimilarity measure is expressed pixel per pixel on the basis of mutual information, a probabilistic approach, and second is a global 2D smoothing constraint across multiple direction is introduced (Hirschmüller, 2008). It reduces the streaking effect in DLW, and oversmoothing and bell shape DSM effect of LSM. Because of the intensive per pixel matching along epipolar direction and calculation of cost function along all direction, it takes much time. A hybrid method is suggested in Krauss et al. (2008), Krauss and Reinartz (2009), which combines DLW and SGM for accurate DSM generation in dense urban area. This method considers two scan line before and two scan line after the epipolar line for matching and computing the cost function, instead of earlier only epipolar line. This approach along with some other refinement technique overcomes the streaking effect and results a more accurate DSM. These different DSM generation techniques like LSM, DP, DLW and SGM are compared and a conclusion is drawn in Alobeid et al. (2009). They summarize that the LSM has an over smoothing effect andt, DP and DLW have streaking effect along a certain line. SGM, however, has a good result but it also has some artefacts in a non-homogeneous urban areas and it takes more time for matching.

Different matching techniques are successfully used for DEM generation from different high resolution satellite imagery. Many researchers have studied extraction of DEM from stereo pairs of the HRS images. Generation of Digital surface model from CORONA satellite images is studied and the results are resented in Altmaier and Kany (2002). A DSM is generated with horizontal accuracy of about 3m and vertical accuracy of about 10m from a CORONA image of spatial resolution 1.83m. A successful process of DEM generation from EROS-A1 stereo pair images observed from multiple direction of Hiroshima, Japan is discussed in Suga et al.(2003). Generation of DEM from different SPOT image data has also been studied. The extraction of DEM from along track SPOT stereo image of 10m spatial resolution and across track stereo image of the same satellite of 5m spatial resolution is presented in Toutin (2006), Kornus et al. (2006) . Study on orientation of the stereo images taken from an ALOS PRISM satellite and extraction of DEM by using different matching techniques also carried out in detail (Gonçalves, 2008; Wolff and Gruen, 2007). The potential of Indian Remote Sensing (IRS) satellite imagery to derive different large scale mapping products is explored and generation of DEM is suggested in Radhadevi et al. (2009).

After the emergence of the first VHRS image Ikonos in 1999, researchers have applied different matching techniques for generation of DEM from it. The results of DEM generation from Ikonos stereo pair by using different matching technique and a conclusion that the Ikonos has quite a high potential for high resolution DEM production and urban feature extraction is presented in (Alobeid et al., 2009; Baltsavias et al., 2008; Büyüksalih et al., 2004; Krauß and Reinartz, 2009; Rau and Chen, 2005; Zhang and Gruen, 2006) .

Similarly, Quickbird is another VHRS satellite with higher resolution than Ikonos, and has been widely used for various geographic information acquisition purposes. Many researchers have studied the DEM generation from Quickbird stereo image with a satisfactory accuracy for various applications. Examples can be found in various literature (Eisenbeiss et al., 2004; Jacobsen, 2003; Krauß et al., 2008; Lehner et al., 2005).

3.2.5. DSM generation from HRS images in urban area: the challenges

The urban environment is always considered as a challenge for accurate extraction of elevation data. To extract DSM from VHRS images, we should take into account the perspective projection of the image, occlusions, shadow, surface discontinuities such as buildings and trees, abrupt change in height, large areas with little or no texture, and repetitive similar patterns (Li and Gruen, 2004). The perspective projection of images is different and it causes many problems such as occlusion behind the objects like building, different reflectance from objects as the light falls with different incident angles. This effect is comparatively very less in a true vertical or nadir images. For this reason, the disparity values are larger in perspective images than nadir images. The disparity is a 2D vector between the positions of corresponding features viewed by the left and right eyes. The horizontal disparity is defined as a difference between the column coordinates and vertical disparity is defined as a difference between the row coordinates of the pixel locations of corresponding pixels in the left and right image of a stereo pair rectified to the normal case. After relative orientation and epipolar rectification, the vertical disparities equal zeros and the horizontal disparities are determined for every location (Fielding and Kam, 2001). Because of this effect of perspective images in urban area, not only the translation but also the rotational parameter and scale difference should also be modelled and affine parameters should be estimated for matching.

Apart from this problem, urban area has very high surface discontinuity and abrupt change in height, shadow and occlusion, different reflectance from same object, repetitive pattern, which cause poor match points detection in conjugate image pairs. To derive a detailed regularly gridded DSM, an interpolation is done in between the matched points. There are many interpolation algorithms such as nearest neighbour, bilinear interpolation, cubic convolution (Maune, 2007). Interpolation method in such a diverse and heterogeneous urban area is always problematic. It always generalises the result and smoothes the resulting DSM. Because of this effect, the DSM of dense urban area is generally, bell shaped and the vertical walls are not truly modelled. Further, because of the perspective viewing angle and occlusion, narrow streets and ground between high buildings cannot be modelled in the DSM in dense area (Krauß and Reinartz, 2009).

The problem caused by the perspective projection can be addressed, in some extent, by using least square matching (LSM) solutions, which considers geometric transformation of image for matching and estimates affine parameters (Vosselman et al., 2004). Simple cross correlation matching only considers gray value translation, which can be applicable in the case of nadir view images. The images with less difference in incident angle can give better result in a highly dense urban area as there will be less occlusion and the ground between two buildings may be visible, although the intersecting geometry may not be optimal in this case. The interpolation algorithm can be selected carefully by considering different characteristics of terrain under study and features of interpolation algorithms (Kerle et al., 2004).

3.2.6. DSM filtering

DSM represents the surface as observed from the space. It includes the surface objects like vegetation, buildings etc. To get a DTM from a DSM, the points on the top of the objects like building, trees are needed to be reduced to the actual bare earth surface. In such case, a technique called DSM filtering is used to get DTM from DSM.

Filtering originally refers to a signal processing operation which processes a signal to manipulate the information. The manipulation of information results in extraction of desired information from the input image (Diniz, 2008). Here, we manipulate the height of the object above the ground to reduce to the bare earth surface.

In order to extract the DTM from DSM, one of the most common methods is the application of mathematical morphological filters (Weidner and Förstner, 1995). Morphological filtering is operated in an image to define the shape of an object with the help of a template, known as structuring element (SE). This SE is defined by its size and geometry. A square, rectangular or circular SE of different size can be used according as per requirement

Mainly four types of morphological operations are used in image analysis. They are Erosion, Dilation, Opening and Closing (Breen et al., 2000). Erosion is one of the basic operators in mathematical morphology. It is generally applied to binary images, but it can also be used on gray scale images. It is used to erode away the boundaries of regions of foreground pixels and making it thinner than the original image. The areas of foreground image shrink in size, and the areas of the background grow. Another basic operator in mathematical morphology is dilation. The basic effect of this operator on an image is to enlarge the boundaries of regions of foreground pixels and making it thicker. Thus the areas of foreground grow in size while the areas of the background shrink. Opening and closing are two other operators widely used in mathematical morphology. Opening is the process of erosion of the image by a SE, followed by dilation. Opening in an image causes removal of some of the foreground pixels from the edges of regions. However its effect is less destructive than that of erosion. It is used in image to preserve those foreground regions which have a similar shape to the SE used (or that can completely contain the SE) and to eliminate all other regions of foreground pixels which do not fit with the SE. Closing is a process of dilation followed by erosion. It enlarges the boundaries of foreground regions in an image and shrinks background, but it is not as much destructive as dilation. Closing is used to preserve the background regions which have a similar shape to the SE (or that can completely contain the SE) and to eliminate all other regions of background pixels (Dong, 1997). The size of the SE is very important and should be chosen very carefully. If the size of SE is too small, undesired area will be interpreted as terrain surface and if the size is too large, actual terrain forms such as peaks will be cut off (Schiewe, 2003). The problem of the size can be solved by the use of adaptive structural element. For the urban areas, the radius of such SE must be larger than half of the largest minimum diameter of a building (Krauß and Reinartz, 2009). The deficiency of the method is, however, produces flattened surface and does not preserve the curvature of land.

Application of a median filter can also be used to get a DTM from the DSM. Similarly there are many other filtering algorithms which can be used to derive a DTM from a DSM. A detailed review on performance evaluation of the different filtering algorithm can be found in Sithole and Vosselman (2004). The filtering method performs well in flat terrain but struggles in undulating areas. Further, these filtering algorithms face greatest challenges in complex urban areas, including multi storied buildings, courtyards, stairways, plazas, elevated roads and bridges etc., and discontinuities in the bare earth (Sithole and Vosselman, 2004)

The DSM and DTM together are used to produce a normalized DSM (nDSM), which is the other kind of elevation data, used in topographic feature (especially building) extraction (Haala and Brenner, 1999). nDSM is generated by subtracting the DTM from the DSM. It gives the absolute height of an

object on the earth surface which is highly useful to distinguish the objects which are higher than the ground level, such as building, vegetation etc. Further, the nDSM can be useful to estimate the height of such objects (Elberink and Maas, 2000).

3.2.7. Quality of DSM

Quality can be understood from different perspective. From a user's point of view, quality means fitness for use and meeting user's expectations. From a producer's perspective, it is some thing which conforms to design, specifications, or requirements and which have no (or very less) defects. From a product based view, the product has something that other similar products do not have and value based approach is that the product is the best combination of price and features (University of Vanderbilt).

The quality of a DTM is generally reflected by accuracy. It can also be said, if there is no (or less) error, the DTM has high accuracy. Error is the difference between the true (or assumed to be true) or reference value and observed value. Normally, the measurements from the equipments/ technique of higher accuracy and reliability are taken as reference and the observed or measured data are compared with those reference value. The difference is considered as error. There are mainly three types of error: random, systematic and blunder. Blunder is an error generally caused by careless observation or measurement, recording and can be detected and removed by careful editing. Systematic error is caused by some instrumental system or data collection procedure or miss interpretation of facts. It can also be detected and corrected as it follows a certain trend and rules. Random errors are those, which are introduced by no known reasons, mostly by circumstances, and cannot be governed by certain standard rules. Hence, these errors cannot be removed (Maune, 2007). The main sources of error in DSM are: method of source data generation, processing and interpolation, and Terrain representation (Fisher and Tate, 2006).

The most widely used statistical measure for accuracy assessment is the Root Mean Square Error (RMSE). It is the square root of the mean squared difference of reference data value and measured data value. Mathematically, represented as

$$RMSE = \sqrt{\frac{\sum_{i=1}^{n} (Z_{i(DEM)} - Z_{i(REF)})^2}{n}}$$

Where, Z_{DEM} is the measurement of elevation from the DTM, and Z_{REF} called reference data or checkpoints obtained from more accurate measure and n is the number of measurements. Other statistical measures like mean error, range, standard deviations are also used in accuracy assessment.

3.2.8. Orthoimage production

Generally, VHRS images do not depict the real world features in their true geometric locations due to perspective geometry and higher incidence (viewing) angle of the satellite and sensor system. Similarly, the height of the object, terrain relief and displacements of the object caused by it introduces geometric error in the image (Toutin, 2004). Perspective projection causes the non uniform scale over the different part of the image. This scale distortion and effect of the tilt and relief displacement is more prominent in outward direction from the nadir point. To avoid or minimize this geometric error in satellite images, orthoimages are used for the measurements and

analysis where a high positional accuracy is needed. Orthoimages are orthogonally projected images having map like geometry in which the displacement due the terrain relief and sensor tilt is corrected by a method known as orthorectification (Schenk, 1999). Without performing orthorectification, the scale is not constant and uniform over the image and consequently, accurate measurements of distance and direction cannot be made.

In order to orthorectify VHRS imagery, a transformation model is required which takes into account the various sources of image distortion such as sensor orientation, topographic relief, earth shape and rotation, sensor orbit and attitude variations and systematic error associated with the sensor generated at the time of image acquisition (Okeke, 2009). The conventional or the simple rectification process cannot remove completely the distortion caused by the terrain relief. Similarly, the effect of very high objects such as high rise building, towers, trees etc is also present in the image. Such objects remain in perspective views in the resulting orthoimages and are distorted from their true positions. This effect causes the distortions like leaning buildings and bent bridges, and much useful information on the ground are remained hidden from the user (Agouris et al., 2004; Zhou et al., 2004). In such images, superimposition of vector data for various GIS analysis cannot be made. To minimize the effect of object height and ground relief and displacement caused by it, a DTM is used for orthorectification. However, only application of a DTM is not sufficient to remove the effect of high rise building and occlusion caused by it completely. The occluded and hidden areas behind high rise building and shaded areas can be replaced by extracting them from other images in which those areas are visible. The orthoimages produced in such a way is called a true orthoimage and are free from all types of geometric errors caused by oerspective projection and height of buildings (Zhou et al., 2004), however production of true orthoimage is not addressed in this study.

3.2.9. Commercial software for DEM and Orthoimage production

Now a days, the integration of several software package into a commercial-off-the-shelf (COTS) systems provide a versatile option for the user with limited expertise to create their own application specific spatial information. There are several COTS systems available in the market, which contain an automated terrain extraction capacity including DEM generation and orthoimage production. These COTS systems may have similarities in workflow, but may differ widely in production environment, operational procedures, available functionality and accuracy achieved of the products generated. In table 3-4, some state of the arts COTS systems, used for photogrammetric operations, are compared on the basis of their functionalities:

3.3. Method adopted

We adopted two methods of DSM generation. The first one is image matching in a COTS system, Leica Photogrammetric Suite (LPS) by ERDAS Inc., and the second one is image matching in a software Satellite Image Precision Processing (SAT-PP) developed by Swiss Federal Institute of Technology (ETH), Zurich. DTM and nDSM were produced from both DSMs. The overall workflow of the method adopted to generate DSM and produce orthoimage is shown in fig 3-1. The whole process is divided in four steps. In the first step, image orientation was done. In the second step, process of DSM generation was carried out. In the third step, DTM and nDSM were produced from DSM by applying morphological filtering method and finally, orthoimage was produced. The following sections discuss the method in detail.

Table 3-4: COTS, a comparison

	Orientation and AT	DEM generation	Ortho Image	Feature extraction
ImageStation by Intergraph	Automatic interior/ relative orientation, AT, blunder detection	All methods, with contour and editing facility no break lines,	Interactive mosaic, True orthoimage possible	Mapping possibility and integration possible with some systems
LPS By Leica Geosystem	Automatic interior/ relative orientation, AT, blunder detection	Area based: least-squares, cross correlation, hierarchical with contour and editing facility no break lines,	Interactive mosaic, no true orthoimage	Mapping facility with 3D shape file also
PCI Geomatics by PCI Geomatics Corporation	Automatic interior/ relative orientation, AT	All methods, with break line and contour generation, editing facility	Interactive mosaic, no true orthoimage	Mapping facility with a wide range of supported format
Info System by Info	Automatic interior/ relative orientation, AT, blunder detection	Area and feature based with contour, and editing facility no break lines,	Interactive mosaic, True orthoimage possible	extracted features can be integrated with CAD/ ArcGIS/ Microstation
SOCET SET by BAE system	Automatic interior/ relative orientation, AT, blunder detection	area and edge matching for DEMs, with break line and contour generation, editing facility	Interactive mosaic, True orthoimage possible	Semi automatic corner points, line features and building extraction, partly can be integrated with other systems
Vr Mapping by Cardinal System LLC	Semi automatic interior, relative orientation, AT, automatic blunder detection	colour balance and colour match, with contour and editing facility no break lines,	Interactive mosaic, no true orthoimage	Wide range of mapping facilities, can be imported/ exported to/ from many other systems
PHOTOMOD by Racurs	Automatic interior/ relative orientation, AT, blunder detection	Hierarchical cross-correlation, with contour, and editing facility no break lines,	Interactive mosaic, no true orthoimage	Mapping facility with possibility of integration with other format
KLT ATLAS KLT Associates	Automatic interior/ relative orientation, AT, blunder detection	All methods, with break line and contour generation, editing facility	Interactive mosaic, True orthoimage possible	Mapping facility along with the support of almost all format data
PhoTopoL Atlas by TopoL Software	Automatic interior, manual relative orientation, AT, blunder detection	area-based, with contour, and editing facility no break lines	Interactive mosaic, True orthoimage possible	Mapping facility with possibility of integration with other format
Match-T by Inpho	Automatic interior/relative orientation, AT, blunder detection	Feature based, with contour and break lines with editing facility	Orthoimage can be generated	Accurate data capturing facility

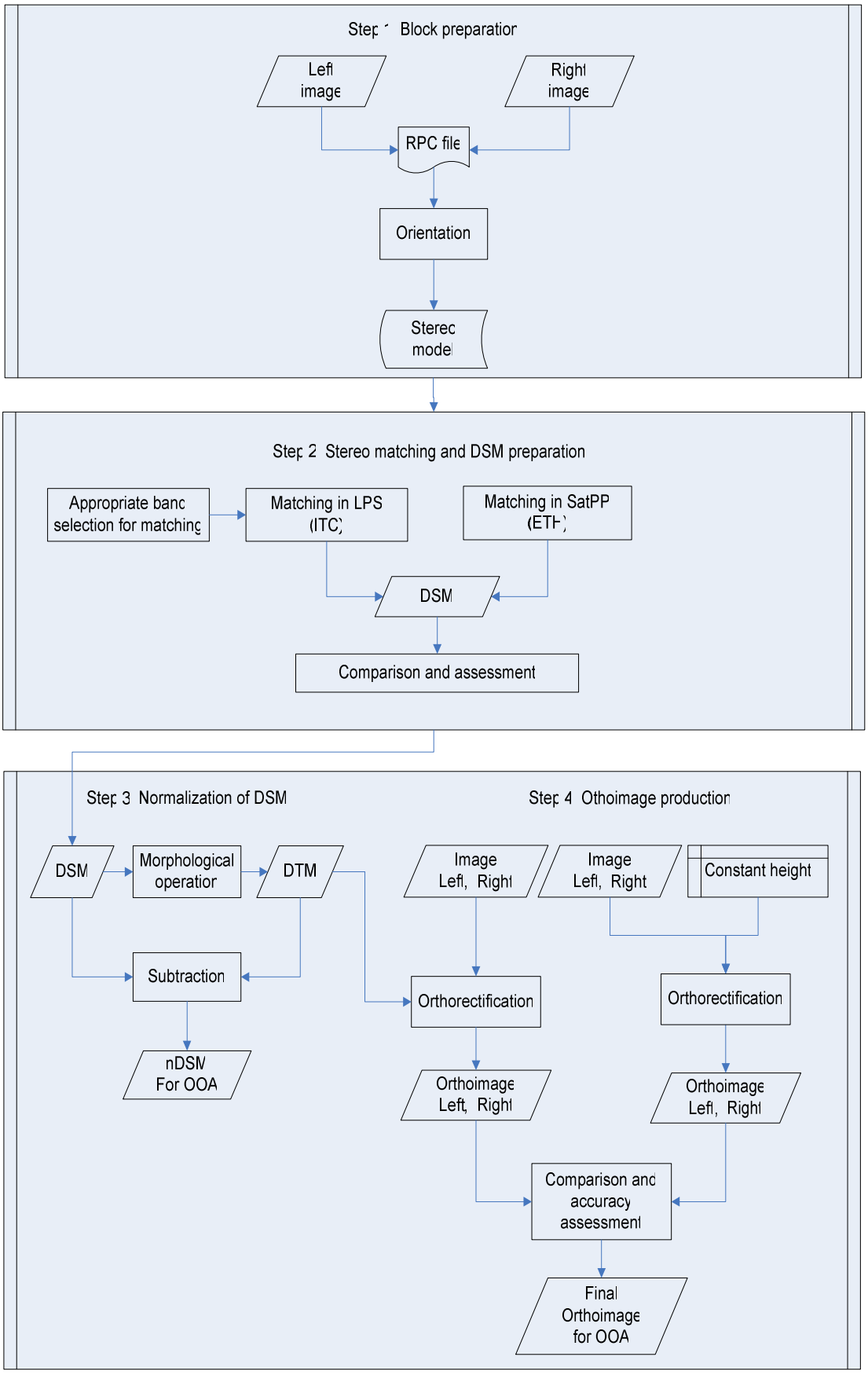

Figure 3-1: Workflow of the method adopted for DSM generation and orthoimage production

3.3.1. DSM generation in LPS

3.3.1.1. Steps in DSM generation

The process of automatic DTM extraction from VHRS satellite image in LPS can be divided into the following three steps:

a. Generation of Mass Point by Automatic Image Matching

In the image, LPS identifies interest points or feature points, the appropriate match of which is searched in the conjugate image pair. An interest operator is used to identify such points. These interest points are usually, the centre of template window, having a sufficient variation of gray level and good contrast and represent features on the ground surface e.g. a road intersection or the corner of a house.

After identifying the interest points to be matched in an image, LPS proceeds to find the matching points which represent the same ground feature appearing on the other images. In the reference image, correlation window is defined and cross correlation coefficient is calculated for each correlation window among the search window. An interest point on the reference image can have more than one possible match point on the conjugate images. In such case, the cross correlation coefficient is calculated for every possible match point and compared. The correlation coefficient considered as the measure of similarity between the image points appearing within the overlapping areas of the image pair. A match point having correlation coefficient 1 is considered as correct match whereas 0 is taken as no match at all. Generally, a value of greater than 0.8 is applied in LPS.

b. Determinations of the Coordinates of the Ground Point

After finding the possible match and computing the cross correlation coefficient, different statistical measures are applied to determine the final matching points. Row and column pixel coordinates of these final image points are recorded. From these image points, the 3D coordinates of the ground feature are computed and the DTM mass points are generated with 3D positions. These 3D coordinates associated with a mass point are generated by using space forward intersection.

c. DTM Generation

Various types of DTM format as output are possible in LPS such as raster DEM, TIN, 3D shape file, ASCII etc. DTM mass points are used to generate DTM in any format. ASCII file and 3D shape file are simple description of the DTM mass points. A TIN is a digital representation of the earth surface which is composed of different non overlapping triangles. TIN is created from DTM mass points by using the Delaunay triangulation approach. A raster DEM output is generated from DTM mass points by using an interpolation technique.

3.3.1.2. Parameters influencing the matching

The matching result depends upon the various parameters mentioned below:

a. Search window size

The search window is normally rectangular. Parameter X refers the length and Y refers the width of rectangle along and across the epipolar line respectively. The search window length X depends upon the variation of the elevation of the ground surface. If the range of the ground elevation is larger, the length of the window should also be large. The width of the search window, the parameter Y

depends upon the geometric accuracy of the images to be matched. In an image from aerial frame camera, the accuracy of triangulation is generally high, in such case, the width of about 3 pixel is sufficient. For the HRS image from pushbroom sensor, the accuracy of triangulation is not so high and therefore, the suitable Y is 3-5 pixels.

b. Correlation window size

Correlation window is normally defined in square shape, but it can be rectangular also. It defines the size of the window which is used to compute the correlation coefficient between the points on corresponding overlapping images. The default window size in LPS is 7 × 7. But the size can be varied according to the image and ground characteristics. If there is a small variation in topographic relief, gray level, or colour intensity e.g. desert, agricultural fields, grassy areas, a larger window size can be used. Conversely, if the area has large variation in topographic relief, gray level, and color intensity, a smaller window size can be used. Rectangular window can be used if there is a large variation in the ground relief along the epipolar direction

c. Correlation coefficient

The correlation coefficient is a measure of similarity. It decides whether the two points should be considered as the matched points. A certain threshold is defined as the limit and if the correlation coefficient is smaller than this threshold, the two points are not considered as match points. Although the correlation coefficient varies from -1 to 1, it is considered as 0 to 1 in LPS. The default threshold set for the matching is 0.8. If this number is increased, the accuracy of matching may increase but the numbers of match points decrease. On the other hand, if this threshold is decreased, number of match points may increase but the accuracy of matching may decrease.

3.3.1.3. Appropriate band to be used for matching

For automatic matching, LPS take any of the bands at a time. The available images contain four bands; band 1: blue, band 2: green, band 3: red and band 4: near infrared. Different objects have different spectral characteristics in different image bands and, thus the contrast and brightness differ for each band. Not all features are equally and clearly visible in every band. It is already discussed that the matching accuracy also depends upon the radiometric properties of an image. Hence, for matching we need to use a band, in which most features are clearly separable. To find the most useful band for matching, spectral variability is considered.

3.3.1.4. Statistical analysis of the image bands

Spectral values of four bands were analyzed statistically on study sites 1 (sparse area), study site 2 (dense regular area) and study site 3 (dense irregular area). The statistical standard deviation was computed and compared.

3.3.1.5. Image matching

An experiment was carried out to generate DSM by matching all available 4 bands separately to evaluate the fitness for DSM generation. This was done by generating DSM in the output format 3D shape file and raster DEM. Different matching criteria such as search window size, correlation size and correlation coefficient thresholds were used for matching. Experiment was repeated for all three study sites and the result was compared.

3.3.2. DSM generation in SAT-PP

The main steps for the DSM generation in SAT-PP are illustrated in figure 3-2. The main procedure can be summarised as follows (Li and Gruen, 2004):

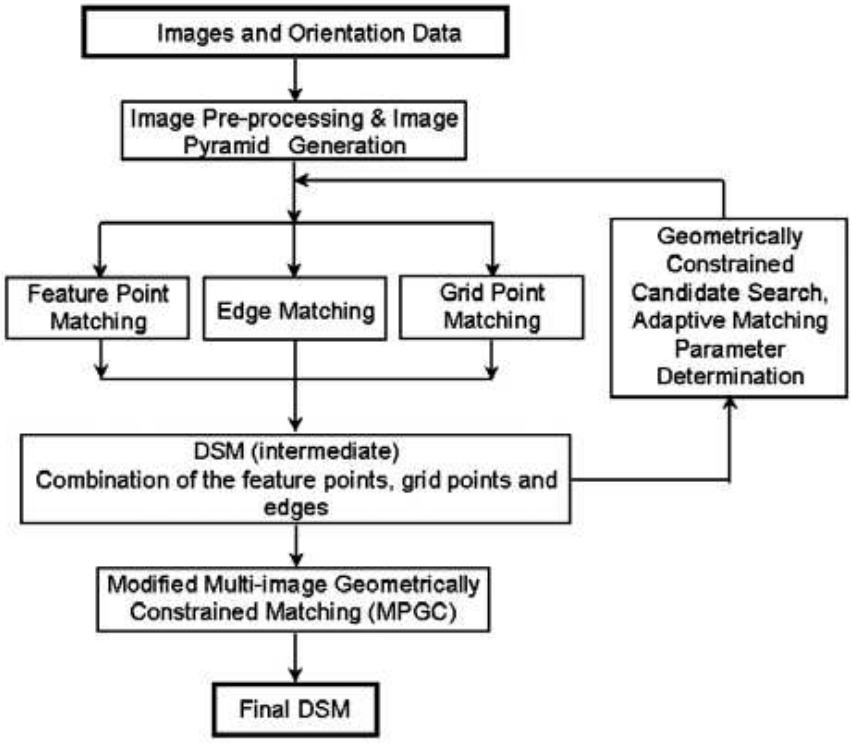

Figure 3-2: Workflow DSM generation in SAT-PP (Li and Gruen, 2004)

3.3.2.1. Image pre-processing

In the first step, image pre-processing is done. Some of the radiometric problems like strong bright and dark regions are removed by applying edge preserving smoothing filter and Wallis filter. The edge preserving smoothing filter reduces the noise while sharpening edges and preserves fine detail such as corners and line endpoints. The Wallis filter strongly enhances already existing texture patterns even in shadow and homogeneous areas. This pre-processing is necessary for optimising the images for subsequent feature extraction and image matching. Then, the image pyramid is generated. The image pyramid starts to generate from the original resolution of images. Each new pyramid level is generated by reducing the previous resolution by a factor of 2. The pyramid level number can be a pre-defined user input value or can be determined by the system itself.

3.3.2.2. Multiple Primitive Multi-Image (MPM) Matching:

This step is the core of the approach for accurate and robust DSM generation. This matching technique applies multiple matching primitives such as feature points, grid points, and edges in successive stages, integrates local and global image information, and utilizes a coarse-to-fine hierarchical matching strategy.

Foerstner interest operator is used to extract well-defined feature points, which are appropriate for image matching. The correspondence of the given points on the search images is determined by using the geometrically constrained cross-correlation method. The matching candidates are computed by using the technique of cross-correlation with a set of adaptive parameters such as the image window size, the threshold of the correlation coefficient, and the search distance. The

approximate DSM that is derived from the higher-level of the image pyramid is used to estimate these parameters. The edge features are matched to solve the problem in DSM generation, especially in urban areas, caused by surface discontinuities, occlusions and the significant perspective projection. These line features play important role for capturing and modelling the ground features such as ridgelines and breaklines. The grid points are matched to create uniformly distributed points over the whole images.

3.3.2.3. Refined matching:

To refine the DSM and get sub pixel accuracy, a method known as modified MultiPhoto Geometrically Constrained Matching (MPGC), developed by Armin Gruen in 1985 is used. MPGC integrates the principle of least squares matching and geometric constraints, which are formulated either in image or in object space and allow a simultaneous determination of pixel and object coordinates, and achieve accuracy in the subpixel range. The modified algorithm is an extension of the standard MPGC, which combines the geometric constraints derived from the linear array sensor models. These geometric constraints force the matching process to search the conjugate point only along a small band around the epipolar line and reduce the possibility of false matches.
The detailed process of DSM generation by matching in SAT-PP can be found in (Li and Gruen, 2004; Wolff and Gruen, 2007; Wolff and Gruen, 2008; Zhang and Gruen, 2006).

3.3.3. DSM filtering

Morphological operation, opening was carried out for DSM filtering. It is a process of mathematical erosion followed by dilation. The height of the buildings, trees, etc are removed from the DSM and only the ground level remained in DTM. Finally, the DTM was subtracted from the DSM to get nDSM

3.3.4. Orthoimage production

Orthoimage production process consists of two main steps: orthorectification and resampling. This process uses an oriented image and elevation data related to the image area. Elevation data can be supplied in the form of raster DEM, TIN, 3D shape or contour line. A constant height, representing the earth surface of the image area can also be used for orthorectification. This method of producing orthoimage by using a constant height can be applicable for the flat areas. Resampling computes the new geometric/radiometric properties of the image after orthorectification.

3.4. Implementation, Results and Discussion

This section presents the implementation of the methodology, processing task, results and outcome of the processing. Short discussion is followed after each implementation and results. The main task carried out here was DSM generation, filtering, and orthoimage production.

3.4.1. DSM Generation

For DSM generation, matching was done in one particular band at a time. It is necessary to explore which band is the most useful for matching. Therefore, suitability of bands was analysed, then matching in LPS was done, and its results were discussed, followed by matching in SAT-PP, result and a comparison between DSM produced in both systems.

3.4.1.1. Statistical analysis of image bands for suitability of matching

Statistical analysis of 4 bands to explore the spectral variability was done. Standard deviation (SD) was used to make a comparison among each band. The result is shown in table 3-5.

Table 3-5 shows, the standard deviation is highest for band 4. Similarly, the histogram analysis was also carried out for each band (see figure 3-3). It also shows the spectral variation is the highest for band 4. This variation of pixel value in different band is shown by the spectral profile of different object class in different image bands (see Annex 1) and spatial profile through different objects/class such as building, water, road, bare ground, vegetation and shadow (see Annex 2).

These analysis and results show the band 4 has the highest spectral variability and offers the most details among the 4 bands. Therefore, the NIR band can be used for matching as it can improve the ability to correlate on features during image matching.

Table 3-5: Statistical analysis of 4 image bands on the study sites

Statistical Measures	Bands used	Pixel value		
		site1 Sparse Area	site2 Dense regular Area	Site3 Dense irregular Area
Standard Deviation	Band1 (B)	78.5	68.2	73.44
	Band 2 (G)	150.6	129.7	138.75
	Band 3 (R)	120.3	100.1	111.09
	Band 4 (NIR)	252.9	232.7	236.82

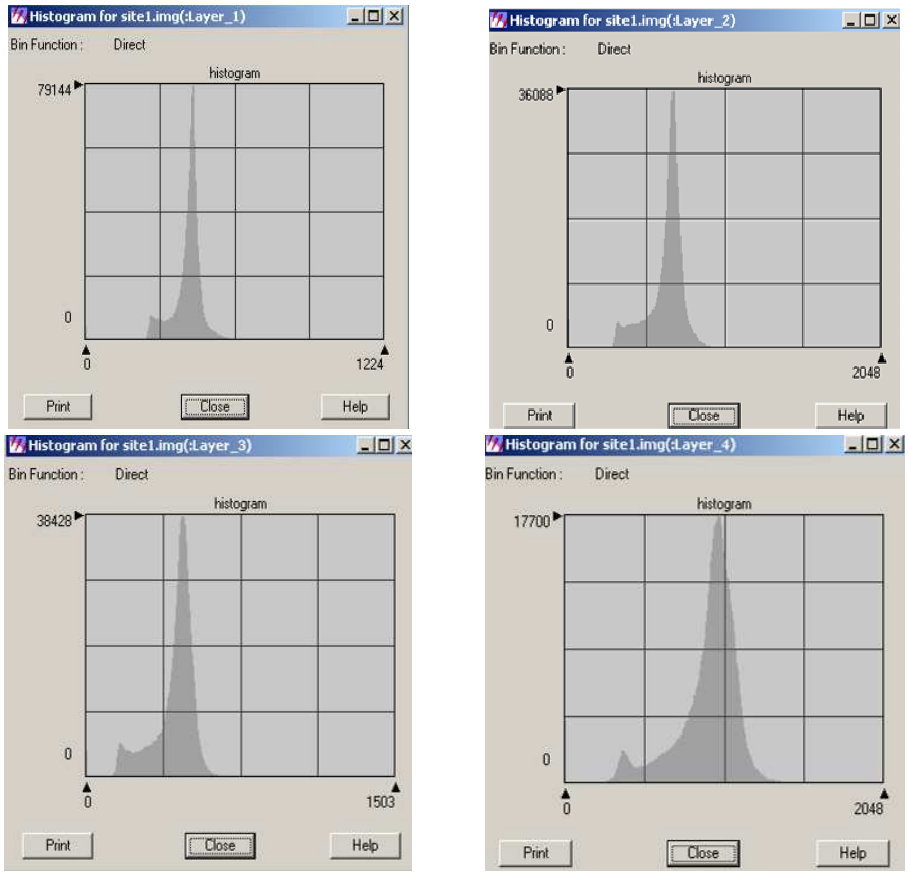

Figure 3-3: Histogram analysis for study site 1

3.4.1.2. Matching in LPS

The previous section showed that band 4 (NIR) is more suitable in matching for DSM generation. However, the result was further verified by performing matching in all 4 bands and comparing the results.

Several experiments were done for matching all 4 bands in original 16 bit image by using different matching strategies and parameters, but the results showed many inconsistencies in generated DSM. These inconsistencies (see annex 3,4,5) were mainly inability in matching band 4, partial matching in band 2, no sufficient match points in matched areas of image, band 1 has more match points than band 4 (table 3-6 and Annex 3), and unexpected problem in software (e.g. window shuts down). Similarly, adaption of parameter for automatic terrain extraction function built in LPS also gives inconsistency in the matched result such as the number of matched points found in DSM are same under different matching criteria (see table 3-6).

Table 3-6: Inconsistency in matching with 16 bit image

Matching Criteria	Bands	No. of match points in site1	No. of match points in site2	No. of match points in site3
Search window 61x3 Correlation window 3x3 Correlation Coef. 0.8	1	39912	26835	5360
	2	7930 (partly)	13986	2963 (partly)
	3	44345	25817	4955
	4	No match	5792	566
Search window 21x5 Cor. 5x5 Correlation Coef. 0.8	1	39912	26835	5360
	2	7930	13986	2963
	3	44345	25817	4955
	4	No match	5792	566 (partly)

To overcome these inconsistencies, the images were rescaled to 8 bit and matching was done. Experiments show the matching in 8 bit image gives better result in LPS. The different matching strategies and parameters were experimented in a trial and error basis. Matching was carried out without using the parameter adaptation functionality of LPS and parameters were set manually. It gives a significant improvement in the matching result. A comparison is made in table 3-7. With adaptive parameter, the number of match points for different matching criteria were same whereas matching without adaptive parameters, the number of match points were different and according as the principle of matching. The result of so produced DEM is shown in figure 3-4 (left), 3-5 (left) and 3-6 (left) respectively for study site 1, 2 and 3.

Table 3-7: Comparison of match points by using different matching criteria

Study sites	Bands	Number of Match Points / Image / Matching Criteria			
		Search window: 61x3 Cor. Window: 3x3 Correlation Coef.: 0.8		Search window: 21x5 Cor. Window: 5x5 Correlation Coef.: 0.8	
		8 bit /without adaptive parameter	8 bit / adaptive parameter	8 bit /without adaptive parameter	8 bit/adaptive parameter
1	1	32865	7611	30568	7611
	2	80543	18924	77204	18924
	3	77323	18312	73755	18312
	4	122316	30861	118403	30861
2	1	82724	12380	73907	12380
	2	136979	20336	123876	20336
	3	135650	19835	122930	19835
	4	146499	27187	130183	27187
3	1	12604	2259	11764	2259
	2	21750	3863	20423	3863
	3	21451	3656	20353	3656
	4	23571	5430	22237	5430

3.4.1.3. Matching in SAT-PP

It has been already mentioned that, the matching in SAT-PP was done at ETH Zurich and resulting DSM was provided. The matching at ETH was also done in 8 bit images because of the similar problems as in LPS. The method and technology behind the matching have been mentioned already in previous sections. The resulting DSM generated in SAT-PP is shown in figure 3-4 (right), 3-5 (right) and 3-6 (right) respectively for study site 1, 2 and 3.

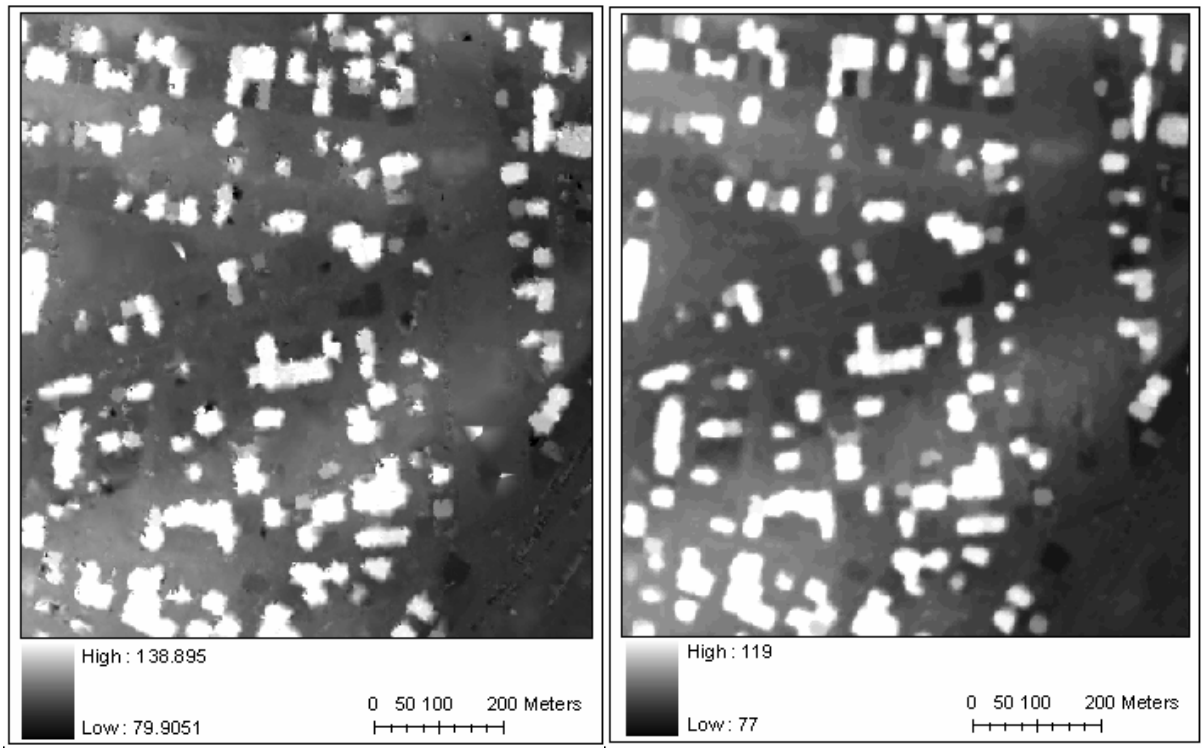

Figure 3-4: DSM of study site 1 by using LPS (left) and SAT-PP (right)

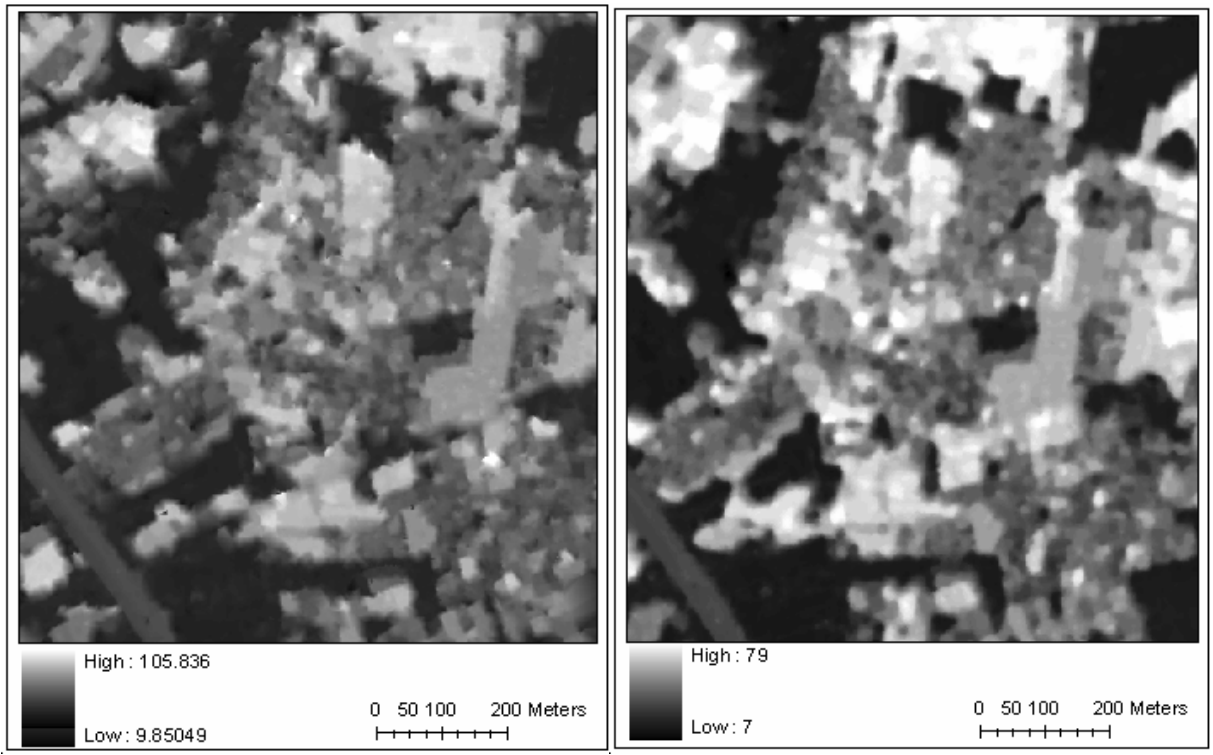

Figure 3-5: DSM of study site 2 by using LPS (left) and SAT-PP (right)

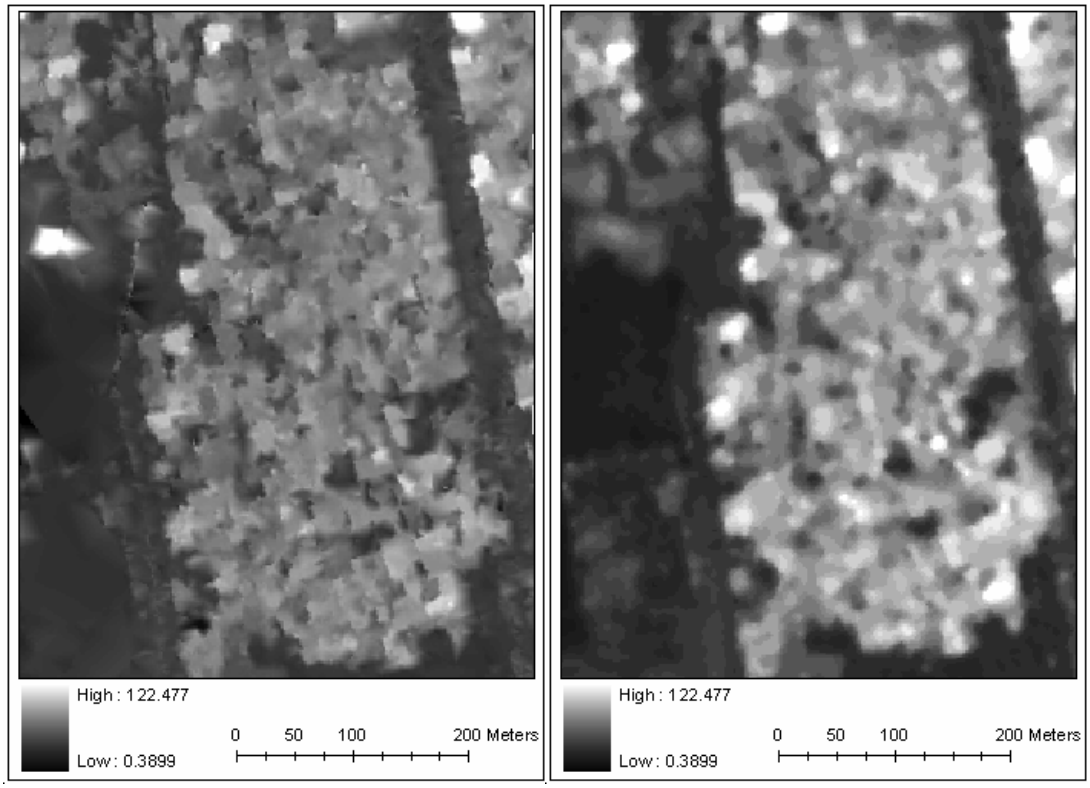

Figure 3-6: DSM of study site 3 by using LPS (left) and SAT-PP (right)

3.4.1.4. Visual Comparison of DSM generated in LPS and SAT-PP

A visual comparison can be made between the DSM produced by LPS and SAT-PP from figure 3-4, 3-5 and 3-6. In study site 1, although the DSM from LPS has satisfactory delineation of shape and buildings, DSM from SAT-PP has clear distinction over it. SAT-PP DSM has less noise, clear shape of building, good identification of details and building edges preserved more clearly. In LPS DSM there is more noise and unclear visualization of detail with less preserved building edges.

In study site 2, the dense area are not clearly modelled, however, the general shape and size of building blocks and other infrastructures like road/flyover is preserved. Both DSMs look similar in quality. In study area 3, the representation of terrain in DSM is not clear, except the road. All building seems meshed up in the DSM.

3.4.2. DSM filtering

Mathematical morphology filtering operations opening was used successively for filtering the higher elevation objects like building and trees from DSM. Opening was achieved by erosion followed by dilation. Removing the higher object from DSM, a DTM was produced. The ground surface height in so produced DTM was compared with the manually measured height of same point in stereo image. And a variation of 1-4 m was observed. This is because some of the ground objects were still not filtered well in the DSM.

Later, the DTM was subtracted from DSM and nDSM was prepared. It contains the absolute height of buildings from the ground level. The individual absolute heights of the building in this nDSM were also verified by comparing them with the measured height of same building in stereoimage. A difference in of 1-4 m in height of building was observed. The produced DTM and nDSM are shown in figure 3-7.

Figure 3-7: Original DSM (left), DTM (middle) and nDSM (right)

3.4.3. Orthophoto production

Orthoimages were produced by using both, left and right images of stereo pair. The output cell size was kept 50 cm to preserve the resolution of the detail similar to that of the image. The elevation data was supplied as output DTM, which was produced by morphological filtering of the DSM generated in LPS.

Since the quality of DSM generated and filtering operation was not much reliable, it was suspected that the orthoimage produced may not be very accurate. Therefore, filtered DSM and constant height was used to produce two different orthoimages. Since the topography of the study sites is fairly levelled, the average elevation of the earth surface was measured in stereo model and a constant height of 95, 15 and 17 m for study sites 1, 2 and 3 respectively was used for orthoimage production.

3.4.4. Quality assessment of orthoimage

To assess the accuracy of the orthoimage produced from left and right stereomate by using DTM (produced by filtering of SAT-PP DSM) and constant height, position of the buildings in both orthoimages were compared. The comparison was made with respect to the buildings, which were manually digitized from stereo model. A visual comparision made between the building digitized from orthoimage from left and right image are shown in figure 3-8 (left). Similarly, the positional displacement in the location of buildings in the orthoimages produced by using SAT-PP DTM and constant height are shown in figure 3-8 (right).

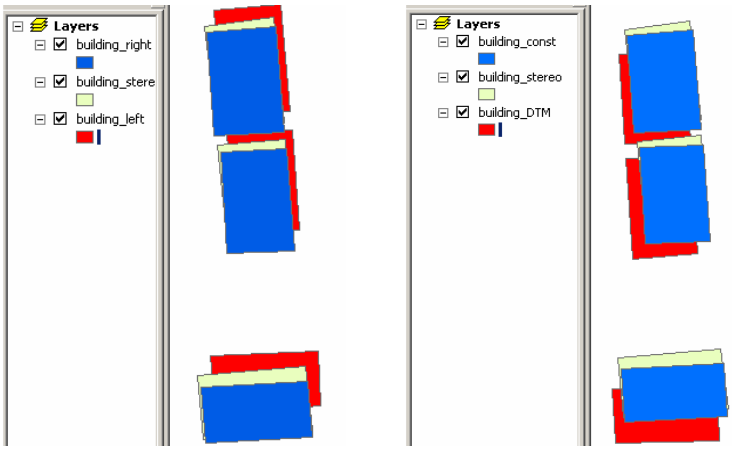

Figure 3-8: Positional shift of buildings in orthoimages from left and right images (in left) and from LPS DTM and constant height (in right)

Figure 3-8 (left) shows that the buildings extracted from left orthoimage (red) were more displaced along north-east than the buildings extracted from right orthoimage (blue) displaced only along

south in comparison with reference buildings extracted from stereo model (yellow). The reason behind this is the incident angle (viewing angle of satellite) for right image is less (13.3^0) than that of left image (17.4^0), which causes less relief displacement in right image. Similarly, the nominal collection azimuth of the left image is 214^0 (south- west), which causes a larger displacement along north-east whereas in the case of right image the azimuth is 340^0 (almost north), which causes the displacement only along the south. This fact suggests that the orthoimage produced from right stereomate is more accurate than that produced from left and therefore, for the further task, orthoimage from right stereomate is used.

To assess the accuracy of the orthoimages produced by using two different elevation data (DTM and constant height), the positional displacement of the buildings with respect to the reference buildings was done. The building centroid was identified and the distance between buildings centroids were compared. Detailed calculation is in Annex 6 and the result is shown in the table 3-8.

Table 3-8: Comparison of building displacement in orthoimages

Statistical measures	Building displaced in orthoimage by using SAT-PP DTM	Building displaced in orthoimage by using constant height
Mean displacement in X	-1.17	-0.62
Standard Deviation	0.41	0.45
Mean displacement in Y	4.55	2.88
Standard Deviation	1.10	1.13
Mean distance vector	4.73	3.08
Standard Deviation	1.02	0.84

Table 3-8 shows that the buildings extracted from constant height orthoimage are less displaced than those from the orthoimage produced by using SAT-PP DTM. The reason behind this could be the poor DSM quality and imperfect filtering for producing DTM from DSM. Hence, for the next step in this research, the orthoimage produced by using and right image with constant height is used.

3.5. Concluding Remarks

Band 4 (NIR) is found the most suitable band for image matching to extract DSM because this band has the highest spectral variability. But the matching in original 16 bit image was found problematic and inconsistent in LPS. Similarly, parameter setting is also vary important and cannot be relied on automatic adaptive terrain extraction parameters. Reducing the radiometric resolution to 8 bit, and careful and interactive parameter setting gives better matching results and more reliable DSM.

Matching in open areas produces more reliable DSM than dense and crowded areas. DSM in study site 1 is more reliable than study site 2 and 3. Because of the large amount of shadow, occlusion and height of building, the matching process suffers and do not yield accurate result in dense urban areas with tall buildings. The quality of DSM generated in SAT-PP is found slightly more reliable than the DSM generated in LPS. The LPS DSM has some artefacts, discontinuity, and noise on the terrain surface whereas the SAT-PP DSM is smoother than LPS DSM.

The orthoimage produced from right stereomate has less displacement of objects from their positions Because of the lower incident viewing angle. The DTM generated was not accurate enough for removing the distortion in orthoimage, a constant height was used for orthoimage production as it was found more accurate than the orthoimage prepared from the DTM.

4. Building Extraction by Object Oriented Image analysis Technique

4.1. Introduction

This chapter deals with the sub objective 2: to extend the method of building extraction by OOA technique, using photogrammetric DSM generated from VHRS stereo image. This chapter starts with a brief introduction to key terms used in this chapter (section 4.2), followed by a review on the OOA and building extraction by this technique (section 4.3, 4.4, and 4.5). The adopted method for this study is discussed in section 4.6. Then the results obtained and the accuracy assessment is presented in 4.7 with a brief discussion and finally a concluding remark in presented in section 4.8.

4.2. Introduction to the terms

This section briefly introduces the terms, which are commonly used in this chapter. These terms may have several and broad meanings but in this chapter they are used in the context of OOA, unless stated otherwise. Some of these terms are explained further in detail in the chapter according as necessity.

Object: A discrete individual spatial entity, e.g. an individual building.

Class: Collection of similar object, e.g. all buildings.

Segmentation: Process of partitioning an image in several pieces on the basis of certain criteria. The partitions are called segments (or image objects, object primitive). An object may be either a single or a combination of segments, based on its properties.

Feature property: Property that characterises the image segments, e.g. area, length, brightness etc.

Scale: A parameter used for image segmentation in OOA based software, Definiens, which is crucial to determine the size of the segments.

Shape: A parameter used for image segmentation in Definiens, which is used to define the homogeneity of the segments.

Colour: A parameter used for image segmentation Definiens, which is used in relation with shape to determine the homogeneity of the segments.

Spectral information: Information related to the spectral properties of the objects/segments, characterised by colour (hue, value) in the image, e.g. NDVI, brightness etc.

Spatial information: Information regarding to the spatial extent of the objects/segments, e.g. area, length, asymmetry, length/width ratio etc

Contextual information: Information regarding the spatial arrangement and association of objects/segments in relation to other objects/segments, e.g. *relative boundary with* (e.g. shadow)

Building extraction: A term, used for building identification, detection and measurement in image

Individual building: single isolated building

Building block: two or more buildings grouped or connected to form a bigger cluster of building.

Building outline: Outline of a single building or building block.

4.3. Review on building extraction techniques

Building extraction in urban areas is one of the important fields of research in remote sensing. Many methods have been mentioned in literature for extraction of building by remote sensing technology (Baltsavias et al., 2001). Studies show that buildings can be extracted successfully from several data sources using different methods. Traditionally, aerial photographs were most popular and widely used data sources for extraction of buildings. Very high spatial resolution, robust geometric property and good radiometric quality, make building extraction possible from aerial photographs and many studies are conducted already for this (Baltsavias et al., 2001).

After the emergence of VHRS, researchers have the other option for extraction of buildings. The spatial resolution of these images is high enough, and the geometric and radiometric properties are found suitable for extraction of buildings (Eisenbeiss et al., 2004; Jacobsen, 2009). These VHRS images are widely used for building extraction, examples are found in several literature (Baltsavias et al., 2001; Jin and Davis, 2005; Rottensteiner and Briese, 2003; Sohn and Dowman, 2007).

With the advancement of technology, new methods are developed. LIDAR is one of them. The LIDAR data are produced by scanning the earth surface by a laser scanner in an aerial vehicle. By using LIDAR DSM with VHRS images and applying different techniques, many researchers extracted urban building successfully (Brenner, 2005; Miliaresis and Kokkas, 2007; Vu et al., 2009).

One of the (semi)automatic algorithms for extraction of features from VHRS image is the pixel based approach. In this approach, pixels of similar spectral values are clustered into different classes. Sample pixels are chosen for different feature type and the system classifies these pixels accordingly. The main limitation of this approach is not considering the spatial and contextual information for classifying the object and hence result suffers from salt and pepper effect (Benz et al., 2004; Blaschke and Strobl, 2001; Burnett and Blaschke, 2003). Improvement of pixel based approach is based on the introduction of semantic knowledge in the classification process. The knowledge about spatial relationship between the different land-cover types is applied to improve pixel based classification (Lhomme et al., 2009). The main objective is to improve delineation of building boundaries during classification.

The other approach for building extraction is based on extracted edges to reconstruct the buildings. This reconstruction is usually constrained by rules defined by the user, e.g. perpendicular orientation, right angle corner, etc. The main limitation of this approach in VHRS image is the resolution of images is too coarse to extract the edges very accurately (Lhomme et al., 2009).

Another alternative for urban object extraction is object oriented approach. This approach is based not only on individual pixel and its spectral characteristics, but also on the spatial, contextual, and textural information of the surrounding. The image is first segmented on the basis of homogeneity criteria, mainly guided by colour and shape and then different spectral, spatial and contextual features are computed for each segment. These features are then used for classifying the segment. This research uses OOA approach for building extraction and is further discussed in the following sections.

4.4. OOA technique

There are several methods for information extraction from images (Baltsavias et al., 2001). However, the main requirements for the extraction of required information from the images in a state - of - art

image analysis system are: to understand the sensor characteristics, to identify the appropriate analysis scales and their combination, to identify typical context and hierarchical dependencies, and to consider the inherent uncertainties of the whole information extraction process, starting from the sensor, to fuzzy concepts for the requested information (Benz et al., 2004).

Information extraction from remotely sensed images is combination of the smallest processing unit of the image, features used for processing and classification algorithm (Liu et al., 2006). The smallest processing unit may be either pixel or object (group of similar pixels). Features may be spectral characteristics, DN values, textures etc for pixels and spectral characteristics, shape, size, texture, context, semantic knowledge for object under observation. Classification algorithm may be minimum distance, maximum likelihood, nearest neighbour or fuzzy membership.

Since the start of the first Landsat satellite in 1972, most of the methods for information extraction from images have been depending upon the single pixel by measuring reflectance at the Earth's surface (Blaschke and Strobl, 2001). These traditional pixel based methods may not be fully successful to exploit the strength in information extraction of recently emerged VHRS images. The reasons behind this are mainly: similar spectral reflectance from more than one class, not taking consideration of spatial relationship among the neighbourhoods, inapplicability of the semantics and prior knowledge about the object and class, meshed up information and artefacts (Blaschke and Strobl, 2001). Since the starting of earlier this century, OOA of VHRS is being studied and documented. This study shows that the OOA could overcome the above mentioned problems of pixel based analysis (Blaschke, 2010).

The concept of OOA is to break images down into spectrally homogenous segments or objects. The shape and size of such segments can be constrained by a number of parameters which control the maximum allowable heterogeneity within a segment (Benz et al., 2004). Additional thematic data layers, such as DSM, parcel boundary, and roads can be used to create meaningful segments in the image (Teo and Chen, 2004). Different characteristics of these segments like spectral characteristics, shape, orientation, texture, proximity or adjacency to other objects can be calculated and then can be used to develop rulesets which are used to classify the segments.

To represent the different hierarchical level of objects in real world situation, different level of segmentation can be applied. It leads to easier extraction of image objects in different scale level. Furthermore, we can establish a topological relationship to the neighbouring objects (in same segmentation level) or the objects in a different segmentation level (so called sub or super object level) (Burnett and Blaschke, 2003). The most important characteristic of OOA is to integrate different datasets, process and semantic knowledge regarding features, which is not possible with most of the other image processing methods.

OOA is not only based on the spectral characteristics of the image but also based on the spatial and semantic knowledge about the objects ant its context, texture, association with spatial arrangement and neighbourhood. The main advantages of the OOA over pixel based analysis are: it takes a homogeneous object element or image segments as a fundamental building block for classification, considers spatial relationship among the neighbouring objects, and applies semantics and prior knowledge about the objects for analysis (Benz et al., 2004). The main constituents of OOA and the steps involved in it are discussed in the following subsections.

4.4.1. Image Segmentation

Segmentation is a process of creating homogeneous and continuous region of an image, called image object, object primitive or segment. A successful image segmentation process should follow the following criteria: summing up all individual segments must be equal to the whole image, interior area of segments must be mutually exclusive i.e. should not overlap, pixels in same category should have similar values, pixels of one category should form continuous region and neighbouring pixels that are in different categories should have dissimilar values (Miliaresis and Kokkas, 2007).
Mathematically a segmentation procedure can be represented as:

$$I = R_1 \bigcup R_2 \bigcup ... \bigcup R_n$$

Where, I is whole image, $R_1, R_2, ..., R_n$ are the non-overlapping, contiguous individual regions and $\bigcup$ is the mathematical operator union.
Many segmentation techniques can be found in literature such as thresholding, edge based and region based segmentation (Miliaresis and Kokkas, 2007; Rekik et al., 2007). Further discussion in this section is limited to region based segmentation as this technique is used in this research.

Region-based segmentation:

This technique extracts information from an image by grouping similar pixels together to form an image object by finding a homogenous region. It can be divided into

(a) Region growing: In this method, a seed pixel is chosen and adjacent neighbouring pixels are checked. If they are similar to the seed pixel, they are added to form a region. This region starts growing until it finds the similar pixel and stops if no more similar pixels can be added. The similarity of pixel can be defined on the basis of homogeneity criteria. The process of growing starts from single pixels and gradually become bigger and thus it is called a bottom up approach. Multiresolution segmentation (Definiens 2008) is the example of region growing.

(b) Region splitting: In this method, whole image is split into a number of homogenous pieces of images depending upon certain user defined criteria. The region is split in the smaller image objects starting from a whole image and can be split to a minimum of a single pixel. Chessboard segmentation (Definiens 2008) is the example of region splitting in which the image is broken down in a numbers of regular tiles like in a chess board. This approach is called top down approach

(c) Split and merge: This technique is a combination of region splitting and merging. The whole image is split down into a number of pieces and then the pieces are merged together to form image object based on their homogeneity. It finally yields the image segments on the form of quadtree. Quadtree segmentation (Definiens 2008) is the example of split and merge segmentation.

4.4.2. Feature property analysis

The next step after image segmentation is the analysis of the feature property of the image objects. These feature properties are mainly spectral (hue, colour, value), spatial (shape, size, area), contextual (shadow, pattern, relation with neighbouring objects) and textural information of the image objects. The image segments are classified on the basis of these feature properties.

4.4.3. Classification

The third step in OOA is classification of image objects. There are many classification algorithms mentioned in literature. Supervised nearest neighbourhood classification algorithm uses samples of

image objects from each class and classifies the image objects by comparing their feature properties with the provided samples. The fuzzy membership function uses feature characteristics and ranges from 0 to 1. The possibility of an image object falling in certain class is decided on the basis of fuzzy membership function.

4.5. Building extraction by OOA

Emergence of VHRS images and limitation of traditional pixel based classification creates an opportunity for new technique to adopt automatic building extraction from remotely sensed images. With the beginning of the new century, OOA has been widely used for extraction of buildings from VHRS images. One of the first studies in this field is documented in Hofmann (2001). In this study the OOA technique is used to extract the informal settlement of Cape Town, from Ikonos image. Image segmentation and successive classification of segments under a complex class hierarchy by using different object characteristics like shape, size, context, and textures is done. The same technique is used in more enhanced and improved way to extract an informal settlement of Rio de Janerio. The method is used in a more simplified class hierarchy in a Quickbird image with fuzzy membership function and their combinations (Hofmann et al., 2008).

In OOA, some additional input data layer can be integrated with image for effective extraction of information. For building extraction, a DSM is widely used with VHRS image as it contains the information regarding the height of building, which can help to differentiate buildings from the ground objects like roads, parking areas and bare grounds. OOA method is used for detecting urban building in Aubrecht et al. (2009) . This study uses a four channel pan sharpened Ikonos image along with ALS elevation data. The mean height of each segments derived from ALS data was helpful to separate the objects like building having certain height above the ground.

OOA technique is used for studying urban social vulnerability assessment in Ebert et al. (2009). In this study, Quickbird image and a laser derived DSM is used for extraction of urban buildings which are further used for vulnerability assessment. A DTM and nDSM is generated from LIDAR DSM. The nDSM was used to identify the buildings of certain height from the ground level in the segmented image and finally to classify the segments as building.

A VHRS images with ALS DSM data is used for building extraction in an urban area in Jiang et al. (2008) . Multiresolution segmentation approach is used for image segmentation and the image objects are classified on the basis of various feature characteristics. The height of the buildings is considered as the most useful information and hence nDSM is used to extract higher objects. The trees are also included in classification as they also have certain height. The NDVI is used to distinguishing trees and buildings, and finally the building information is extracted. There are some similar approaches found in literature in which VHRS images in combination with ALS elevation data are used to extract the urban features, and land cover classification, especially buildings (Chen et al., 2009; Syed et al., 2005; Teo and Chen, 2004). The inner complexity of the urban area is considered and the hierarchical image classification approach is used to extract buildings. Moreover a new spectral index called SSI (spectral shape index) is introduced in (Chen et al., 2009) which is quite effective to separate dark features like building shadows and water in urban area.

Some researchers have extracted urban building by OOA technique without using DSM data also. A Quickbird image was used for OOA to extract urban features for making a building inventory of Bangkok city in (Dutta and Serker, 2005). Multi level segmentation approach was used to detect different urban object in appropriate size and the segments are classified in a hierarchical scheme. Fuzzy membership function is applied to utilize different shape, size and spectral feature characteristics for building detection. In another study, a VHR orthoimage is used to extract the very dense urban slum dwellings and population living in it is estimated (Aminipouri et al., 2009). Chessboard segmentation is applied first to reduce the area of the interest and then multiresolution segmentation is used for efficient and meaningful segmentation of the image to carry out classification of buildings. Fuzzy membership and nearest neighbour classification are applied for extraction of different types of roof structures based on colour, shape, size, texture and context.

OOA technique has been used for some different types of mapping. A VHRS image Ikonos is integrated with ALS elevation data and used for urban landcover classification in Kressler and Steinnocher (2006). The extracted residential buildings by hierarchical classification approach are used in estimation of the population living on those buildings and finally a dassymetric mapping is done. Another study is carried out to identify the elements in an informal settlement of an urban area which are at risk of flooding (Shamaoma, 2005). Quickbird image and LIDAR elevation data is used for building extraction. The nDSM and Quickbird imagery are segmented by using multilevel segmentation approach and buildings are extracted along with other information. These buildings were classified on the basis of height to assess and model the risk of flooding in the dense urban informal settlements area.

Multi-scale segmentation in combination of subsequent contextual analysis is the real strength of OOA. The spatial, spectral, and contextual properties of the segments at different spatial scale level are used for creating rules which are used further for subsequent classification (Sliuzas et al., 2008). It indicates that the accuracy of the classification is normally dependent on the segments. The usefulness of a segment depends on the resemblance of the segment with the actual object i.e. the shape and size of the image segment should be similar to the natural boundary of the object (Tian and Chen, 2007). In case of building extraction in dense urban area from VHRS images, only the spectral, spatial and contextual properties are not sufficient to identify the building. Because of low spectral and high spatial resolution, buildings have very high within-class spectral variation. Moreover, the buildings in a dense urban area of a developing country generally do not have uniform shape, size, colour texture and pattern.

One of the main characteristic in all building is the height; however it varies among different building. The height of the building is depicted in DSM. In OOA, the height can be used for segmentation and classification of the image segments. Most of the study mentioned above used LIDAR DSM. LIDAR DSM offers certain advantages over photogrammetric DSM, since measurements are denser and more accurate. Surface discontinuities like building walls are represented better in LIDAR DSM which allows the easier detection of regular surfaces, e.g., planar faces on building roofs (Baltsavias, 1999). In contrast, the photogrammetric DSM suffers from many problems such as the areas occluded behind a tall building, the gaps between the buildings, and narrow streets cannot be matched which results an inaccurate DSM. Furthermore, the wall of the buildings cannot be modelled accurately because of the interpolation and oversmoothed DSM near the foot of buildings.

The application of photogrammetric DSM is not widely seen in the previous works. The positives strengths which support and challenges which restrict the photogrammetric DSM in the building extraction process in OOA are not explored. This research is carried out to extract urban buildings by using the photogrammetric DSM. In this sense, this research differs with the above mentioned studies and tries to investigate the possibilities of using photogrammetric DSM alongwith spectral, spatial and contextual information for building extraction in an urban area.

4.6. Method adopted

The overall methodology is shown in fig 4-2. First, the orthoimage is visually interpreted and analysed by using different interpretation elements. It provides a general overview of the image. Then the image segmentation was done in the software Definiens Developer 7. The image objects and their feature properties along with nDSM are used for building extraction. The method is briefly discussed in the following sub sections.

4.6.1. Visual Image interpretation

Visual interpretation is important to get an insight of an image, feature properties and their relationships which are useful for further analysis and supports building extraction from orthoimage.

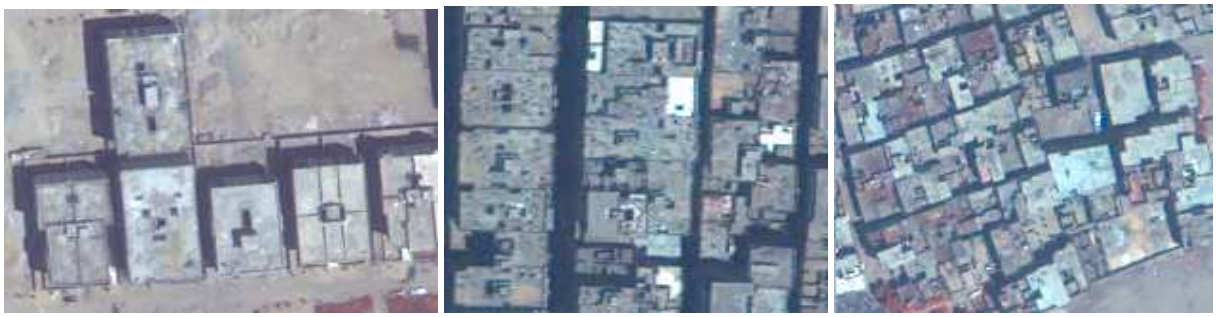

Figure 4-1: Overview of study site 1 (left), 2 (middle) and 3 (right)

A visual image interpretation was carried out. The pattern of buildings in the image can be classified in three basic categories: single buildings, regularly spaced dense buildings and irregularly spaced dense buildings. Therefore, three different study sites were identified. Study site 1 comprises single and sparse buildings; study site 2 contains dense but regular buildings whereas the study site 3 contains dense and irregular buildings. Figure 4-1 shows an overview of 3 study sites, the detailed study site is given in figure 2-2 in section 2.2.5.

Considering the complexity of the study sites, it is decided to extract the individual buildings from study site 1 whereas the building blocks from study sites 2 and 3. In study site 1, single buildings can be identified and described clearly. They have certain shape size and relationship with their surroundings. In case of the study site 2 and 3, the buildings are grouped and connected to each other in such a way that the building boundaries can not be identified clearly. The shape and boundary of the individual building can not be judged even by the human eye-brain system. Therefore, in study site 2 and 3, building blocks are extracted.

The findings of visual image interpretation in 3 different study sites are summarized in table 4-1.

Table 4-1: Visual image interpretation

Interpretation element	Observation from image Study site 1	Observation from image Study site 2	Observation from image Study site 3
Shape	Mostly rectangular	Mostly rectangular	Mixed
Size	medium, varying from 10–600 sq. meter	Medium, large	Small, medium, large
Height	Mostly homogeneous, varies from 7-18 m	Roughly 3–40m, homogeneous in a group (from stereo)	Roughly 3–20 m, varies abruptly (from stereo)
Association	Single house, mostly fenced, surrounded by bare ground and /or vegetation	Mostly clustered building blocks, surrounded by other buildings, narrow roads or streets	Mostly buildings connected to each other, surrounded by narrow roads ,streets and other building,
Shadow	Clear shadow in north and west,	Shadow of taller building in shorter building,	Shadow of taller building in shorter building,
Texture	Rough texture on the roof	texture on the roof is highly rough	Texture on the roof is highly rough and difficult to discriminate from open area
Tone	Most are Grey/brownish, few are dark and few are bright	Most are Grey/brownish, few are dark and few are bright, variation is high	Most are Grey/brownish, few are dark and few are bright, variation is very high
Pattern	Linearly arranged, single buildings separated by certain distance	Group of building, mostly regularly spread along roads and composed in block	Connected to each other, irregularly situated and mixed haphazardly

4.6.2. Segmentation

Definiens Developer 7 (Definiens, 2007) is used for image segmentation and building extraction. It embeds seven different types of segmentation algorithms (Definiens). Brief review of Multiresolution segmentation and chessboard segmentation is made as these two segmentation types are used for this study.

4.6.2.1. Multi resolution segmentation

Multi resolution segmentation is based on a bottom up region based segmentation algorithm. It starts from a single seed pixel and the seed grows by pair-wise merging the similar segments in its neighbourhood to form a bigger segment. The merging decision depends on a homogeneity criterion, which describes the similarity among adjacent segments. The pair of image objects, having small increment and within the user-defined threshold of the homogeneity criterion is merged. The process continues until it finds the image objects fulfilling the defined criteria and terminates when the increment on homogeneity exceeds the threshold (Benz et al., 2004; Tian and Chen, 2007). In multi resolution segmentation, the homogeneity criteria are defined on the basis of three parameters: scale, colour and shape (figure 4-3). Scale parameter is used to determine the maximum allowed heterogeneity in image objects throughout the segmentation process (Benz et al., 2004).

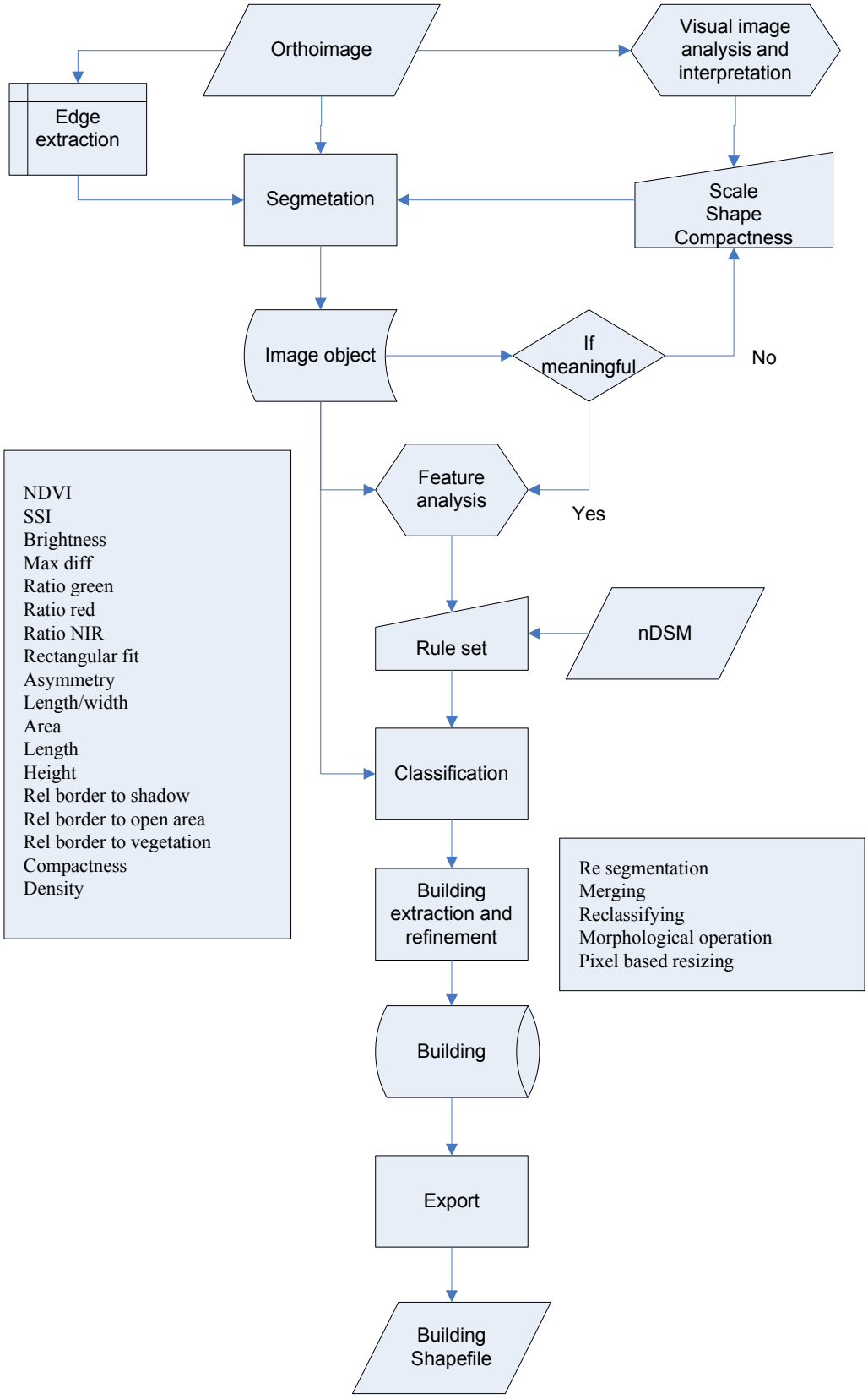

Figure 4-2: Schematic diagram for building extraction

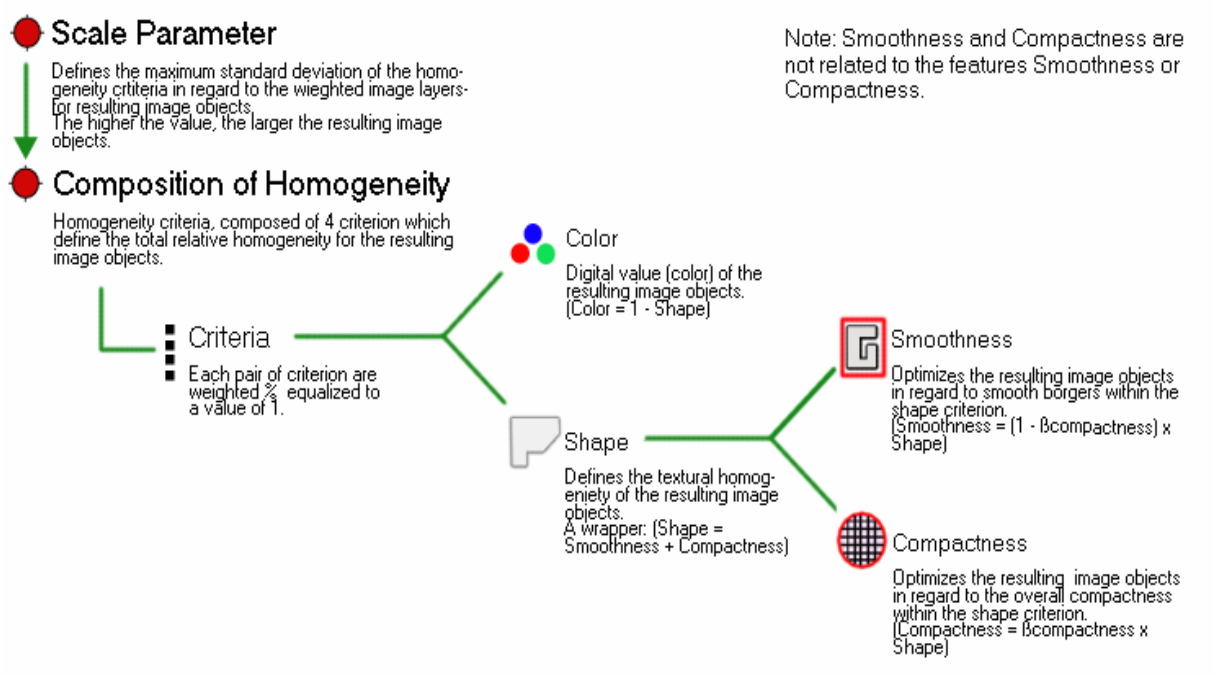

Figure 4-3: Multiresolution segmentation, concept flow diagram (Definiens, 2007)

The scale parameter determines the average size of image object. Higher scale parameter results bigger image objects in size but less in numbers, and vice versa.

The homogeneity criterion further depends on a combination of colour or the spectral value and shape properties. If the colour homogeneity is w_1, the shape homogeneity will be $1-w_1$. It means, higher the spectral criteria, lesser the influence of shape in image object formation and vice versa.

The shape criteria are further split in smoothness and compactness. Smoothness influence the resulting image objects by making their boundary smoother whereas the compactness determines how compact will be the image objects. Compactness is relation between boundary length l of the object and the square root of the number n of the pixels ($l/\sqrt{n}$) of the object. Smoothness is relation between boundary length l of the object and the perimeter of the bounding box of the object (l/b). Smoothness and Compactness together determine the shape homogeneity, i.e. if the compactness is w_2, then the smoothness will be $1-w_2$. The shape and size of the image object can be adjusted applying different combination of scale, colour and shape (compactness, smoothness) parameters.

4.6.2.2. Chessboard segmentation

Chessboard segmentation is based on the top down region splitting principle and splits the pixel domain or an image object domain into square image objects. User can control the size of chessboard tile by applying certain number which represents the number of pixel. For instance, chessboard segmentation by size 5 implies the chessboard tile size of 5 by 5 pixels.

Chessboard segmentation is simple and fast. It is used mainly when the whole area is to be split in some specific tiles and only certain tiles are used for further analysis. It reduces the area of interest efficiently. It can also be used in the refinement of the shape and size of extracted objects.

4.6.3. Feature property analysis

By using the clues obtained from visual image interpretation and prior information on the features and their semantics, we can develop knowledge about the image and the objects in it. This knowledge helps to analyse and identify useful feature properties for object extraction. The example is shown in table 4-2.

Table 4-2: Feature property analysis of the image objects.

Observation from image	Semantics/Knowledge	Features property
Most of the buildings are Grey/ brownish, few are dark and few are bright	Building roof are made of different materials such as asphalt, concrete, brick, cement or metal and therefore are varying in tone.	Different spectral properties like colour, brightness
Mostly, rectangular, few are irregular and mixed shape	Residential building are normally rectangular with regular length and width, some building may be irregular in shape	Rectangular fit, Asymmetry Length/width
Most of the buildings are small and medium, a few are large in size	In the Residential area, normally the buildings are small and medium size, in commercial area they are large, in informal settlement, they are irregular	Area Length
Buildings are associated with shadow in north west direction	Buildings have certain height, they cast shadow and share boundary with shadow, which is in opposite to sun	Height of the building Relative border to shadow
Building are mostly single, separated by certain distance in sparse area	Single building, surrounded by shadow in north and west and by bare ground/ asphalt / concrete / vegetation in south and east	Rel. border to shadow Rel. border to open area Rel.border to vegetation
Sharp edges and outline in north-west, but fuzzy outline in south	Building outline in north and west shares boundary with shadow and have a large gray value change, gray value difference is less in south /east	Edge of building
Same building roof has varying colour	Building may be made in parts, in different time with different material	Spectral variability within same object
Buildings are not similar in colour	Different building made in different time, uses different construction material	Spectral variability within same class
Some buildings are similar with road and/or bare ground	Most of the land is covered with sand. So building roof made of sand, bare ground and unpaved road could be similar in colour.	Spectral similarity among different class

4.6.4. Complexity of the urban OOA

Normally, the buildings are made of different materials, such as concrete, bricks, sand, metal, synthetic materials, bitumen, tiles, mud and so forth. The spectral characteristics of buildings may have major overlap with parking area, road and other open surfaces since they may be made of the same materials. Some of the buildings may contain several parts made by different construction material during various time periods. Hence the single building may have different spectral properties from these different parts. Figure 4-4 shows, the different spectral property of a single building within circle 1, similar spectral properties of different buildings and the different objects, building, road and bare ground (Annex 7). The buildings, in such situation, cannot be separated only

on the basis of spectral information. Similarly, the buildings may have different irregular shape, size and other properties which can be similar to other objects and cannot be differentiated. Therefore the buildings are extracted by integrating spectral (e.g. colour), contextual (e.g. shadow) and spatial (e.g. shape) information. This multiple information can be embedded to formulate a ruleset and a fuzzy membership function can be applied to classify the image object. Spatial and contextual information provides an additional help along with spectral information to discriminate buildings from the other land cover/ use classes.

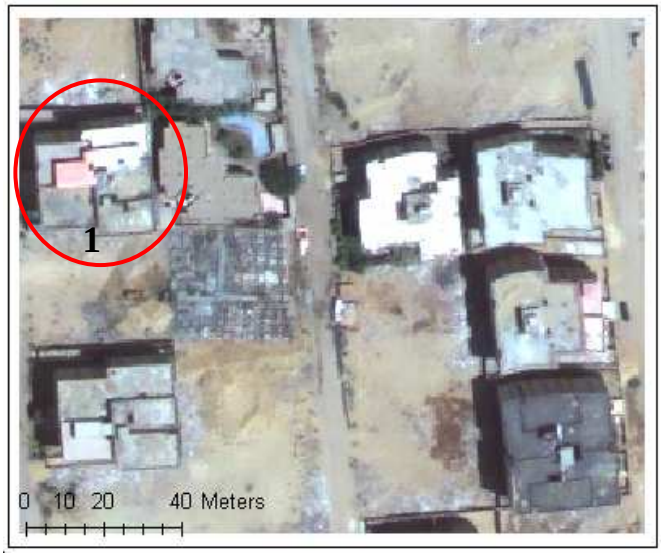

Figure 4-4: Spectral properties of different objects

In a dense and highly crowded urban area, like Cairo, the extent of the problem is more severe. The buildings are generally not as regular and homogeneous as we understand them semantically. The height difference is abrupt and structure is irregular. Top surface of the objects is covered with the dust which restricts the spectral properties of individual object. Buildings are clustered, connected to each other, streets and roads are narrow, open spaces and vegetations are less. Because of the height of buildings and viewing angle of satellite, there are large shadow and occlusion. These all problems make the image analysis and extraction of building difficult. Application of information like spectral, spatial and contextual may not fully help.

4.6.5. Application of DSM

In a complex urban environment, as mentioned in 4.6.4, a DSM can help to extract the buildings. All the objects which have similar characteristics like building are generally ground objects. Buildings are normally taller than these ground objects. So applying a height threshold, the buildings can be separated from other objects. There are some other taller objects apart from buildings in urban areas, such as trees, flyovers, bridges etc. These objects can easily be differentiated from buildings by using spectral, spatial and contextual information. For example, trees have higher NDVI value than any of the other objects.

In this research, the DSM used in OOA is a photogrammetric DSM which is not as accurate as the LIDAR DSM. In this DSM, the vertical wall and the edges of the buildings are not preserved and the gaps between the buildings are not modelled. Figure 4-5 shows the problem of photogrammetric DSM which is not matching with the building. The outlines of the buildings are drawn to show that the DSM area which lie outside the building area and can erroneously classify the bare ground areas

as building if we only consider height as the deciding factor for classification. Therefore the application of spectral, spatial and contextual information in combination of DSM is important.

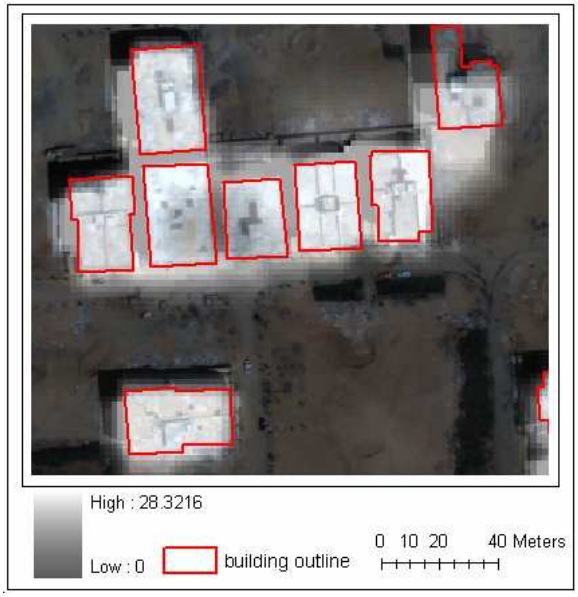

Figure 4-5: Photogrammetric DSM overlaid on top of the building in orthoimage

4.6.6. Applying knowledge to create rulesets

The visual image interpretation, feature property analysis, complexity of urban area and available DSM, and semantics of the area helps to construct a knowledge base for extraction of the buildings. Since, the objective is to extract the building, we use an approach to separate out the other objects/class and remain with buildings only.

Firstly, the distinct objects in the image, which can be extracted easily by using spectral properties, are separated. Vegetations in the image have very high *NDVI* value in comparison to any other objects. Hence by applying a threshold vegetation can be separated clearly. The shadow and water are the other elements, which can be separated by spectral properties. The shadow was extracted by using an index, *spectral shape index* (SSI), which is found very effective to classify shadows in VHRS images (Chen et al., 2009) and water was classified by using the spectral property of water (high absorption of the blue radiation).

The other objects in the image have the complex mesh up in their spectral, spatial and contextual properties. Hence we need to apply them in combination of each other. The approach is now to extract building and leave out other as unclassified image objects.

The nDSM was used to differentiate the taller objects in the image first. Because the trees were already extracted, the main elevated objects remaining are buildings. Buildings are normally taller than 3 m. So applying this threshold, the building areas can be approximately separated. Because the nDSM is not accurate enough and do not model the buildings only (figure 4-5), the bare ground areas around the buildings are also classified as buildings. Similarly, because of the other uncertainties in the nDSM, some bare ground/road areas can be classified as building whereas some buildings may not be extracted well and classified as ground. In this situation, the extracted building class is considered as the temporary class and the image objects contained in this class are further investigated for separating the actual building and other erroneously extracted bare ground objects. Several spatial properties like area, length, asymmetry, rectangular fit, and spectral characteristics

like standard deviation of pixels values, maximum difference of neighboring gray values, and ratio of different bands are used to differentiate building objects from remaining other objects. Similarly contextual properties like relative border with shadow, building or unclassified objects or a combination of these properties are also used. On the other hand, the buildings, remained unclassified can also be classified by using the similar approach of utilizing spatial, spectral and contextual information or a combination of these properties.

The schematic diagram of the approach for developing rulesets and extracting building is shown in figure 4-6.

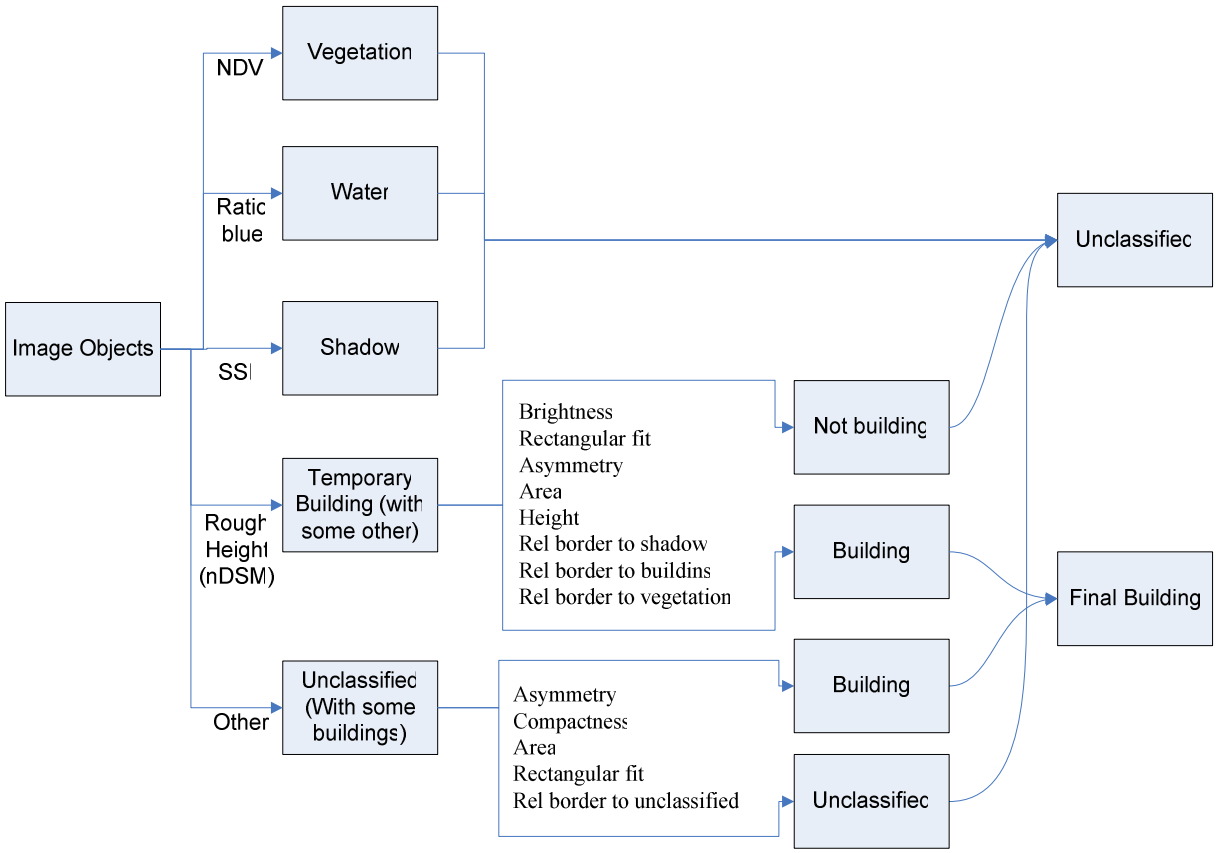

Figure 4-6: Approach adopted for building extraction

4.6.7. Building refinement

All extracted buildings may not be in smooth shape and therefore refinement is needed. The chessboard segmentation is applied to divide the image in small grids and morphological operations, pixel based reshaping, merging etc operations are applied to get the buildings in final smooth shape.

4.6.8. Accuracy assessment

Building outlines extracted by manual digitization on the orthoimage are used as reference dataset. The extracted buildings by OOA are compared with reference dataset for accuracy assessment. Mainly three approaches of accuracy assessments are used, each are described as following:

4.6.8.1. Object based approach

In this approach, the individual building objects were taken into account. Total number of building in reference data of study site was compared with the number of extracted buildings by OOA. Then the

number of correctly extracted, missed and wrongly extracted buildings was identified. On the basis of this statistics, percentage of building extraction, completeness and correctness of building extraction was calculated. This approach was used for assessing the quality of individual buildings detection in study site 1.

4.6.8.2. Position based approach

In this approach, the positional accuracy of the extracted building was considered. The centroids of the building extracted by OOA and the reference buildings were compared. The positional displacement of each individual building was calculated and the statistical measures like minimum, maximum mean and standard deviation in displacement was assessed. This approach was also used only for the individual buildings.

4.6.8.3. Area based approach

In this approach, the extracted building area was compared with the reference building area and several accuracy measures were calculated. In figure 4-7, if ABCD is a reference and PQRS is extracted buildings, then the following three types of area can be defined for accuracy assessment:

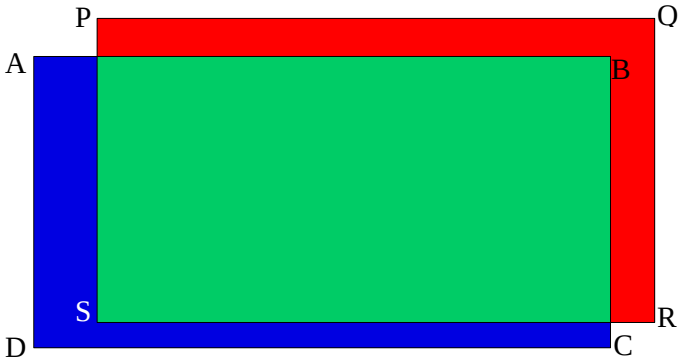

Figure 4-7: Accuracy assessment method

True Positive (TP) is the area which is present in both, the extracted and the reference building, in figure, the area in green is TP. False Positive (FP) is the area which is present in the reference building but not in the extracted building. The area in blue is FP in the figure. False Negative (FN) is the area which is present in the extracted building but not in the reference building, in figure, the area in red is FN.

From these three types of area, the following quality measures were calculated

Split factor (SF) or branching factor = $\frac{TP}{FP}$

Missing factor (MF) = $\frac{FN}{TP}$

Percent of building extraction = $\frac{TP}{TP+FN}\times 100$

The accuracy measures were also expressed in other way round as follows:

Correctness = $\frac{TP}{TP+FP}$

Completeness = $\frac{TP}{TP+FN}$

Correctness is a measure which indicates the correct detection rate with respect to the reference building and ranges from 0 to 1 or can be shown in percentage. The converse of correctness is error of commission. The sum of correctness and error of commission is 1. Similarly, completeness is a measure which indicates how complete the extracted buildings are. It is the converse of error of omission and the sum of completeness and error of omission is 1.

4.7. Implementation, Results and Discussion

This section deals with the implementation of the OOA methods, the results and discussion simultaneously.

4.7.1. Study site 1: Area with sparse buildings

4.7.1.1. Image segmentation

As the buildings in the image are spectrally different and not homogeneous in shape, size and other characteristics (see section 4.6.1), there was no such set of parameters which was equally applicable to get best fitting segments for all building in the study area. However, a set of parameter, which fits approximately for the extraction of certain object in a particular image, can be judged by trial and error method. It should be kept in mind that the image should not be over or undersegmented. The oversegmentation can be fixed in successive steps by merging the segments having similar properties, but undersegmentation may cause more difficulty in fixing later. Some results of segmentation with different parameters are shown in figure 4-8. The image is little bit oversegmented in fig 4-8 left, slightly undersegmented in middle, and a serious under segmentation in right. Based on these experiments a comparatively more suitable set was found as scale: 50 shape: 0.6 and compactness: 0.8.

In the image, the colour of many buildings is not unique and similar to its surrounding whereas the shape is more prominent. Therefore the shape value was given higher priority over colour. Similarly, we need a compact building boundary rather than a fragile and zigzag area; hence we used a high value of compactness. Regarding the scale, although the scale parameter 50 gave slightly over segmented image, but it addresses most of the buildings well in comparison of higher scale values. The scale parameter 75 and 100 gave some building undersegmented (see figure 4-8, middle, right) which was not optimal case of further extraction process.

Figure 4-8: Segmentation with scale, shape and compactness 50, 0.6, 0.8 (left), 75, 0.5, 0.7 (middle) and 100, 0.7, 0.9 (right)

nDSM was not used for image segmentation, as the outlines do not matches with the building outlines. This problem can influence the segmentation process which further creates problem in extracting the accurate buildings.

4.7.1.2. Building extraction without DSM

The approach shown in fig 4-6 was adopted to extract the building. First, vegetation was separated by using *NDVI*, then shadow was extracted by using *SSI* and water was extracted by using *ratio blue*. The rest of the objects like bare ground, car park, unpaved roads and buildings have generally the similar spectral characteristics and were not further classified individually but considered as either building or not building areas. Finally, the buildings are placed in a class and all other objects are remained as unclassified.

To separate buildings, several experiments were carried out. Without using a DSM, it was found difficult. The spectral similarity among buildings and others objects, and spectral variability among building was discussed already. Still the experiment was carried out by using different spectral (*ratio green, ratio blue, max. diff, standard deviations*), spatial (*asymmetry, length/width, compactness, area, length, rectangular fit*) and contextual (*relative border to shadow, building, unclassified*) properties. The buildings extracted by this method are not much satisfactory (figure 4-9, right). Result shows, some of the buildings were not extracted and some of the non building areas were extracted as buildings.

The main problem was noted on the southern edges of the building where there was not much contrast between building and surrounding. The colour of the building is similar to the bare ground and roads around the building. Shape couldn't discriminate the segments either. The clear context like the association of shadow was not there because the direction and incident angle of the sun.

The poor segmentation in the southern part of building due to the lack of clear spectral differentiation and/or shape is one of the reasons. The quality of segments in southern edge can be compared visually with the other part of building (figure 4-8).

To solve this problem, some other experiments were done. Building edges were extracted from image by using Canny's operator and used for segmentation as an extra input layer. In multiresolution segmentation, the extracted edges were used as an input layer along with the other image layers with equal weight. But the edges couldn't support the segmentation process and couldnot improve the result because the edges were very weak on the southern part of the building (figure 4-9, middle). Similarly a disparity image (prepared by dense matching and having information on the difference of y- parallax, and represent height difference on the image, defined in chapter 3) (figure 4-10, left) of the same area was also used for segmentation and classification of the image. It also suffered from problem as the image was not matched well on the southern part and there was much disturbances and noises in the form of black and white areas (figure 4-10, right). This problem led the disparity map not preserved the edges well and couldnot support segmentation and classification (figure 4-10 middle, right).

Application of context is useful to separate objects and was used to extract the building by using the context of shadow. In the areas with tall building and their large shadow on other shorter building influence the classification process.

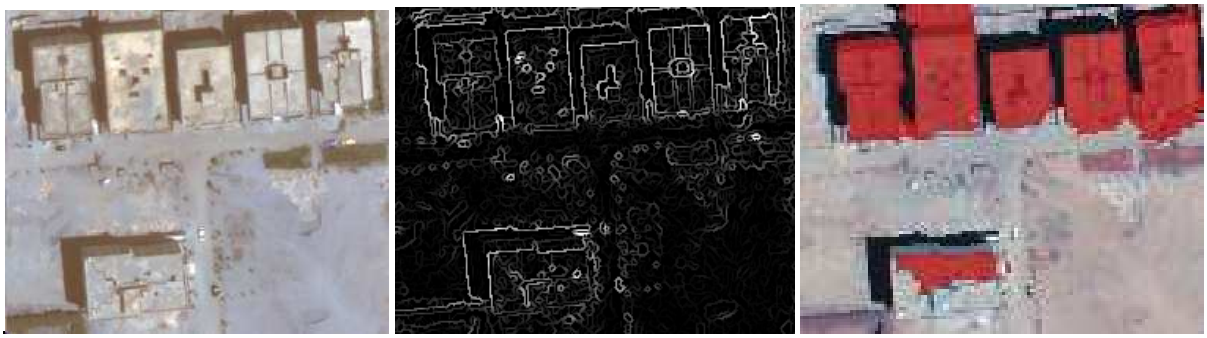

Figure 4-9: Extracting building without DSM, problem in lower (southern) edge, orthoimage (left), extracted edge (middle) and classified buildings (right)

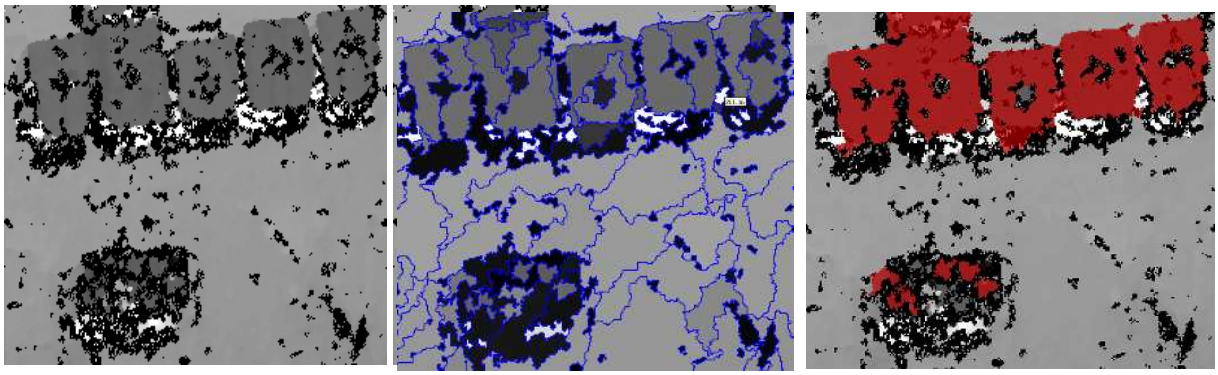

Figure 4-10: Extracting building with disparity map, disparity map (left), segmentation (middle) and classified buildings (right)

4.7.1.3. Building extraction with DSM

The nDSM was used for classification of image segments. It was not used for segmentation because the building outlines were not preserved in nDSM which can influence the segmentation result. The other approach for building extraction was similar as mentioned in figure 4-6 and explained in the section 4.6.6. First, *NDVI, SSI* and *ratio blue* are used to separate vegetation, shadow and water. Then the nDSM was used with a height threshold of 3.5m to separate building. The result of applying this height threshold is shown in figure 4-11 (right). Most of the building areas were separated from bare ground/ roads. At the same time, because of the error in nDSM, some of the ground areas near the building were classified as building (see the areas in rectangle) and some of the building areas (see the circle) remained unclassified.

Figure 4-11: Application of photogrammetric nDSM in building extraction

To deal with this problem, spatial properties of the segments (asymmetry, length/width, compactness, area, length, rectangular fit) and contextual information (relative border to shadow, building, unclassified) were used in the similar way as illustrated in figure 4-6 and mentioned in

section 4.6.6. Finally, all other classes except building were merged together to unclassified leaving out building only. The experiment was repeated by using both set of nDSM, from LPS and SAT-PP. The result is shown in figure 4-12.

The result shows much improvement over building extracted without DSM. Still the both set of extracted buildings were not identical (compare figure 4-12, left and right), although the same parameters of segmentation and similar approach for building extraction were used. The only difference was the height threshold used for building separation. This is because the quality of nDSM from LPS and SAT-PP was different and both do not have identical gray value to represent height of building and nDSM did not exactly match with building outline. Further, both sets of nDSM are slightly different in shape, size and height values. This effect of nDSm led to slight changes in the rulesets and adjustment with height threshold.

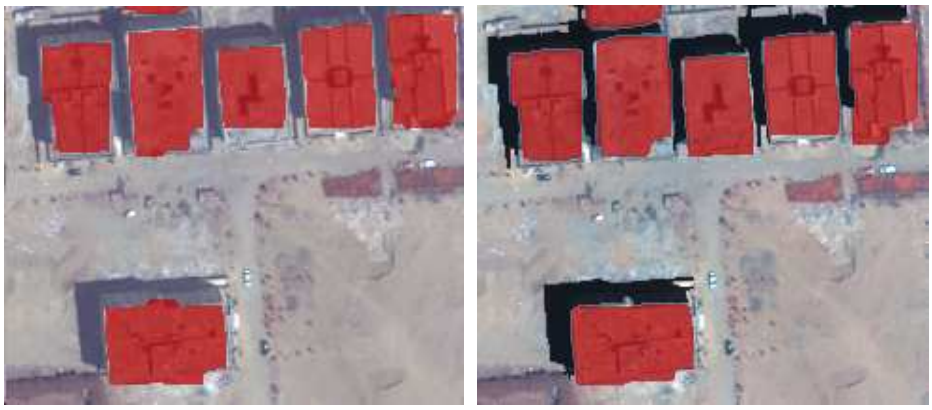

Figure 4-12: Extracted building by using nDSM from LPS (left), SAT-PP (right)

Overall result of building extraction by OOA technique is satisfactory (figure 4-13). In spite of the problems in nDSM, the spectral, spatial and contextual information can be used to extract individual building. The application of photogrammetric nDSM is useful to separate most of the ground objects from taller object in such areas where spectral, spatial and contextual characteristics do not support the classification process.

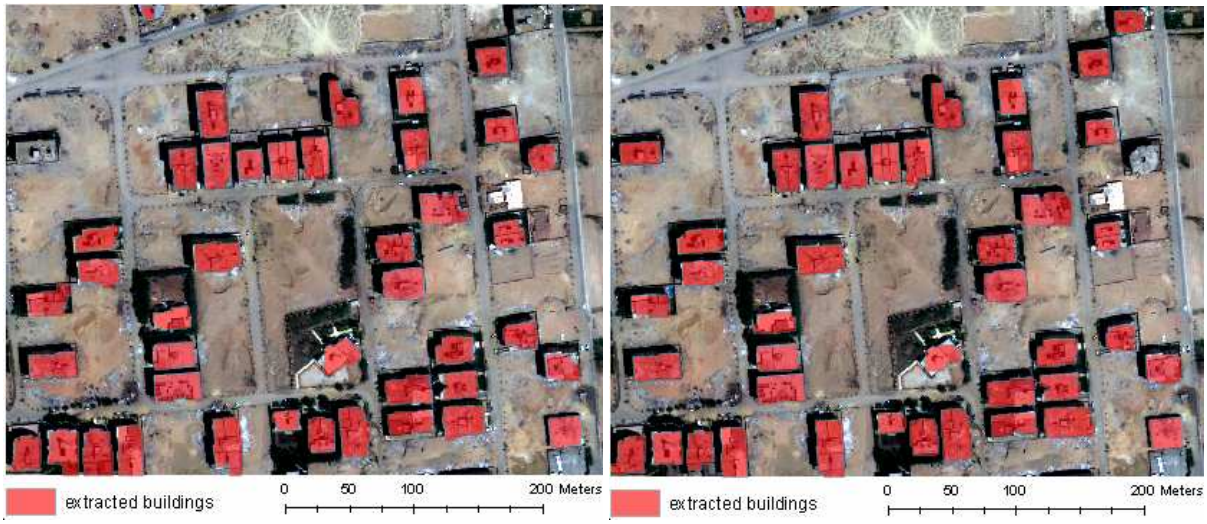

Figure 4-13: Extracted buildings in study site 1 by using nDSM from LPS (left) and SAT-PP (right)

4.7.2. Study site 2: Area with dense regular buildings

This study site contains clustered buildings and building block with more or less regular linear pattern although they are varying in terms of height. Our main objective is to extract the building blocks. The

same segmentation parameters, as used in study site 1, (scale 50, shape 0.6 and compactness 0.8) were used. The result of segmentation is shown in figure 4-14.

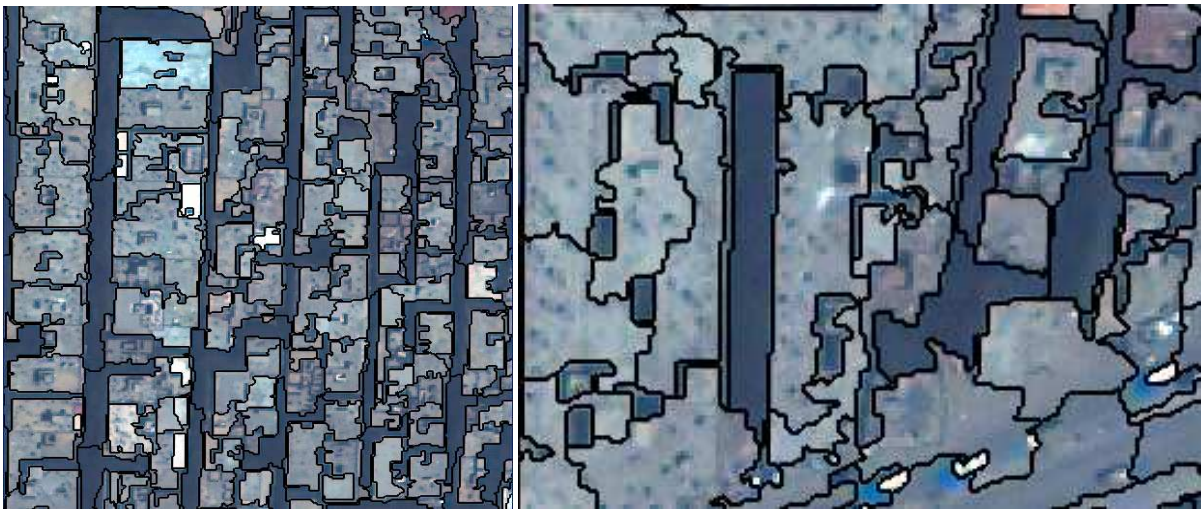

Figure 4-14: Image segmentation in study area 2, an overview (left) and closer view (right)

The resulting segments were mostly fit to the large buildings, building blocks and small dwellings. Most of the area in the image is covered by the buildings and shadow. Open areas, wider roads and vegetations are less. Some problems were seen in those areas where the boundary between southern part of building and the open area/ road exists. The reasons are already discussed in section 4.7.1.2.

The building extraction approach used in this study site is similar to that used in study site 1. Complexity increased because of the heterogeneous and complex building structure and shadows. The nDSM used in this area was not as accurate as in study area 1 and application was limited to less crowded open areas and wider roads only. The small and narrow open ground in dense area is not represented well in the nDSM. Similar approach with slightly modifying the thresholds as used in study site 1 was applied to extract the building blocks. The final result of building block extraction is shown in figure 4-15.

4.7.3. Study site 3: Area with dense irregular buildings

The study site 3 comprises connected buildings and building block with irregular pattern and abruptly varying height. Objective is to extract the building block rather than individual buildings. The same segmentation parameters, as used in study site 1 and 2; (scale 50, shape 0.6 and compactness 0.8) were used. The result of segmentation was similar to that in study site 2.

This approach is also similar as used in study site 1 and 2. The result shows most of the building blocks were extracted. Some open areas were also extracted as buildings whereas some building blocks were left out. The roads, wide open areas, clear shadow and vegetation are separated well. But the main problems are in the building blocks of dense area (figure 4-16).

The reasons may be the shape and sizes of the buildings along with spectral characteristics are not consistent. Blocks, generally surrounded by wider road/street, are extracted well, but the buildings blocks inside the narrow road mesh are not clearly distinguishable even by human eye-brain system (See figure 4-1, right). They are mainly confused with small open ground. The colour and texture of the buildings are similar to open ground and the pattern is not regular. The taller building has its shadow on the shorter buildings, which makes using the context difficult. The height of the building

and small ground between building network is not well represented in nDSM and it did not help to extract building accurately.

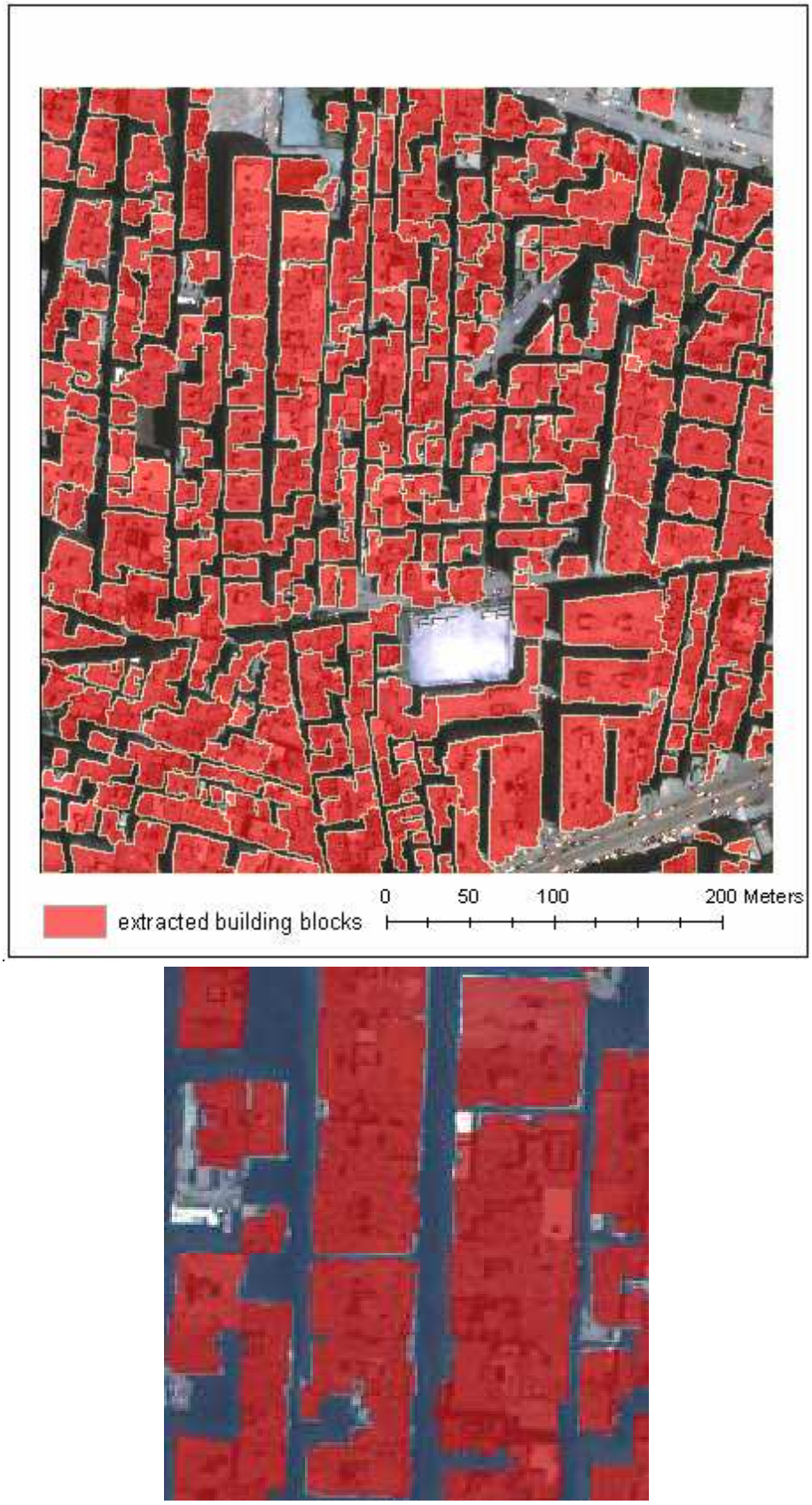

Figure 4-15: The final extracted buildings from study site 2 (top) and zoomed portion (bottom)

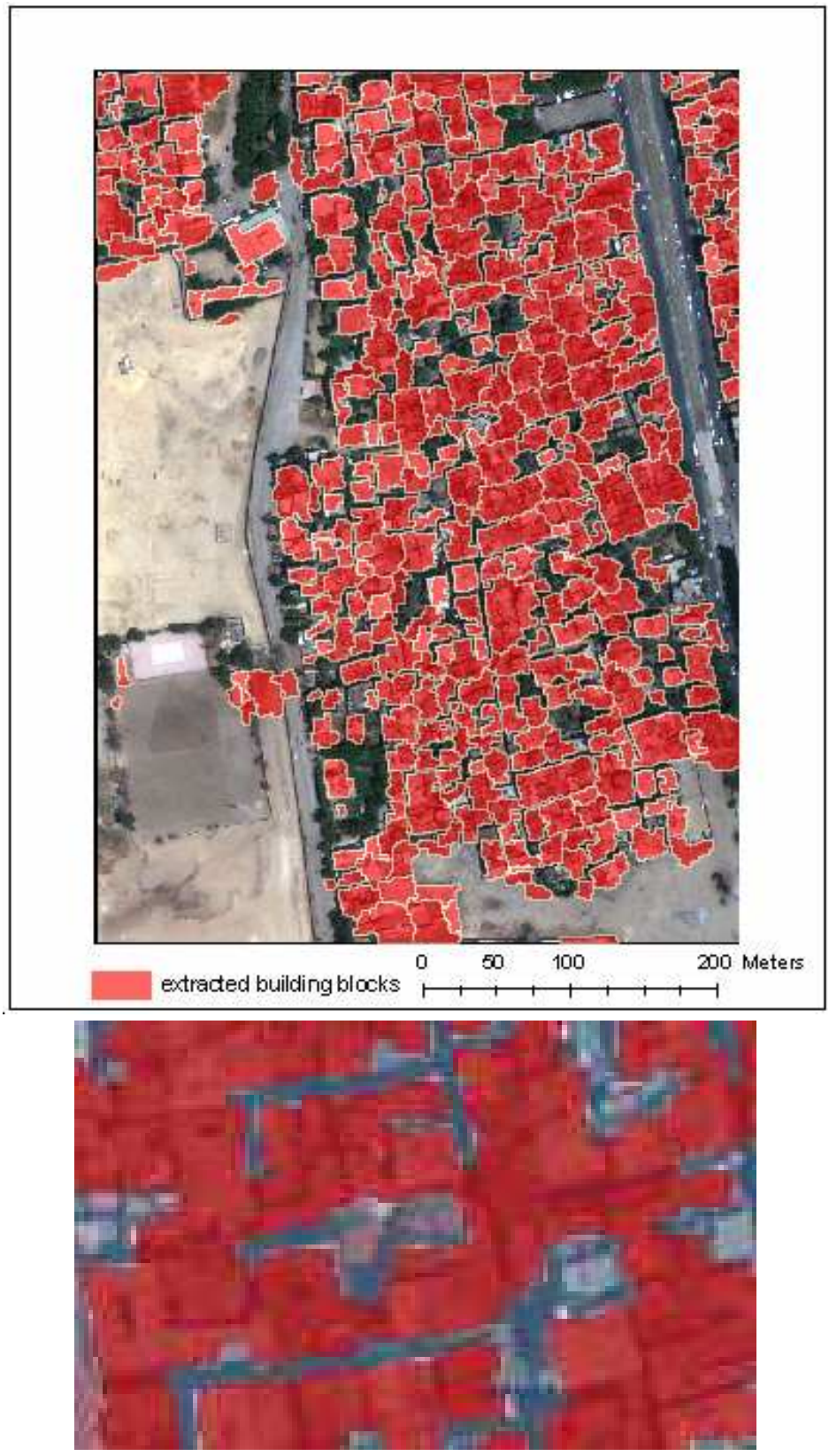

Figure 4-16: Final extracted buildings in study site 3 (top) and zoomed portion (bottom)

4.7.4. Quality assessment

In study site 1, the buildings were extracted individually. The quality of extraction was assessed on the basis of individual object, its location and area covered by the building. In study site 2 and 3, buildings were extracted as the building blocks. Therefore, in those areas, the quality assessment on the basis of the individual building and building position is difficult and only area based quality assessment was performed.

4.7.4.1. The object based approach for study area 1

This approach is based on the number of buildings in the reference image and extracted by OOA technique. The assessment was done on both extraction results, i.e. the extracted buildings by using LPS DSM and SAT-PP DSM. A comparison is shown in table 4-3.

Table 4-3: Object based accuracy assessment of single building detection

Accuracy measure	Building by using LPS DSM	Building by using SAT-PP DSM
Buildings in reference image	44	44
Extracted building	42	43
Extraction percent	95.5	97.7
Completeness	95	98
Correctness	100	100
Error of omission	5	2
Error of commission	0	0

Result shows, the completeness of building extraction is very high. For the extracted buildings using SAT-PP DSM, it is about 98% and for LPS DSM it is around 96%. The correctness is 100% in both cases. For this experiment, a small subset of image containing 44 buildings was taken and it shows a very good result for the subset. Similarly, the result using SAT-PP DSM is better than the result of LPS DSM, which supports the fact that the better the nDSM, higher the quality of building extraction.
This method gives only the overview of building detection quality. It doesn't show how accurately the shape, size, area and position of the buildings are extracted. To deal with these issues, position and area based quality assessments were used.

4.7.4.2. Position based approach for study area 1

In this approach, the accuracy of the extracted buildings was calculated on the basis of position of the building. To calculate this, the building centroid was identified in both, reference and extracted building and the displacement between them was measured. The result is shown in table 4-4.

Table 4-4: Position based accuracy assessment of single building detection

Accuracy measure	Building extracted by using LPS DSM (m)	Building extracted by using SAT-PP DSM (m)
Minimum displacement	0.25	0.29
Maximum displacement	3.58	3.53
Mean displacement	1.26	1.14

The positional displacement between the reference and extracted building is measured for 41 buildings. For the buildings extracted by using LPS DSM, the result shows the majority 51 % of the

buildings are found within the positional error of 1 m, other 32 % has positional error of 1m to 2 m, 12 % has positional error of 2-3 m and 5% has 3-4 m. Similarly, for the buildings extracted by using SAT-PP DSM, 61 % of the buildings are found within the positional error of 1 m, other 27 % has positional error of 1m to 2 m, 10 % has positional error of 2-3 m and 2 % has 3-4 m. The distribution is shown on the figure 4-17.

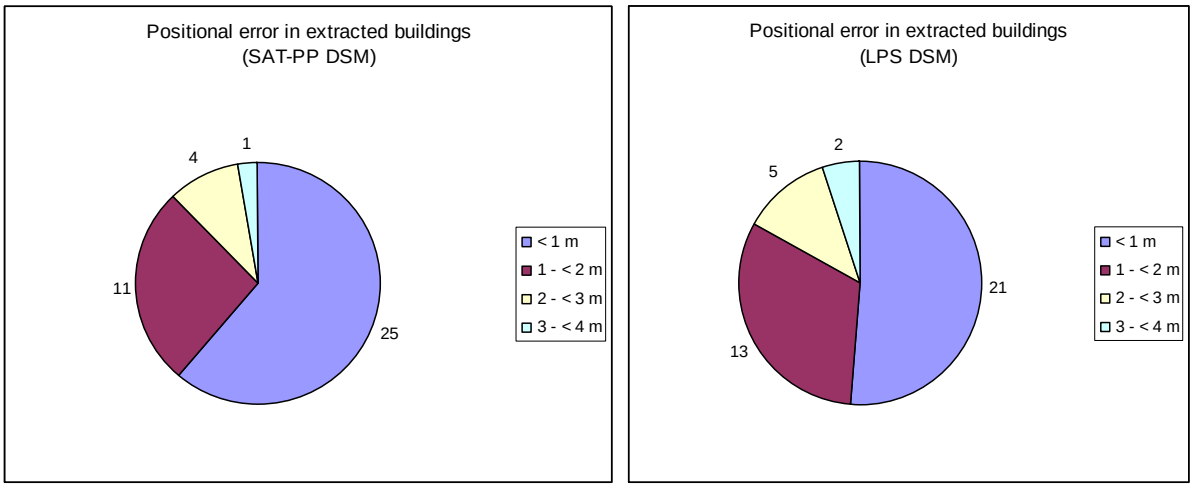

Figure 4-17: Positional error in buildings extracted by using SAT-PP DSM (left) and LPS DSM (right)

4.7.4.3. Area based approach

This approach compares the area of reference and extracted building. The three types of area: TP, FP and FN were identified. Different quality measures such as correctness, completeness, and extraction percentage were calculated. This approach was used for all 3 study areas. The results are shown on the table 4-5. In study site 1, accuracy was assessed by comparing the area of extracted building by using SAT-PP DSM and LPS DSM whereas that of study site 2 and 3 was assessed only from the buildings extracted by using SAT-PP DSM. The error in extraction of building is visualized in figure 4-18 (site 1) and 4-19-top (site 2) and 4-19-bottom (site 3).

Table 4-5: Area based accuracy assessment of building detection in study site 1, 2 and 3

Accuracy measures	Study site 1 (SAT-PPDSM)	Study site 1 (LPS DSM)	Study site 2	Study site 3
Area of reference building (m^2)	25906.87	25906.87	118954.72	110375.04
Area of extracted building (m^2)	26185.20	24392.10	116016.24	111451.34
True positive (TP) (m^2)	23905.88	22768.95	106230.11	94847.40
False positive (FP) (m^2)	2001	3138.04	12724.59	15527.64
False negative (FN) (m^2)	2280.31	1624.16	9786.16	16603.94
Branching factor	0.08	0.14	0.12	0.16
Miss factor	0.09	0.07	0.09	0.17
Building extraction percentage	91.29	93.34	91.56	85.1
Correctness (%)	92	88	89	86
Completeness (%)	91	0.93	0.92	0.85
Error of omission (%)	8	12	11	14
Error of commission (%)	9	7	8	15

In study site 1, the result shows, the accuracy of building extraction using SAT-PP DSM is slightly higher than using LPS DSM. The accuracy of extracted building is slightly dropped down in study site 2 and considerably in study site 3. In study are 2, although the buildings are dense and clustered in a group, they are situated in a regular pattern. The buildings are separated by roads in a regular spacing. Because of homogeneity in a block, they can be identified clearly. Their shadow is also regular and mostly falls on road or streets. These facts about the buildings make it easy to use the contextual and structural characteristics. In study site 3, the buildings are irregularly situated. They do not have any specific and regular pattern. Abrupt change in height results shadows of higher building on a lower one and the context couldn't be used effectively. Because of irregular structures of buildings and similar spectral characteristics, there is a strong confusion between building and open areas. The small open areas between large building blocks are not well represented in DSM. These problems make the extraction of building more difficult and less accurate in study site 3.

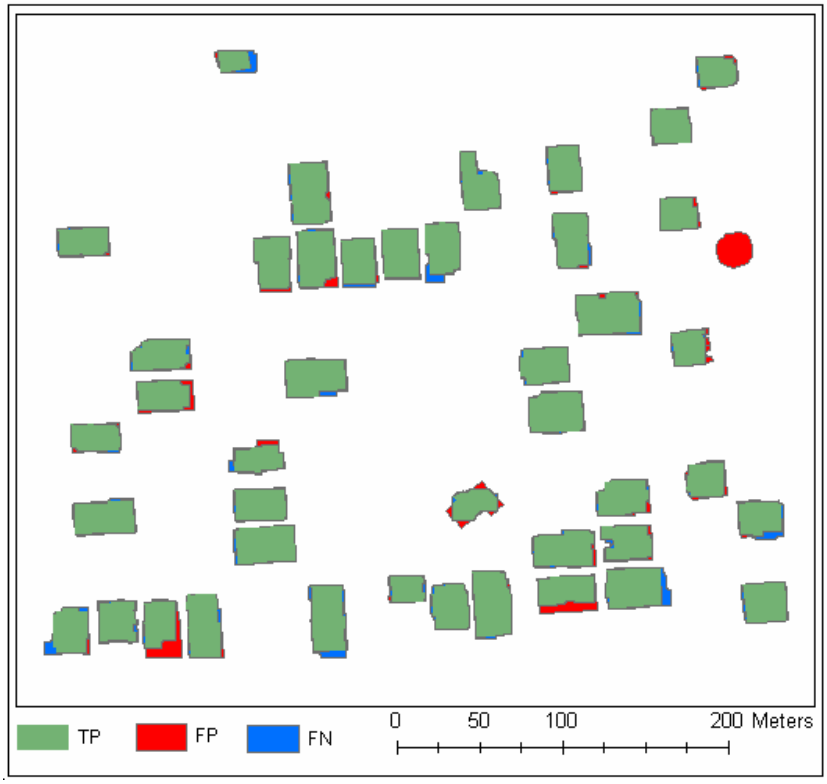

Figure 4-18: Accuracy Assessment of study site 1

Figure 4-19: Error in building extraction in study site 2 (top) and study site 3 (bottom)

4.8. Concluding Remarks

Building extraction in urban area by using OOA technique depends upon the spectral, spatial and contextual information of image objects. A good segmentation of image is always helpful for accurate building extraction; however the quality of extraction does not completely depend upon the initial segmentation. Because of the spectral variability within an object and/or within a class and spectral similarity among different class, the extraction of building is not straightforward in dense urban area in a VHRS image. Furthermore, the shape, size and contextual information are, sometimes, not much useful because of the heterogeneous urban environment. In such a situation, along with the different feature characteristics of image objects, extra input information such as nDSM plays very important role in building extraction. As buildings are taller than ground objects, a certain height threshold separates building from the other objects.

The results show the accurate height information would helpful to extract building. In study site 1, because of the fairly good quality of nDSM, open and sparse area, regular structure of buildings and well identifiable context, building extraction is more accurate. In study site 2, because of the highly crowded and connected settlements, buildings blocks were extracted instead of single building. In this area also, the buildings are regularly placed along wider streets. Well identifiable context of shadow help to extract building block satisfactorily, however the nDSM was not so accurate. Therefore, some of the areas are not extracted very well. Iin study site 3, the nDSM was not accurate enough to separate the buildings from other objects. Similarly, the colour, shape, size, structure, context etc are not sufficiently clear to separate them from other objects especially, small open areas. Therefore, the building blocks cannot be extracted as accurate as in the study sites 1 and 2.

5. DSM Quality Improvement

5.1. Introduction

This chapter is the third phase of the research, which deals with the sub objective 3: To develop an algorithm for improving the quality of DSM by using building outlines extracted by OOA technique. Improving the quality of DSM involves using appropriate methods to fill the gap between existing and expected quality of DSM. The DSM was produced by photogrammetric image matching technique in phase 1 (see chapter 3) and building outlines were extracted by using OOA method (see chapter 4). This chapter deals with combining the results from chapter 3 and 4 to improve the quality of DSM. A 2.5D DSM of individual/block of building with preserved edges and improved shape/size is expected. This chapter starts with a review on DSM improvement and related techniques (Section 5.2), followed by the main issues of improvements (Section 5.3) and method used for DSM improvement (Section 5.4). Implementation and results obtained are discussed in (Section 5.5) and quality assessment in (Section 5.6). Finally, the chapter ends with a concluding remark (Section 5.7).

5.2. DSM Quality Improvement: a review

There are several methods for generating DSM from different data source (see chapter 3). Especially, in this research, we discussed the DSM generation from VHRS stereo image by using image matching technique. Chapter 3 also discussed the problems with different DSM generation techniques and the errors on the produced DSMs. This chapter is mainly focussed on the improvement in quality of building DSM in urban areas.

Many urban applications need accurate DSM which delineates the building edges sharply. In the DSM generated from image matching, this sharpness on the boundary of building is generally not preserved. Similarly the narrow streets and gap between buildings are not represented well in urban DSMs. Because of this reason, the LIDAR DSM is being widely used in urban building modelling. Some researchers used LIDAR DSM for reconstruction of shape of the building and producing a 3D building model from it (Rottensteiner and Briese, 2003) whereas the others used VHRS satellite or aerial images to detect the edges of building and integrate with LIDAR DSM to construct 3D model (Syed et al., 2005). The similar quality like LIDAR DSM cannot be achieved from photogrammetric DSM generated from VHRS stereo image by image matching technique, but it can be improved to achieve a quality which would be comparable to LIDAR DSM and can be used in many applications.

Many researchers have discussed on the quality and accuracy of urban DSM generated by image matching technique from VHRS stereo images. The main concern is about the vertical accuracy (Poon et al., 2005). There are not many studies discussing the shape and positional quality of the generated DSM which is also a big issue in urban modelling. The generated DSM normally is not accurate enough to match exactly with shape and position of the corresponding building. The improvement

processes are targeted to improve the digital surface model in such a way that they have a crisp enough boundary and match with the corresponding buildings as much as possible.

Some approaches have been developed to improve the quality of DSM generated from VHRS stereo image in an urban area. In a recently developed approach, vector and raster data are integrated to develop a more reliable and accurate DSM, which can be used for urban city modelling (Devriendt et al., 2008). In this study, a DSM was generated by image matching in urban area. The stereo image suffers from occlusion, which caused the erroneous DSM on those areas, especially on and near the foot of the building on the ground and in the narrow strips and areas between two tall buildings. So, the building roof boundaries were digitized and added to the stereo image as a break lines. These break lines were used as a restriction for matching algorithm. The 3D vector features, mainly building polygons were integrated with raster DSM to improve the quality of DSM. The unmatched areas because of occlusion were interpolated by the surrounding DSM values. In this method, the building features, which are used for improvement of DSM and create a 3D city model, were extracted manually. This process leads a lot of human interaction and time consumption.

A vector based enhancement of a raw DSM is mentioned in (Scholten et al., 2003). In the research, building contours, extracted from priory available image data source, were used in an automated process to enhance the crude DSM. Later, this improved DSM was successfully used for accurate high resolution orthoimage production.

In above mentioned methods, the vector outlines of the buildings are successfully used for improving the quality of DSM in terms of shape and size although the level of automation is low. Therefore, different programming environment embedded with the image processing software can be used for integration of building outline (vector) and DSM (raster) data for improving the quality of DSM in an automatic way. The objective of this part of study is mainly dedicated in developing an automated technique for improving the quality of DSM by using building outline and DSM and it is discussed in the following sections.

5.3. Issues for DSM improvement

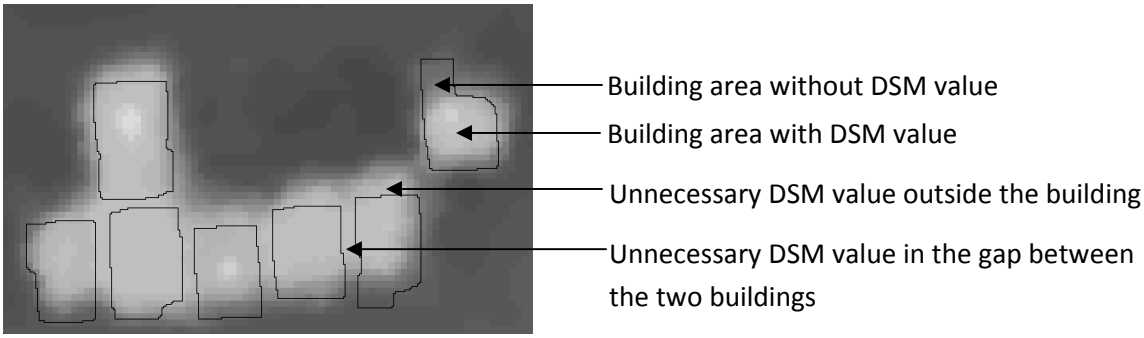

Figure 5-1: Problem in generated DSM and need of improvement

The DSM of urban area cannot preserve the edges of the building correctly. Further, it cannot discriminate the building area and the gap between two buildings and narrow streets. There are unnecessary height values outside the building area and in some regions, no height values in building area (figure 5-1). To improve such DSM, building outlines extracted from orthoimage by OOA technique are used.

In this chapter, mainly two issues are addressed for improving the quality of DSM. The building outlines were extracted from an orthoimage by OOA, which already had some error in the form of

relief displacement (section 3.4.4). Using such building outline in improving the quality of DSM would propagate error in final DSM as well. Therefore, the first issue is, the error due to relief displacement of orthoimage in building outlines is needed to be corrected before using them in DSM quality improvement (figure5-2: d). The second issue is the assignment of height values to the corrected building outline to get an improved DSM. These issues and problems with DSM improvement can be illustrated as following:

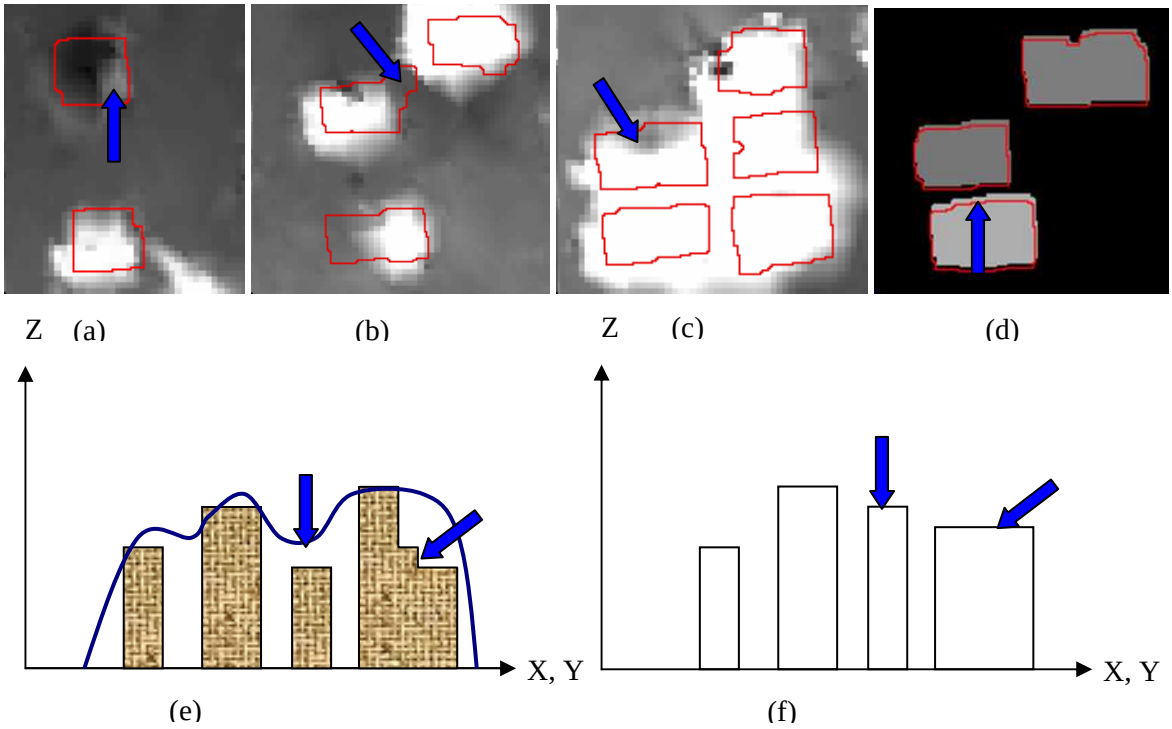

Figure 5-2: Problems in DSM and difference in height between DSM before and after improvement

Figure 5.2 shows mainly the following problems: (a) Missing building elevation values in DSM, (b) erroneous building outline extracted by OOA, (c) different gray values within one building because of stepping multiple height building and high DSM gray values in the gap of buildings (d) Translation for correcting relief displacement, (e) a short building in between two tall building is modelled higher than its actual height in DSM and a building of multiple height (stepped) also represented as oversmoothed bell shaped building. Figure5-2 (f) shows a DSM after improvement, the DSM cannot be improved in case of shorter building in between the two taller building and height is generalized and multiple stepped stories cannot be modelled in the improved DSM.

The nDSM can be used for input source data for height value improvement. The gray values from nDSM can be extracted and applied to the corresponding pixels in the corrected building outlines, but there are several options for applying the gray values in building regions. These can be; same pixel to pixel gray value as in nDSM, or any of the mean, median, maximum, and rank filtered gray value over the building region. The first option, individual pixel to pixel gray values cannot improve the result at all as there are large variation of gray values of the pixels within one building region (figure 5-2: a, b, c). As we wish to improve the DSM in the form of 2.5D DSM having same height value within a building region, we can use any of the mean, median, maximum and rank filtered gray values per building.

Figure 5-2(a) shows a building polygon, overlaid on nDSM, which has gray value only at a small corner inside the building (see arrow). The reason is: error in matching (in DSM) or error in producing nDSM. In such case, if we apply the mean of the gray value within the polygon to the building, the black pixels (zero) values influence (reduce) largely the height of the building in improved DSM, although we can get a homogeneous gray value in the building region. This holds for the case in figure 5-2 (b) and (c) also. If we apply the median gray value in the situation in (a), the result would be worse, because median gives the middle value of the population and in (a) the median would certainly be near zero because of the majority of black pixels. However, median improves the result in (b) and (c) as the majority of the population is near higher gray value.

Applying maximum gray value within the building gives a better result than mean and median but if there would be outliers within nDSM gray values, they can cause exaggeration on the height in resulting improved nDSM. To cope with this problem, a rank filtered gray value from nDSM is introduced and applied to building outline. It filters the certain percentage of highest gray values within the building outline and then out of remaining, the maximum gray value is applied to the building. This process removes the possibility of outlier and exaggeration in improved DSM, but the problem shown in figure 5-2 (e) cannot be solved by any of the method as the shorter building in between two taller building may already get higher gray value from input nDSM.

5.4. Method Adopted

Commercial software Halcon (Halcon, 2009) was used for improving the quality of DSM. Because of its working environment in graphical window as well as easier programming interface, this software is user friendly and can be handled easily. For a user with comparatively less knowledge and skill of programming environment, it is a very effective tool for composing algorithms and programs by using its inbuilt operators in graphical environment (Eckstein and Steger, 1999). The detailed methodology and workflow of implementation are shown in figure 5-4.

5.4.1. Preparation

To process the nDSM and building outline in Halcon, the data were converted to appropriate format. The nDSM produced in image (.img) format was converted to the 8 bit continuous tiff format by applying a linear mapping from 0 to 255. The building outlines extracted by OOA technique were in ArcGIS shapefile format, which is not accepted in Halcon environment. So, the building shapefiles were converted in to arcinfo generate text file. The generated text file is such that it contains X and Y coordinates of each nodes of polygon starting from and ending to the same point e.g. $(x_1, y_1), (x_2, y_2), (x_3, y_3), (x_4, y_4), (x_1, y_1)$ to represent building polygons. This conversion was done in python.

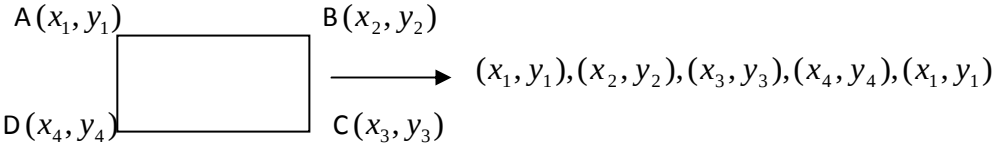

Figure 5-3: Conversion of building shapefile in text format

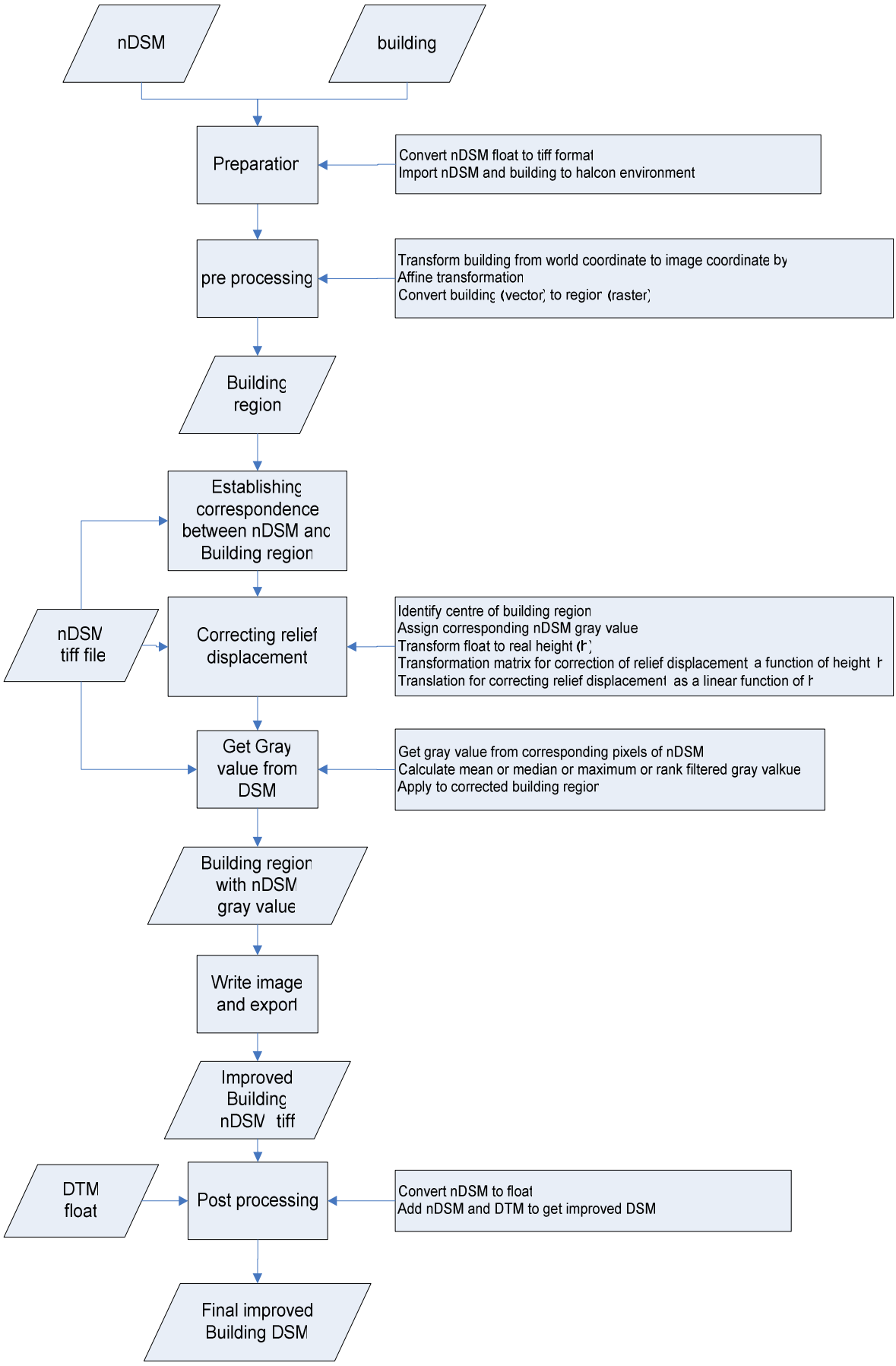

Figure 5-4: Detailed method and work flow for refining building DSM

5.4.2. Pre-processing

Pre-processing involves necessary operation on the nDSM and building outline data to make them ready for processing the main task. The main steps performed are applying an affine transformation to the building, to get it in image coordinate system and converting building vector to building raster region.

5.4.3. Processing

Correction for relief displacement was applied to the building region. This relief displacement, along with many other factors, is influenced by the height of the building. After analysing the results in section 3-4-4, it was found that the relief displacement in Y direction is linearly dependent on the height of the building whereas the displacement in X direction did not show any significant relationship with height. The displacement was found as a linear function of height as:

$$d_y = ah + b$$

Where d_y the relief displacement in y direction, h is the height of the building, and a and b are constants. The relief displacement in x direction did not show any significant effect and linear relationship with the height of the building.

To apply the correction on the building regions for relief displacement, the building region should be assigned a height value, because the relief displacement is a function of height. To do this, the centre of each building region was identified and their corresponding gray values were extracted from nDSM. These gray values were in float data type and should be converted in real height value. These gray values were transformed to actual height values by using a linear relationship

$$h = pg + q$$

Where, *h* is the actual height value and *g* is the nDSM gray value, and p and q are the constants. This relationship was established by measuring the gray value in 8 bit float data type DSM imge with corresponding image with actual height value.

Then, a homogeneous matrix was generated with translation parameters d_y in Y direction and 0 in X. A translation was applied to displace the building region by a distance d_y in Y direction and 0 in X direction.

The gray values were extracted from nDSM and a maximum gray value was applied to the corresponding building regions after using a 5% rank filter. This filtering process sorts out the maximum value and avoids the possibility of outlier or blunder.

5.4.4. Post processing

Finally, in this step, the improved nDSM is added to the existing DTM (chapter 3) to get improved DSM.

.

5.5. Implementation, Results and Discussion

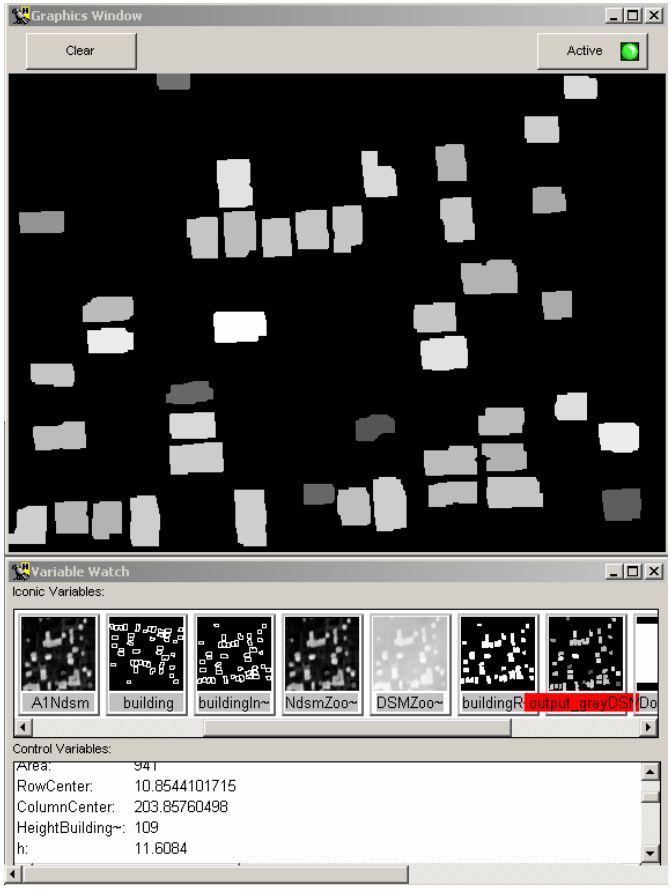

Figure 5-5: Resulting nDSM after processing in Halcon

The DSM generated from stereo image by matching technique in LPS (see chapter 3) was filtered to get DTM, and nDSM was produced by subtracting DTM from nDSM.

The building outlines extracted from OOA, after necessary pre-processing, were overlaid on nDSM. The building regions were translated and applied the correction for relief displacement. Then gray values were extracted from nDSM and rank filtered maximum value was applied to each building and the rest of the area in the building image was remained as background, with zero value (figure 5-5).

The Improved nDSM was exported as image and transformed back to world coordinate system. The gray values were also transformed to actual height values by applying linear transformation.

Finally, the improved nDSM and DTM were added to get a DSM. Both the datasets have same coordinate system, grid cell size and gray value scale to represent the actual terrain surface height. The addition of building height values in nDSM to the ground height in DTM gives the height of building above ground. Other background 0 values in nDSM were added to the bare terrain height value of DTM without any influence in the final DSM.

Figure 5-5 shows a brief procedure of the implementation and results obtained from it (the technical details of procedure and results are in Annex 9. To make the whole process clear and comparable, the DSM, DTM and nDSM produced in earlier steps (chapter 3) are also shown.

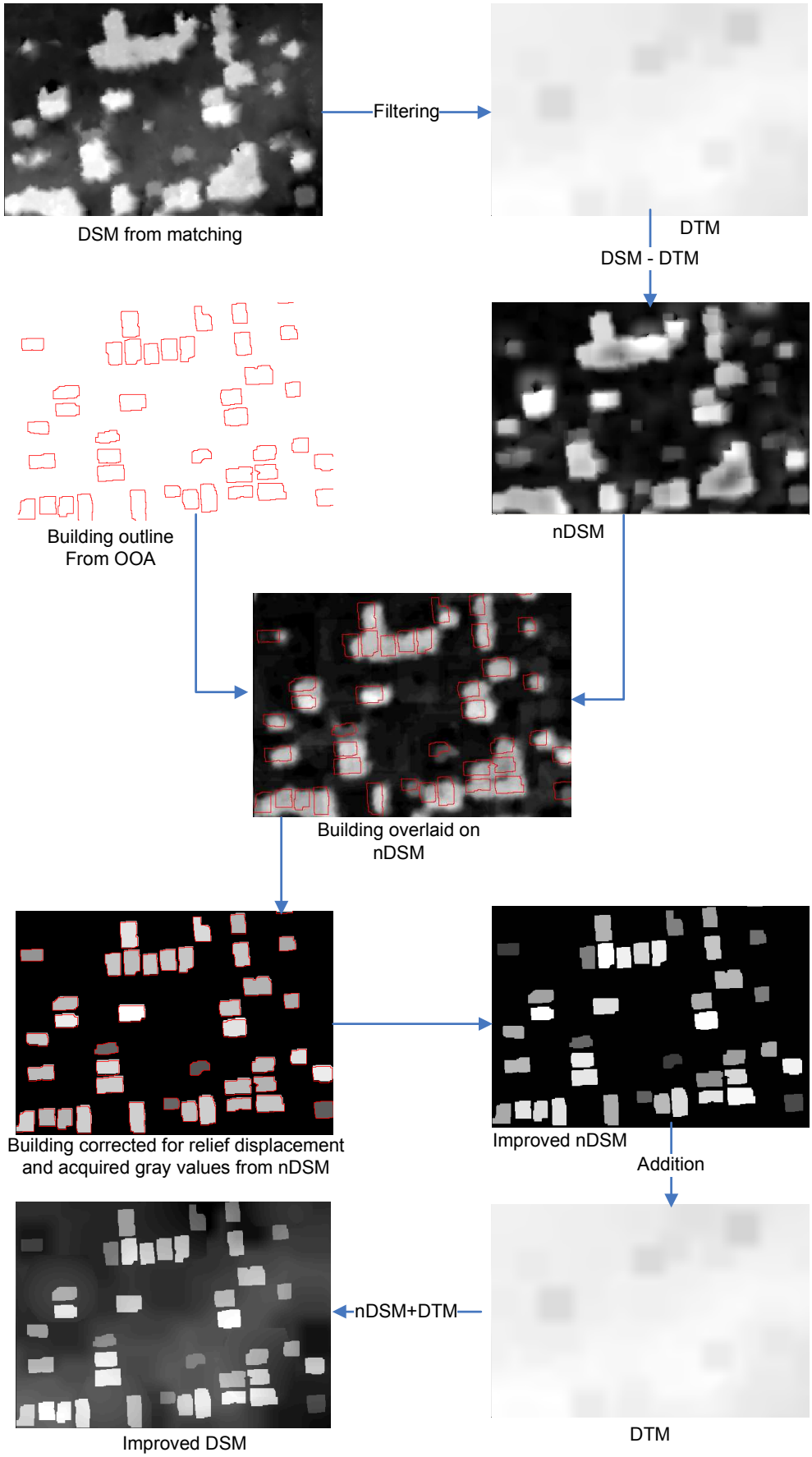

Figure 5-6: Implementation and results of DSM quality improvement process, study site 1

The above mentioned process was repeated to improve the quality of DSM for study site 2 and 3 also. The result obtained is shown in figure 5-7.

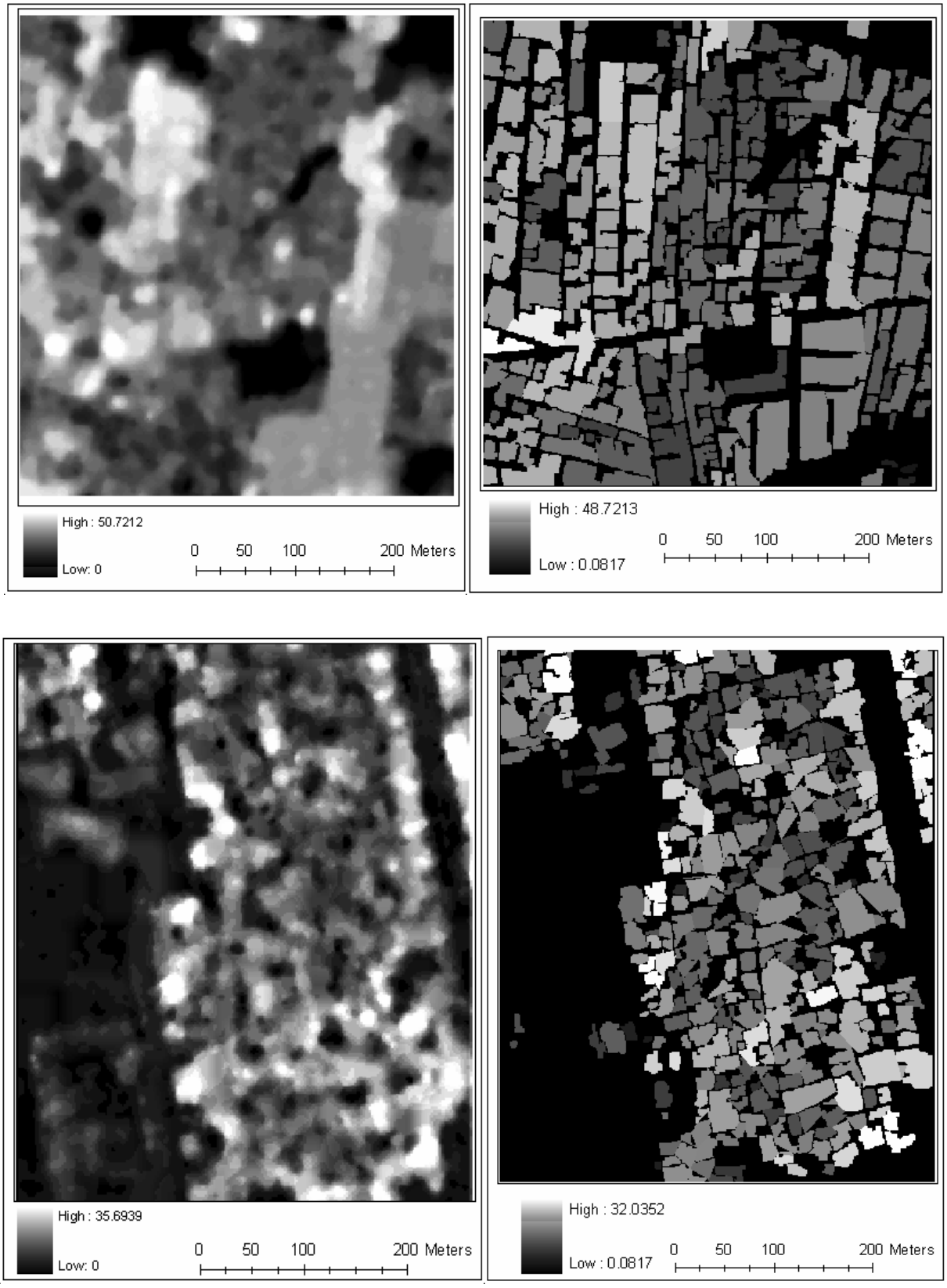

Figure 5-7: DSM of study site 2 (top) and 3 (bottom), before improvement (left), after improvement (right)

5.6. Quality assessment of improved DSM

The quality of the DSM was assessed after improvement. Although a DSM dataset with higher level accuracy was not available for result validation, we performed it in three different ways. Firstly, the DSM before improvement was compared with the DSM after improvement and differences in terms of improvement were mentioned descriptively. Secondly, the position and shape of improved DSM were compared with respect to the original DSM, and finally, the average heights of the building in DSM were compared with respect to manually captured heights of the building in stereo model.

5.6.1. Visual comparison and analysis

The DSM and nDSM before improvement were compared visually to the DSM and nDSM after improvement. Some major differences are mention in table 5-1.

Table 5-1: Difference between before and after improvement nDSM, study site 1

nDSM before	nDSM after
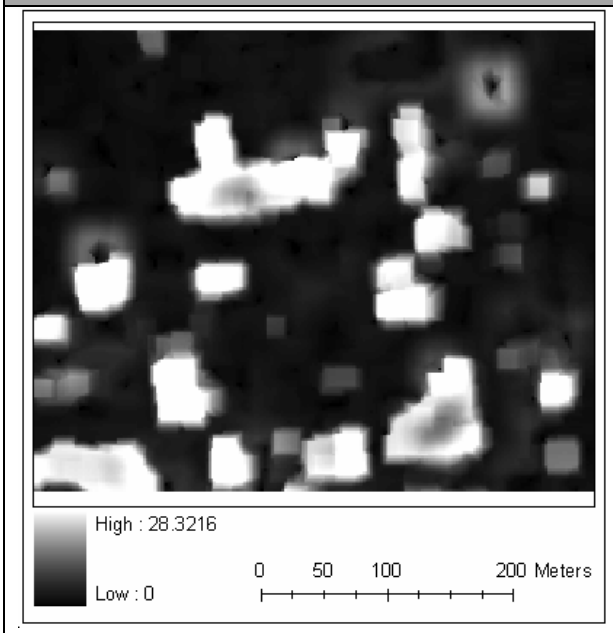	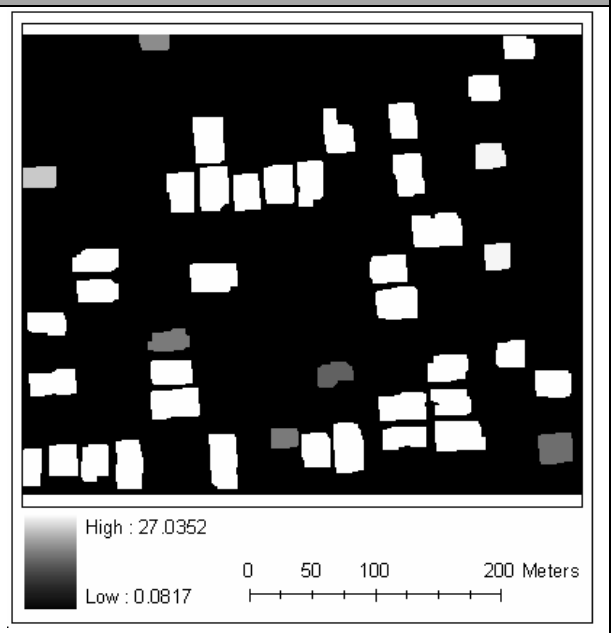
• Rough • Fuzzy boundary, building edges cannot be separated clearly • Buildings are in block • Gap between the building or narrow streets cannot be identified • Height values from matching, individual height value over building • Outlier and blunders may present	• Smooth • Crisp boundary, building edges can be separated clearly • Buildings are individual • Gap between building and narrow streets are identified • No individual height value, same 2.5D height over a building • Smoothed, no possibility of outlier

Figure 5-8 shows the difference between before and after improvement of the DSM. The red areas were present in the DSM before improvement and they were removed in new DSM after improvement. These areas were basically around the building foot edges, in the gap between two buildings or narrow streets. The green areas were additionally included in the new DSM after improvement.

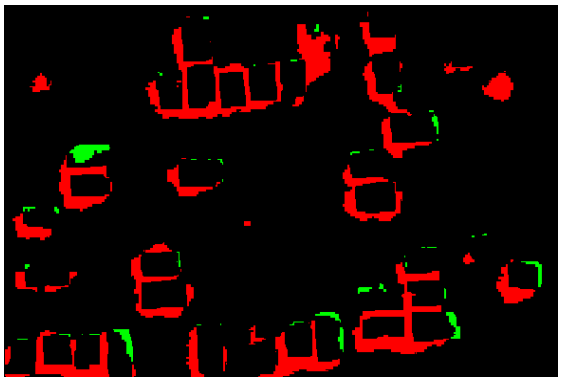

Figure 5-8: Change in the new DSM after improvement (study site 1)

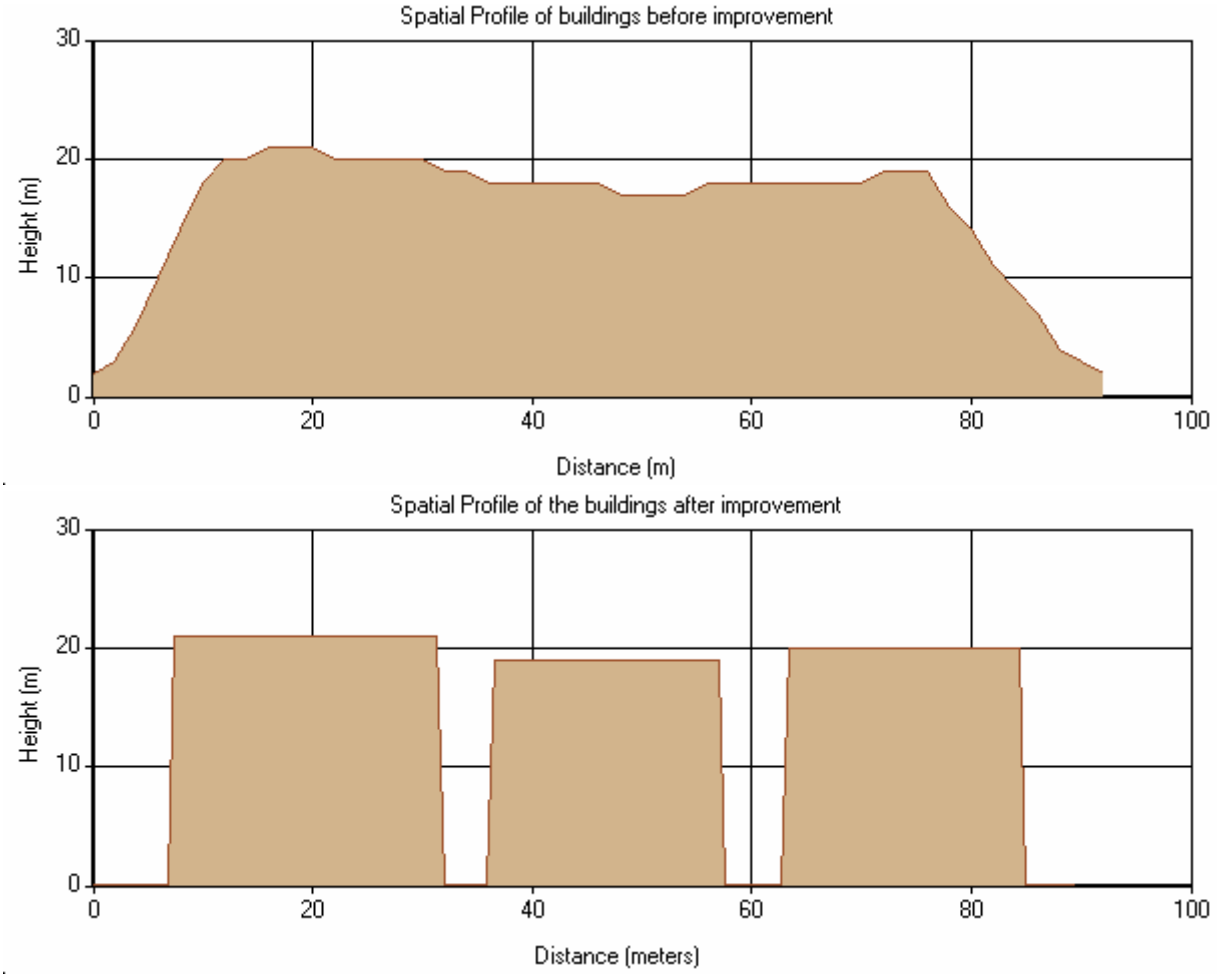

Figure 5-9: Spatial profile of the 3 buildings, before improvement (top) and after improvement (bottom)

Figure 5-9 illustrates the spatial profile of 3 buildings in a row in the nDSM before and after improvement. The spatial profile before improvement shows the problems in a photogrammetric DSM explained earlier in chapter 1 (bell shape, edge of the building not preserved, gap between building not modelled) and the spatial profile after improvement is free from all these problems and accurately model the actual shape of the building.

5.6.2. Position and shape

The position and shape of the improved DSM can be compared with respect to the actual building position and shape in stereo model. For shape, the building outlines were extracted by OOA and they were already compared in section 4.7.4. In this improvement, since the same outlines were used, no need to compare the shape again. For position, during the improvement process, the correction for relief displacement was applied on boundary outline and hence it is necessary to assess the accuracy of the building position after correction. To carry out this assessment, the same reference dataset digitized over stereo image which was used in section 4.7.4, was used.

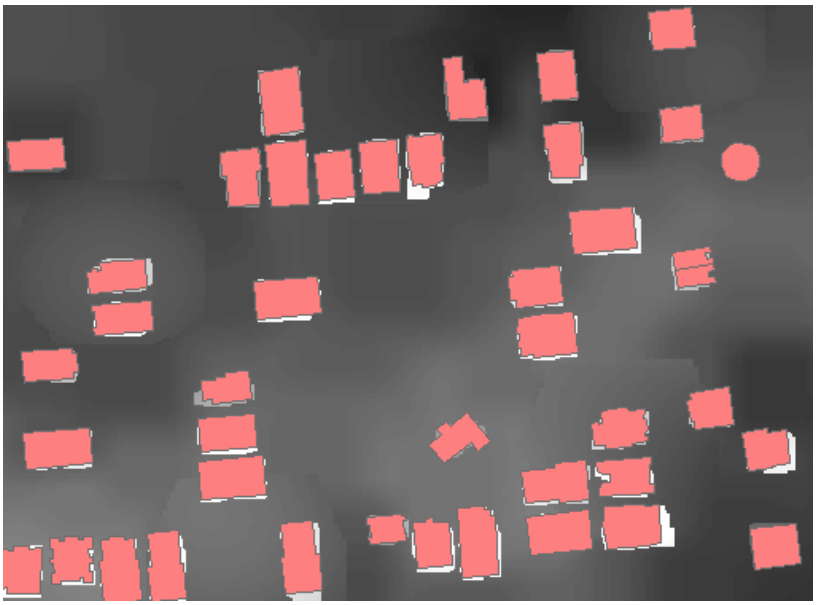

Figure 5-10: Comparison of the shape of DSM with the original building, study site 1

For this comparison, the building areas manually digitized from stereo image were overlaid on top of the improved DSM. Fig 5-10 shows, the improved DSM generally fits over the original building outline. In some building, we can see some difference between the shape of DSM and building outline. This is mainly because of the error in building outline extracted by OOA.

To compare the position of the original building and improved DSM, a vector polygon file was created from DSM raster and the centroid was identified. Similarly, the centroid of the original building polygon was also identified and the difference between the coordinates of the centroid was calculated to find the relative displacement of DSM from original building outline.

The result shows that the displacement of DSM in X direction ranged from 0.02 m to 2.94 m with mean displacement of 0.55m and standard deviation of 0.81 m. Similarly, the displacement in Y direction ranged from 0.04 m to 2.39 m with mean displacement of 1.08 m and standard deviation of 0.84 m. These displacements in X direction do not show any specific characteristics whereas those in Y direction were mostly negative values, showing the systematic nature of error. The average (distance between the centroids of the building) building displacement is 1.48 m with standard deviation of 0.77m. The positional error in root mean square error (RMSE) is 1.18 m. The detailed table showing the calculation is attached in Annex 10.

The comparison of the shape and position can be effectively done by the 3 D visualization of the terrain. This can be done by draping the orthoimage over the DSM. Two different 3 D models were prepared by using before nDSM and after nDSM. The models of study site 1, 2 and 3 are given in figure 5-11, 5-12 and 5-13 respectively.

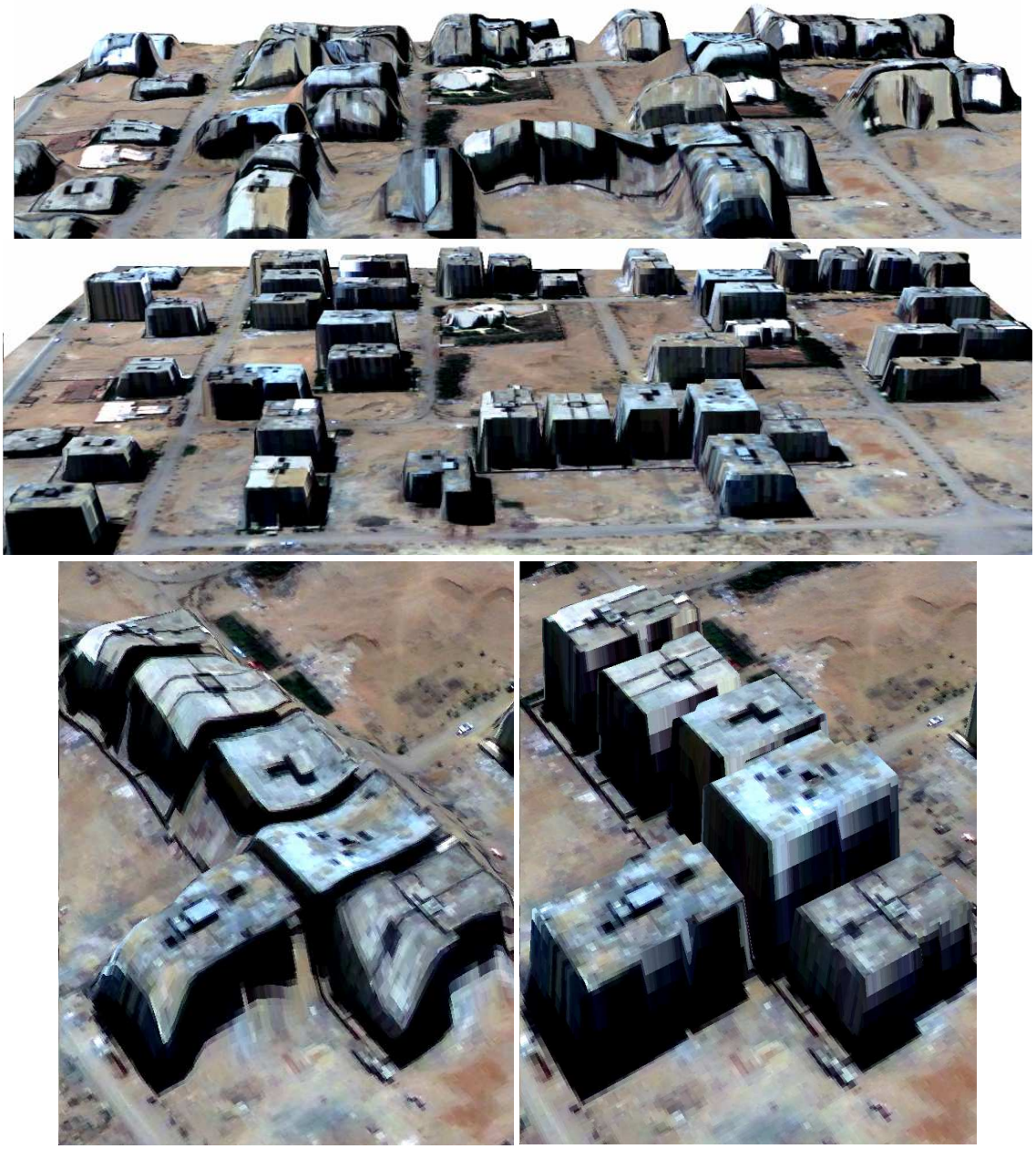

Figure 5-11: Orthoimage draped over nDSM of site 1, before and after improvement (top and middle), a closer look (bottom) before (left) and after (right)

The result in figure 5-11 shows the most of the problems of the DSM mentioned in chapter 1 are improved. The building outlines and edges are preserved. The gap between the building and narrow streets are clearly modelled. Hill shaped terrain (because of the bell shaped DSM) in the model from original DSM is not seen in improved model.

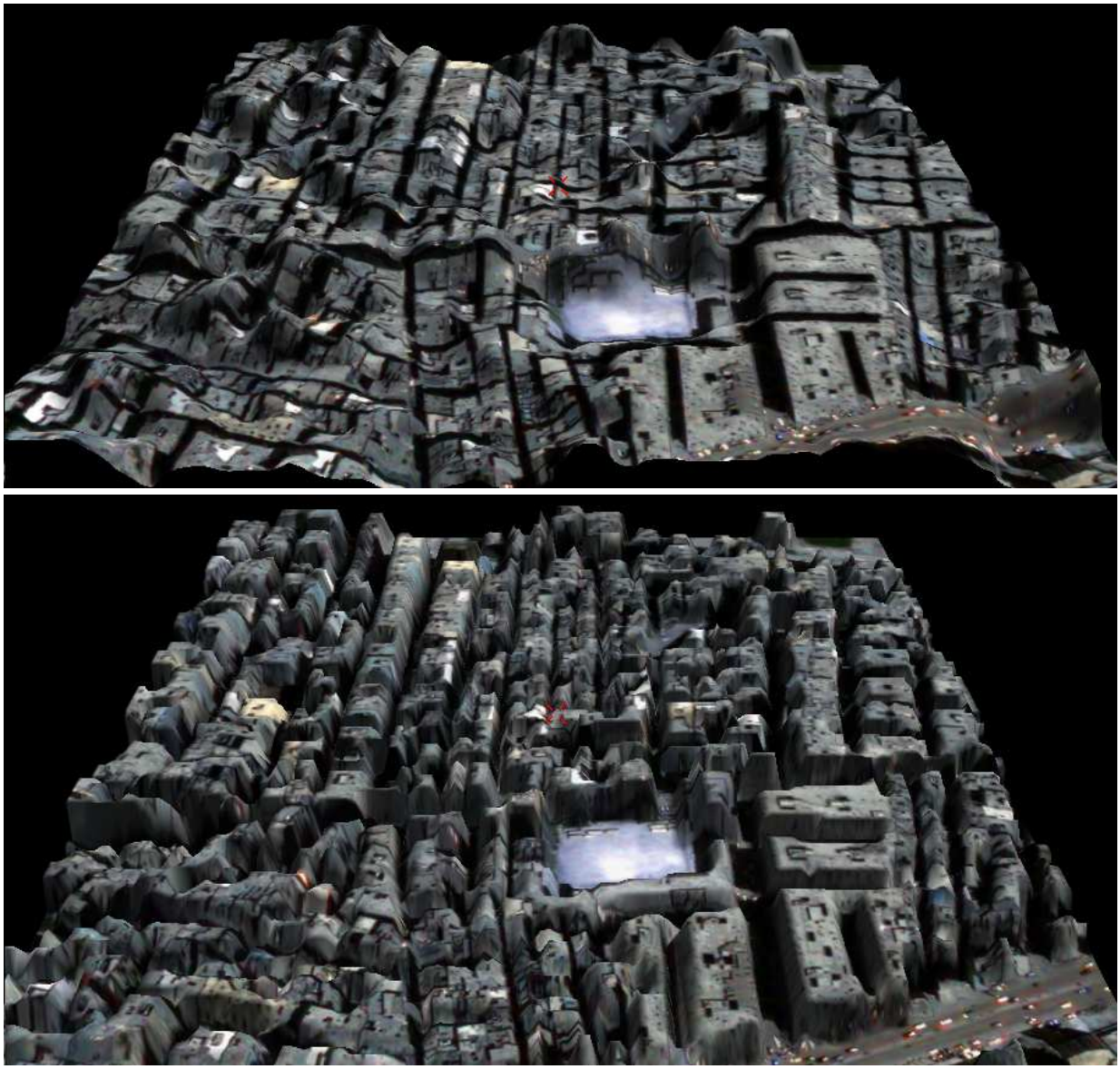

Figure 5-12: Orthoimage draped over nDSM of site 2, before and after improvement (top and bottom)

Figure 5-12 shows the 3D model of the terrain of study site 2. Improvement in the model is clearly visible in the figure. The large blocks, regularly spread buildings along the wider streets are delineated clearly. However, some blocks where the buildings are smaller, dense and irregularly situated are not accurately modelled.

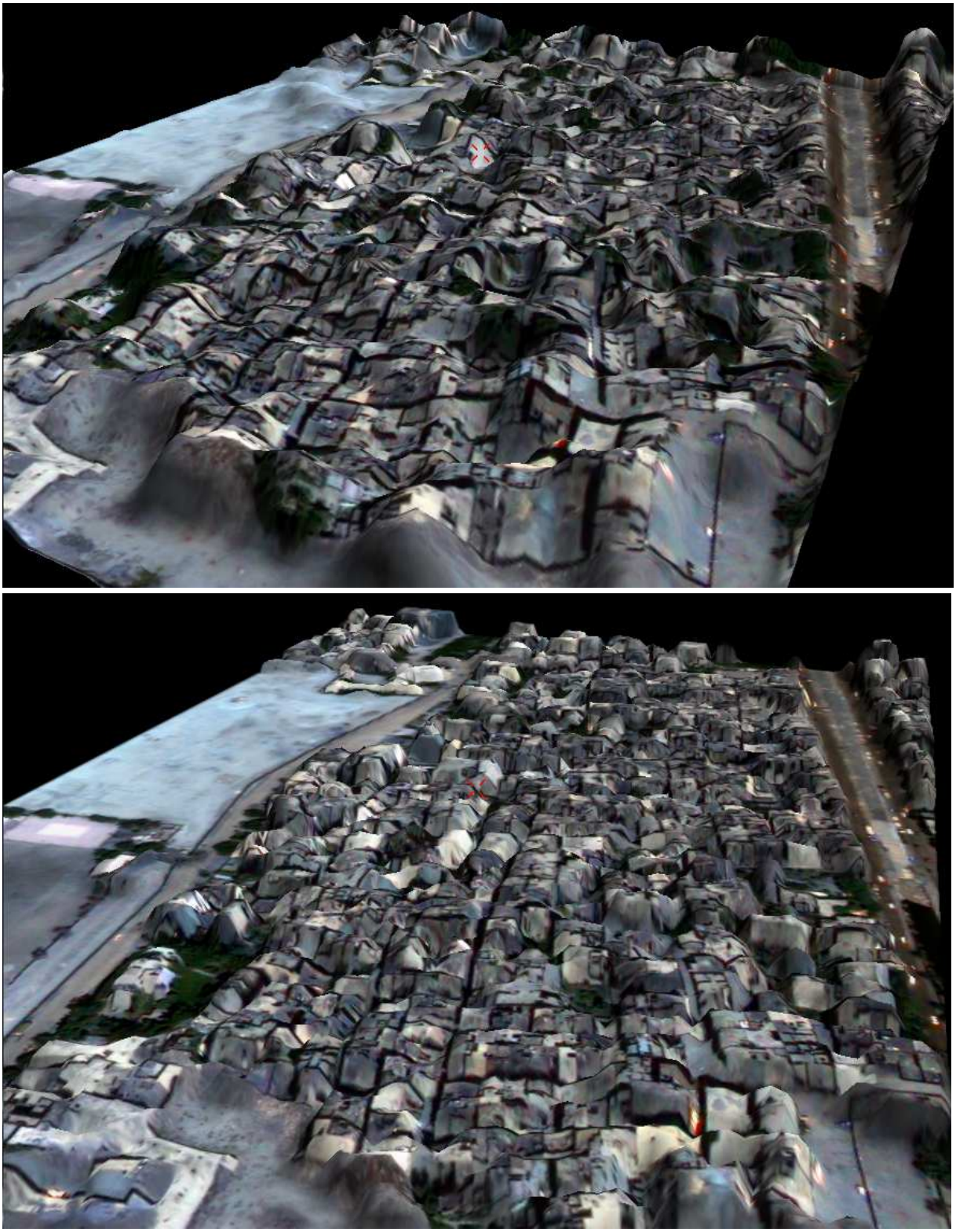

Figure 5-13: Orthoimage draped over nDSM of site 3, before and after (top and bottom)

Similarly, figure 5-13 shows the 3D terrain model of study site 3. Improvements can be seen with respect to the original model but it is not as clear as in study site 1 and 2. In this site, some building blocks are not accurately identifiable. Some open ground can also be seen as building. Similarly the outlines and edges are also not seen sharp and natural.

5.6.3. Height

Accuracy assessment of height value in DSM needs a reference data of higher accuracy. In this case, such a reference was not available. Therefore, the average height of the individual building top was measured manually from the stereo model and it was compared to the corresponding building height approximated from DSM, before and after improvement and given in table 5-2. The detailed calculation is shown in Annex 11.

For this comparison, the height of 41 buildings in study site was measured individually. The comparison shows that there is not much difference in the height of building measured from stereo image and DSM before improvement. The average difference between the height measured on stereo model and before DSM is 0.58 m; however, the maximum difference in height is 5.01 m shows there may be some outlier in the DSM from matching (table 5-2).

The height accuracy of the DSM after improvement depends upon the method of acquiring the gray height value from nDSM. The possible methods of acquiring height from nDSM are already mentioned in section 5-3. Here, the result obtained by using mean height value and maximum height value after applying 5% rank filter are shown (table 5-2).

Table 5-2: Comparison of height accuracy of DSM after improvement, by using different method of height value acquisition

difference with reference height from stereo model	DSM before improvement	DSM after improvement	
	Mean height on DSM over building (m)	Mean height over building (m)	Maximum height after applying 5% rank filter (m)
Minimum difference	-0.05	-0.06	-0.17
Maximum difference	5.01	13.32	-3.68
Mean difference	0.58	4.63	-1.65
Standard deviation	1.11	3.16	1.00

Table 5-2 shows, acquiring maximum height value after applying 5% rank filter gives much better result than mean height over building. The reasons behind this were explained in section 5-3 (see figure 5-2 also). It can be described as:

- Because of the effect of averaging over an area, the building with higher elevation are reduced significantly, it can be seen in table 5-2, the maximum difference of 13.32 m shows the problem in matching over the particular building and result with partial DSM values within the building see figure 5-2(a). In the rank filtered maximum value, this problem does not exist.

Some sources of error in acquired height value may be common in both DSM, they can be as follows:

- A smaller building in between two taller building gets the larger height from nDSM since the shorter building is not modelled accurately in DSM and the DSM has similar height in a block.
- The DTM used in producing the final DSM may not be sufficiently accurate and may contain error. The error would propagate when adding nDSM to DTM to get DSM.

5.7. Concluding Remarks

In this chapter, improvement of DSM was done by using building outline extracted by OOA. The quality of improved DSM, in terms of shape and position, depends upon the quality of extracted building outline. As in the result of OOA in the study area 1(chapter 4), individual buildings were extracted with highly accurate outlines, the quality of improved DSM is also high in this site. For study area 2, building block outlines were extracted with a fairly good quality; the similar result can be seen here in DSM improvement. In case of study site 3, since the building block outlines cannot be extracted very accurately; the DSM cannot be improved very significantly. Further, the relief displacement of the building outline was corrected, which increased the accuracy of the resulting DSM with respect to the outline extracted by OOA. Hence, it can be concluded that higher accuracy of the extracted building outline may increase the quality of improvement of the DSM in terms of shape and position.

In this chapter, the main concern was to improve the quality of urban DSM in terms of its shape and position over the building areas. However, it was taken into consideration that the accuracy of height values in the DSM should be improved. Gray values were extracted from nDSM and same maximum value after 5% rank filter was applied throughout a building to reconstruct the improved nDSM. By using this improved nDSM and DTM, new DSM was produced, the quality of which is improved significantly in comparison to the original DSM.

6. Result Synthesis and Discussion

This chapter synthesizes the results of chapter 3, 4 and 5 and includes discussions on the results. The discussion is presented in relation to the input data used, method applied and result obtained in accordance with the objective and research questions.

6.1. DSM generation and orthoimage production

This section presents discussion on the results of chapter 3. The objective of chapter 3 was to explore the DSM generation techniques and produce DSM and orthoimage from VHRS stereo image.

6.1.1. Data used and method

The input data used for the DSM generation is Geoeye-1 stereo image. This image was provided with RPC file and necessary metadata. The additional ground control points collected by using differential GPS were used for bias correction with an overall RMSE 0.87 pixels. Any accuracy achieved within RMSE of one pixel is regarded as good enough and accepted for orientation.

Photogrammetric software LPS and SAT-PP were used for DSM generation. LPS is widely used commercial software for photogrammetric purposes. It uses a combined (area and feature based) matching algorithm for image matching, which is used for DSM generation. SAT-PP is specialized software developed by ETH, Zurich for different photogrammetric product generation. It also uses a combined and improved matching method for DSM generation. DSM generation in LPS was carried out at ITC whereas it was carried out in SAT-PP at ETH, Zurich with the help of the researchers at ETH.

6.1.2. Band selection for matching

An experiment was carried out to find the most suitable band for matching to generate DSM. Statistical analysis shows that the NIR band can be most suitable since it has the highest spectral variability and can acquire most of the details, which increases the possibility of correlating the features during matching. This fact was verified by comparing the number of match points generated by matching algorithms using different bands. The result shows matching in the NIR band has the highest and blue band has the lowest number of match points.

Several inconsistencies were observed during the matching process of original 16 bit Geoeye images in LPS and SAT-PP. Therefore, the original radiometric resolution was rescaled and 8 bit image was matched. It gives satisfactory results. The reason behind these inconsistencies may be the inability of LPS and SAT-PP to handle very high radiometric resolution and large range of gray values but the actual causes can be investigated in separate research. However, it would be more informative to match original 16 bit image because of its high radiometric resolution, which can not be exploited in this research.

6.1.3. DSM in sparse area

The DSM produced for sparse area represents the general surface characteristics of the study area. The buildings are well represented in DSM in terms of shape and size; however the DSM does not exactly fit with the individual building boundary. The areas near the building foot, narrow streets and gap between two tall buildings are not modelled truly as the ground. This is because the sensor cannot 'see' these areas as they are occluded behind the buildings or covered by shadow. During matching, the system cannot find any match points in those areas and DSM gray values are interpolated on the basis of other nearest surrounding DSM values.

6.1.4. DSM in dense area

In highly dense areas, the quality of DSM generated by matching is questionable. Most of the small ground areas are covered by shadow and occluded behind the tall buildings. The building roofs and bigger open areas, wider roads, which can be seen through the sensor, are modelled well. The high rise buildings and their abruptly changing height within a small distance make matching difficult. Because of these reasons, the DSM generated by matching in study site 2 and 3 are not much reliable.

6.1.5. Comparison of DSM generated in LPS and SAT-PP

When comparing the resulting DSM from LPS and SAT-PP, it can be observed that the SAT-PP DSM is smoother than LPS DSM. Similarly the DSM generated from LPS has some artefacts which are not present in SAT-PP DSM. Moreover, some buildings or building parts are not represented well in LPS DSM, their shape and size do not match with the same building in SAT-PP DSM and original buildings in image.

This difference in the quality of the DSM generated is because of the different matching strategies used in both softwares. The LPS uses the distinct feature points like road crossings, house corners, etc in the images as the interest point for matching, whereas the SAT-PP uses multiple matching primitives such as feature points, grid points and edges in successive stages and integrates local and global image information and utilizes a coarse-to-fine hierarchical matching strategy. LPS used a cross correlation and least square technique for calculating the similarity measure whereas the SAT-PP utilises the principle of least squares matching and geometric constraints.

6.1.6. Orthoimage production

Orthoimage was produced by using the right stereomate of stereo pair. The reason is the satellite viewing angle for right image is smaller than left stereo image, which causes less relief displacement. Similarly, the right image was collected from an azimuth of 340^0 which is almost north and therefore the displacement is in south whereas for left image image, the azimuth was 214^0 which causes the displacement in north and east.

Two different orthoimages were produced by using different elevation data for orthorectification. Constant average ground surface height (measured manually in study site from stereo image) and a self generated DTM (produced by morphological filtering of the DSM generated in SAT-PP) were used as source of height. The accuracy assessment shows the orthoimage produced by using constant height data source is more accurate than the orthoimage produced by using DTM. It could be because of the poor accuracy of the DTM. There may be some errors already in the DSM

produced by matching. Again, due to the imperfect filtering, the produced DTM may not truly represent the actual terrain surface. On the other hand, the constant average height almost represents the actual ground surface as the study site if fairly level and flat.

6.1.7. Accuracy of orthoimage

The orthoimage produced by using constant height as an elevation data is more accurate than the orthoimage produced by using own generated DTM. For the orthoimage by using constant height, the displacement seen in X and Y direction is 0.62 m and 2.88 m in average whereas the displacement in X an Y direction for the orthoimage produced by using filtered DSM is 1.17 m and 4.55 m respectively. The reason behind the error may be the quality of DTM. During DSM filtering, there may be some object remained unfiltered, whereas because of the flat surface of the study site, the constant height represents it correctly and the orthoimage is accurate. Similarly, orthoimages from the left and right stereomate were compared and found that the orthoimage from right stereomate is more accurate than that from left stereomate. The region is the different azimuth and incident angle for left and right image.

Thus, the orthoimage from right image with constant height was found more accurate for building extraction. Although, this orthoimage also suffers from relief displacement because of the height of the building and perspective geometry of image, but it can be modelled as a linear finction of height and can be corrected in some extent.

6.1.8. Limitation

The original 16 bit radiometric resolution can not be exploited because of the software problem. In absence of the reference elevation information, the generated DSM accuracy cannot be assessed. Similarly in absence of accurate DTM, the orthoimage was produced by using constant height. The DTM produced by using morphological filtering of DSM was not reliable. There are not any other reliable inbuilt tools for getting DTM from a DSM. The DTM filtering is itself a dedicated, time consuming and separate study area which was not included in this research.

6.2. Building extraction by OOA

This section discusses on the results of chapter 4. The objective of chapter 4 is to explore the building extraction technique by using OOA technique.

6.2.1. Data and method used

The input data used for this task are orthoimage and nDSM (chapter 3).

Depending on the structure of urban building in study area, three types of settlements were chosen. Site 1 consists of single and separate building having consistent and regular shape. Site 2 consists dense and crowded settlement but having regular building structures and site 3 is an informal settlement with dense crowded and irregular building structure.

The main idea is to segment the image on the basis of homogeneity criteria and classify the segment on the basis of similar feature characteristics and using nDSM, to extract the buildings.

6.2.2. Image segmentation

Image segmentation was done in definiens developer 7. Parameters for segmentation were found by trial and error method. Segmentation parameters are chosen carefully so that the resulting

segments should normally match with the shape of the object, however, same segmentation parameters may not necessarily yield well fitting segments to all objects.

The result of segmentation shows that the image segments mostly fit with the buildings in all other sides except in southern edges. This is because the edges of the building in the other directions are clearly separable from its surrounding because of the large gray value difference. But the surrounding of southern edge is mostly similar with the spectral properties of the building. Because of the sun angle, shadow is casted in the north and west of building which caused strong discrimination between the edge of building and shadow. This strong gray value difference lacks in southern edge and the surrounding is spectrally homogenous, which led to inaccurate segmentation in these areas. Other parameters like shape also cannot help in this situation as the shape is also not clearly identifiable in this direction. Application of DSM in segmentation cannot support to solve this problem as the nDSM itself is not crisp and the boundary edges of the buildings were not preserved. The same fact holds for the application of disparity image in segmentation.

6.2.3. Feature properties used for building extraction without DSM

Several feature properties of the segmented image objects were analysed to identify the most applicable ones for extracting building successfully. Separation of vegetation, water and shadow is straightforward since their spectral characteristics is different than other objects and feature properties like NDVI, ratio blue and SSI can be used to extract them. The main difficulty was to separate buildings from road, bare objects, parking areas etc since their feature properties are similar. Spectral characteristics only are not sufficient because of the spectral variability within building object/class and spectral similarity among different object/class. Shape and size of the image object are also not consistent. Some are rectangular others are not. Some are elongated others are compact. Some are regular whereas others are irregular, and so on. The segments do not follow some specific spatial properties like asymmetry, rectangular fit, size (area, length, perimeters etc). Contextual information like relative border to shadow, relative border to building, relative border to unclassified (bare ground, road etc) supports in some extent to extract the building from other objects but not completely because there are some other image objects which also follows the similar spectral, spatial characteristics and context like buildings. In such cases, the spectral, spatial and contextual information are not sufficient to extract the building accurately. In this context, the height information may help to extract building because; height is the most common property in all buildings.

6.2.4. Building extraction with DSM

The discussion in section 6.2.3 shows only spectral, spatial, and contextual information are not always sufficient and height information provides extra support for building extraction. In the image, the objects, which are similar in characteristics, are mainly the ground objects like road, bare ground and parking areas. These areas have less height in comparison with buildings. Other taller objects like trees can easily be separated by using NDVI. Therefore, by using a certain height threshold, the image segments of ground object can be separated out leaving behind only building segments.

By using height as an extra layer along with the other feature properties mentioned in 6.2.3, most of the buildings are extracted successfully. The results of building extraction in all three areas are different although the approach followed for building extraction is similar. The rulesets used for

building detection in these areas are almost similar except height thresholds and some refinement steps. This is mainly because of the difference in the quality of nDSM used building detection. Since the quality of nDSM is better in study site 1, the result of building extraction is also better in study site 1 in comparison with the site 2 and 3.

6.2.5. Single building detection in sparse area

Result shows in sparse areas, single buildings are extracted successfully. This is mainly because in most of the cases the image segments are fit with the building object and applying feature properties for building extraction is more convenient. The shape and size of the building are consistent and regular and contextual information like shadow is mostly clearly distinguishable. Only difficulty is the spectral dissimilarity with same object/class and spectral similarity with other objects/class. This problem was solved by using height information, which is fairly accurate enough to discriminate ground object (road, bare ground) from buildings. Although the individual buildings are not separable and differentiable in nDSM, they are well identifiable in orthoimage. Because of the small gap with dark shadow in between the building, they are separated.

6.2.6. Building blocks detection in dense area

Result shows that the building block extraction is satisfactory in study site 2 (dense regular building) but there are still some problems in study site 3 (dense irregular building). In the dense area, most of the properties of the sparse area, discussed in 6.2.5 are missing. The buildings are so close and clustered in the group that cannot be identifiable as individual building. Furthermore, the buildings are connected to each other; shadow of the taller building is casted on shorter buildings which causes difficulty and confusion on applying context. In a regularly structured settlement, however, the pattern of the building is clear, and size and height of the building is almost regular and uniform. Wider streets and shadow casted on street can help to apply the context. These characteristics make extraction of building blocks convenient. On the other hand, in a dense informal settlement area, all above discussed characteristics are missing. Furthermore, the small open areas in between the buildings are strongly confused with buildings. Irregular pattern of building and their shadow on one another do not favour applying context. Narrow streets and shadow of building also creates confusion. Connected buildings of different spectral properties and small open patches, parking area are also confusing. The building and non building areas cannot be separated, in some cases, even with a human eye-brain system. Because of the matching problem in dense urban environment, the DSM was also not reliable and good quality. This DSM cannot represent the narrow streets, gaps between the building and small open areas between the dense buildings. These problems guided the quality of building block detection in site 3 less accurate in comparison to study areas 1/2.

6.2.7. Quality of extracted building

The accuracy assessment of extracted building was done in 3 steps for single buildings and a single step in building blocks. Extracted single building can be compared in different ways to the reference datasets such as on the basis of number of individual object, comparison in their spatial positions and area occupied by the buildings, but in case of large building block, the individual object wise comparison cannot be done and comparison of position does not give significant result.

Result of object wise comparison of extracted building in site 1 shows that the completeness about 96 % (LPS DSM) and 98 % (SAT-PP DSM) and 100 % correctness. The result seems extremely encouraging. We have a subset of image containing only 44 buildings; the high percentage of extraction may be because of this small subset also. Similarly, these extracted buildings are within an average positional displacement of 1.14 (SAT-PP DSM) and 1.26 (LPS DSM), which shows a good positional accuracy. Finally, the accuracy assessment on the basis of area extracted shows the completeness of 93%, 92% and 85% and correctness of 92%, 89% and 86% in study sites 1, 2 and 3 respectively which shows the building areas are accurately extracted.

6.2.8. Limitation

Because of the limited time, the detailed OOA study for individual building extraction could not be experimented in study areas 2 and 3.

The rulesets developed for extraction of building in this study area were not validated for the other areas/parts of Cairo city. The transferability of these rulesets could not be tested. The selected three study areas do not still completely represents the urban complexity of Cairo. For example, none of the study sites contains the objects like overhead bridges, flyovers etc, which have more confusion with buildings. Therefore, the developed approach cannot be tested against such object.

6.3. DSM quality improvement

This section discusses on the results of chapter 5. The objective of chapter is to develop a method for improving the quality of DSM generated from VHRS stereo images (Chapter 3) by using the OOA technique (chapter 4).

6.3.1. Data and method used

The input data used in this task were DSM/DTM/nDSM generated (chapter 3) by image matching technique and building outline extracted (chapter 4) by OOA technique. Both datasets were integrated to refine the quality of original DSM.

The idea of the DSM improving method is simple and straightforward. The problems in DSM generated by matching method should be removed by making use of building outline. In other words, the building areas within outlines should have correct gray values and unnecessary gray values outside the building should be removed. This task is done in two main steps: 1) correcting the positional error in building outlines caused by the relief displacement and 2) Capturing the height value from a building in the nDSM and applying same gray value throughout the corresponding building.

6.3.2. Applying correction on building outline

The buildings outlines extracted by OOA suffered from a systematic error which is because of the relief displacement on the orthoimage used for building extraction in OOA. This error due to the relief displacement in Y direction is linearly dependent to the height of the building whereas it did not follow any significant trend in X direction. This is mainly due to the perspective geometry of the satellite/sensor system and height of the building.

Since further improvement of the DSM depends upon the building outlines, it should be made free from error. For this, a correction is applied by shifting building outlines by an equal distance but in

opposite direction of the error. A set of translation parameters was defined and the building outlines were translated to correct this positional error. This step provides accurate building outline free from systematic errors, however, the random errors in building outline may not be corrected by this step.

6.3.3. Assigning correct height to building outline

The nDSM was used to extract the height gray values to assign building regions only; rest of the surrounding background in the building region image has a gray value of zero, meaning the ground. This is mainly because the nDSM stores absolute height of building. If we would use DSM instead of nDSM, the building regions would get the height from MSL whereas the ground is still zero. Later, this nDSM with improved absolute height of the building, when added to the DTM, the improved DSM is found.

After extracting the gray values from buildings in nDSM, maximum gray value from 5% rank filtered maximum height was applied to each corresponding buildings to get a homogeneous 2.5D representation in DSM over the building outline.

Applying 5% rank filter has advantage over mean, median and maximum gray values in nDSM. Application of mean and median do not work well in the case of partly matched DSM and they oversmooth and reduce the resulting height, whereas application of maximum gray value may be affected by blunders in nDSM. Rank filtered value is free from these both types of error.

6.3.4. Quality of the improved DSM

The improved nDSM was added to the DTM and a DSM was produced, which was improved in shape and size with respect to the original DSM. The analysis of accuracy (visually and statistically) shows the improved DSM mostly matches with the actual shape and size of reference buildings. The shape and size of the improved DSM is highly dependent on the building outline extracted by OOA. Hence, the accuracy in building extraction in OOA directly affects the accuracy in shape and size of DSM.

The height of the DSM is not much considered for improvement in this research. However, if there are some blunders in original DSM because of the problems in matching, they are removed by rank filtering. Similarly, if there are partially matched buildings, not completely present in DSM because of occlusion or shadow during matching, and if such buildings are extracted in OOA, then the DSM of such building can be reconstructed. In other cases, as the height in the improved building is taken as an input from original nDSM, the accuracy of original DSM/nDSM is crucial.

6.3.5. Limitation

Limitation of the approach mainly remains on the vertical height value improvement. This problem mainly affects in the case of a lower building in between two taller buildings. In such case, the DSM normally includes the higher value equally throughout and cannot represent shorter buildings in between two tall building correctly. Since this approach takes the gray value from input nDSM, which are already inaccurate, and fills the building region, so the new DSM also cannot represent the actual height value of short building. Similar problem would appear in case of stepped multi storied, gable roof, and hip roof buildings. The stepped surface, gable and hip roof would be generalised to flat roof and same gray value would be applied through out the building roof. This problem was not included in the scope of this research and can be explored further in the future research.

Another limitation of the study is the trees and other elevated surfaces on the earth are not considered as the part of DSM when improving; only buildings are taken into account.
The poor quality of the DTM, produced by morphological filtering is also another limitation. The final DSM was produced by adding the improved nDSM to this imperfect DTM to get final DSM; hence the errors would propagate from DTM to final DSM.

6.4. Conclusion in relation to the objective and research questions

The main objective of this research is to develop a method for improving the quality of photogrammetric DSM generated from VHRS stereo image by using the OOA technique. To achieve this main objective, three sub objectives were set. These sub objectives are related to explore the DSM generation techniques and produce orthoimage, to extract urban building by OOA technique and to develop a method for improving the quality of DSM by using building outline extracted by OOA.
Several research questions were posed to achieve these objectives. Main questions for DSM generation and orthoimage production phase are: which image band in Geoeye-1 would give the best result for DSM generation by matching and does this DSM preserve shape and size of buildings in urban area and can a DTM be used to produce an accurate orthoimage? The result shows that band 4 (NIR) is the best suitable band for image matching. This DSM generally preserves the shape and size but not exactly match with the building outline in sparse area whereas in a dense area, the individual buildings are not identifiable in DSM, the buildings are represented in a block. The accuracy of orthoimage depends upon many factors like accuracy of image orientation, sensor geometry, height of the buildings in image, accuracy of DTM used etc. In this research, the orthoimage produced from right image by using constant height is found more accurate than that of using left image and DTM produced by filtering the generated DSM.
Similarly, the questions for building extraction by OOA are: how can we extract building from VHRS image by OOA and what would be the accuracy of the extracted buildings? The results show that the buildings can be extracted successfully in a sparse area by using several feature properties alongwith a photogrammetric DSM, however, the imperfect shape and unpreserved building outline in nDSM can not help to extract accurate building outline. Further in dense urban environment the success of building extraction depends upon the density and structure of settlement alongwith different feaure properties and accuracy of (n)DSM used. In a comparatively well structures and regular dense urban area, buildings were extracted satisfactorily whereas in an irregular area, the building extraction was less accurate. The accuracy of extracted building in sparse and regular dense urban area is extremely encouraging whereas, taking the complexity of the area in mind, the accuracy in irregular urban area can be regarded as satisfactory.
Finally, the questions for DSM quality improvement are: how can we improve the quality of photogrammetric DSM and what are the improvements in the final output DSM? An innovative approach of DSM improvement is implemented. Mainly two issues were dealt in this approach: 1) correcting the relief displacement in building outline, and 2) acquiring the height values from existing DSM/nDSM and assigning it to the building region. Result shows the new technique for DSM improvement implemented in this research gives significantly improved building DSM in terms of shape, size and position as well as the 2.5D gray values over a building surface.

7. Conclusion and Recommendation

This chapter presents the conclusion of this research and recommendations for future studies. The section 7.1 concludes the results in terms of the main findings of the research and the section 7.2 recommends some issues for further research.

7.1. Conclusions

On the basis of results and discussion, the main conclusion of this research can be drawn as:

- In this study, for VHRS image GeoEye-1, the original 16 bit image could not be matched (in LPS ad SAT-PP) for DSM generation but when rescaled to 8 bit, it matched well. Band NIR is found the best suitable for matching and DSM generation. Individual buildings are normally represented in sparse areas but it is, difficult in dense area. This DSM, after filtering, can be used for the orthoimage production, but the accuracy depends upon the quality of filtering and resulting DTM, alongwith many other factors.
- In spectrally homogeneous areas, it is difficult to get image segments which exactly match the object boundary. DSM generated from VHRS image by matching technique does not provide much support for image segmentation, especially, in the case of the buildings. Various feature properties of the image segments such as the spectral, spatial and contextual information can be used but in a heterogeneous urban environment, the application of these feature properties only, cannot produce accurate result of buildings extraction. In such cases, nDSM plays very important role. The DSM generated from VHRS image by matching technique is not much helpful in dense building areas; however it can be used successfully for building extraction in sparse areas. Better quality of nDSM helps to achieve higher accuracy in building extraction.
- DSM generated by matching technique and the building outline extracted by OOA are integrated in an innovative approach to improve the quality of DSM. The implementation of approach yields significantly improved DSM in terms of shape, size and position. Building outline restricts the shape and size, and the correction applied for relief displacement improves the position. Similarly, acquiring the appropriate height value from nDSM and assigning it to the corrected building outline to get an improved 2.5D representation of building DSM improves the quality of final output DSM significantly. The problem with urban DSM such as inability to model the narrow streets and gaps between building, areas near building foot, bell shape and streaking effect in DSM, gray value missing due to incomplete matching in some building areas are solved.
- The DSM is improved by using building outline extracted by OOA. Hence the quality of final DSM strongly depends upon the quality of building outline extracted by OOA.

In conclusion, all the questions posed in the research are well answered and the main objective of he research: to develop a method of improving the quality of DSM generated from VHRS stereo image

by using OOA technique is achieved. We see that, even a low quality of DSM generated from VHRS stereo image, Geoeye-1 is significantly improved by using the building outlines extracted by OOA.

7.2. Recommendation

The following recommendations are made for further research:

- Inability of LPS and SAT-PP to match original 16 bit GeoEye-1 image can be explored further.
- DTM was used in many steps like orthorectification of image, producing nDSM, segmentation and classification in OOA, and improving the quality of DSM. Therefore, it would be worthy to apply an efficient and reliable method for photogrammetric DSM filtering before making its further application in the process.
- The detailed OOA for individual building extraction can be experimented in study areas 2 and 3. This technique can be extended to more complex areas such as dense areas with overhead bridges, flyovers etc, which have more confusion with buildings.
- The rulesets developed for extraction of building in one study area can be validated for the other areas/parts and the transferability of the rulesets can be tested.
- This method assigns a single height value to the building and generalizes as a 2.5 D flat roof. The possibility of extending this method to the slope roof, hip roof, gable roof or stepped multi storied building roofs can be explored.
- This method concentrates only in building DSM. Improvement of a general DSM including trees and other elevated objects can be explored.

References:

Agouris, P., Doucette, P. and Stefanidis, A., 2004. Automation in Digital Photogrammetric Workstations. In: J.C. McGlone, E.M. Mikhail and J. Bethel (Editors), Manual of Photogrammetry. American Society for Photogrammetry and Remote Sensing, Bethesda, Maryland.

Alobeid, A., Jacobsen, K. and Heipke, C., 2009. Building Height Estimation in Urban Areas from Very High Resolution Satellite Stereo Images, High-Resolution Earth Imaging for Geospatial Information, ISPRS Workshop Hannover, Germany

Altmaier, A. and Kany, C., 2002. Digital surface model generation from CORONA satellite images. ISPRS Journal of Photogrammetry and Remote Sensing, 56(4): 221-235.

Aminipouri, M., Sliuzas, R. and Kuffer, M., 2009. Object-Oriented Analysis of Very High Resolution Orthophotos for Estimating the Populations of Slum Areas, Case of Dar-Es-Salaam, Tanzania, High-Resolution Earth Imaging for Geospatial Information, ISPRS Workshop, Hannover, Germany.

Aubrecht, C., Steinnocher, K., Hollaus, M. and Wagner, W., 2009. Integrating earth observation and GIScience for high resolution spatial and functional modeling of urban land use. Computers, Environment and Urban Systems, 33(1): 15-25.

Baltsavias, E., Gruen, A., Eisenbeiss, Zhang, L. and Waser, L.T., 2008. High-quality image matching and automated generation of 3D tree models. International Journal of Remote Sensing, 5(29): 1243-1253.

Baltsavias, E.P., 1999. A comparison between photogrammetry and laser scanning. ISPRS Journal of Photogrammetry and Remote Sensing, 54(2-3): 83-94.

Baltsavias, E.P., Gruen, A. and Gool, L.V. (Editors), 2001. Automatic extraction of man-made objects from aerial and space (lll). A.A. Balkema publishers, Tokyo.

Benz, U.C., Hofmann, P., Willhauck, G., Lingenfelder, I. and Heynen, M., 2004. Multi-Resolution, Object-Oriented Fuzzy Analysis of Remote Sensing Data for GIS-Ready Information. ISPRS Journal of Photogrammetry and Remote Sensing, 58(3-4): 239-258.

Birchfield, S. and Tomasi, C., 1999. Depth Discontinuities by Pixel-to-Pixel Stereo. International Journal of Computer Vision, 35(3): 269-293.

Blaschke, T., 2009. Object based image analysis for remote sensing. ISPRS Journal of Photogrammetry and Remote Sensing, In Press, Corrected Proof.

Blaschke, T., 2010. Object based image analysis for remote sensing. ISPRS Journal of Photogrammetry and Remote Sensing, 65(1): 2-16.

Blaschke, T. and Strobl, J., 2001. What's wrong with pixels? Some recent developments interfacing remote sensing and GIS. GeoBIT/GIS 6: 12-17.

Breen, E.J., Jones, R. and Talbot, H., 2000. Mathematical morphology: A useful set of tools for image analysis. Statistics and Computing, 10(2): 105-120.

Brenner, C., 2005. Building reconstruction from images and laser scanning. International Journal of Applied Earth Observation and Geoinformation, 6(3-4): 187-198.

Burnett, C. and Blaschke, T., 2003. A multi-scale segmentation/object relationship modelling methodology for landscape analysis. Ecological Modelling, 168(3): 233-249.

Büyüksalih, G., Kocak, M.G., Oruc, M., Akcin, H. and Jacobsen, K., 2004. Handling of Ikonos Images from Orientation up to DEM Generation, http://www.ipi.uni-hannover.de/fileadmin/institut/pdf/bueyuek_Ikon.pdf accessed on 12-12-2009.

Chen, Y., Su, W., Li, J. and Sun, Z., 2009. Hierarchical Object Oriented Classification Using Very High Resolution Imagery and LIDAR Data over Urban Areas. Advances in Space Research, 43(7): 1101-1110.

Definiens, Definiens developer 7 Reference Book. Definiens AG, Trappentreustr. 1, D-80339 München, Germany, 2007.
Definiens, 2007. Definiens, official webpage of Definiens Inc., http://www.definiens.com/, Accessed on 30 - 12 - 2009.
Devriendt, D., Goossens, R. and Ghabour, T., 2008. Combination of Satellite Derived Raster and Vector Data for 3D City Modelling. In: C. Jurgens (Editor), Remote Sensing: New Challenges of High Resolution, Bochum, pp. 202-209.
Diniz, P.S.R., 2008. Fundamentals of Adaptive Filtering, Adaptive Filtering. Springer US, pp. 1-63.
Dong, P., 1997. Implementation of mathematical morphological operations for spatial data processing. Computers & Geosciences, 23(1): 103-107.
Dutta, D. and Serker, N.H.M.K., 2005. Urban Building Inventory Development using Very High-Resolution Remote Sensing Data for Urban Risk Analysis. International Journal of Geoinformatics, , 1(1).
Ebert, A., Kerle, N. and Stein, A., 2009. Urban Social Vulnerability Assessment with Physical Proxies and Spatial Metrics Derived from Air- and Spaceborne Imagery and GIS Data. Nat Hazards, 48: 275-294.
Eckstein, W. and Steger, C., 1999. The halcon vision system: An example for flexible software architecture, http://citeseerx.ist.psu.edu/viewdoc/summary?doi=10.1.1.26.9699, Accessed on 31-01-2010.
Eisenbeiss, H., Baltsavias, E., Pateraki, M. and Zhang, L., 2004. Potential of Ikonos and Quickbird Imagery for Accurate 3D Point Positioning, Orthoimage and DSM Generation, ISPRS Congress, Istanbul, Turkey.
Elberink, S.O. and Maas, H.G., 2000. The Use of Anisotropic Height Texture Measures for the Segmentation of Airborne LASER Scanner Data, IAPRS, Vol. XXXIII, Amsterdam.
Fielding, G. and Kam, M., 2001. Disparity maps for dynamic stereo. Pattern Recognition, 34(3): 531-545.
Fisher, P.F. and Tate, N.J., 2006. Causes and consequences of error in digital elevation models. Progress in Physical Geography 30(4): 467-489.
Fraser, C.S., Baltsavias, E. and Gruen, A., 2002. Processing of Ikonos imagery for submetre 3D positioning and building extraction. ISPRS Journal of Photogrammetry and Remote Sensing, 56(3): 177-194.
Fu, L., Soh, L.-K. and Samal, A., 2008. Techniques for Computing Fitness of Use (FoU) for Time Series Datasets with Applications in the Geospatial Domain. GeoInformatica, 12(1): 91-115.
G.J.Hay and G.Castilla, 2008. Geographic Object-Based Image Analysis (GEOBIA): A new name for a new discipline. In: T. Blaschke, S. Lang and G.J. Hay (Editors), Object-Based Image Analysis. Springer, Berlin Heidelberg, pp. 75-90.
GeoEye, 2009. GeoEye: High resolution Imagery, Official webpage of GeoEye-1, http://www.geoeye.com/CorpSite/ Accessed on 24-12-2009.
Gonçalves, J.A., 2008. Orientation and DEM Extraction from ALOS-PRISM Images Using the SRTM-DEM as Ground Control, ISPRS Congree, Beijing, China.
Haala, N. and Brenner, C., 1999. Extraction of buildings and trees in urban environments. ISPRS Journal of Photogrammetry and Remote Sensing, 54(2-3): 130-137.
Halcon, 2009. Official webpage of Halcon, MVTech software GmbH, http://www.mvtec.com/halcon/overview/index.html, Accessed on 03-01-2010.
Hirschmüller, H., 2005. Accurate and Efficient Stereo Processing by Semiglobal Matching and Mutual Information, IEEE Conference on Computer Vision and Pattern Recognition, San Diego, CA, USA, pp. 807-814.
Hirschmüller, H., 2008. Stereo Processing by Semiglobal Matching and Mutual Information. IEEE Transactions on Pattern Analysis and Machine Intelligence 30(2): 328-341.
Hofmann, P., Strobl, J., Blaschke, T. and Kux, H., 2008. Detecting Informal Settlements from QuickBird Data in Rio de Janeiro Using an Object-Based Approach. In: T. Blaschke, S. Lang and G.J. Hay (Editors), Object-Based Image Analysis. Springer, Berlin Heidelberg, pp. 531-553.

Holland, D.A., Boyd, D.S. and Marshall, P., 2006. Updating topographic mapping in Great Britain using imagery from high-resolution satellite sensors. ISPRS Journal of Photogrammetry and Remote Sensing, 60(3): 212-223.

Jacobsen, K., 2003. Orthoimages and DEMs by QuickBird and IKONOS, EARSeL Conference, Ghent, Belgium.

Jacobsen, K., 2009. Very High Resolution Satellite Images - Competition to Aerial Images GIS Development: Geospatial Resource Portal. GIS Development, Noida, India, URL: http://www.gisdevelopment.net/technology/emerging/mwf09_Karsten_SatelliteImages.htm, accessed on 25-12-2009.

Jiang, N., Zhang, J.X., Li, H.T. and Lin, X.G., 2008. Object-Oriented Building Extraction by DSM and Very High Resolution Orthoimages, The International Archives of the Photogrammetry, Remote Sensing and Spatial Information Sciences. , Beijing

Jin, X. and Davis, C.H., 2005. Automated building extraction from high-resolution satellite imagery in urban areas using structural, contextual, and spectral information. EURASIP J. Appl. Signal Process., 2005: 2196-2206.

Kerle, N., Janssen, L.L.F. and Huurneman, G.C. (Editors), 2004. Principles of Remote Sensing. Educational Text Book Series. International Institute for Geoinformation Science and Earth Observation, (ITC), Enschede.

Kocaman, S., Zhang, L., Gruen, A. and Poli, D., 2006. 3D City Modeling from High Resolution Satellite Images, ISPRS Conference, Commission 1, Ankara.

Konecny, G., 2003. Mapping From Space. Nepalese Journal on Geoinformatics, 1(2): 7-11.

Kornus, W., Alamús, R., Ruiz, A. and Talaya, J., 2006. DEM generation from SPOT-5 3-fold along track stereoscopic imagery using autocalibration. ISPRS Journal of Photogrammetry and Remote Sensing, 60(3): 147-159.

Krauß, T., Lehner, M. and Reinartz, P., 2008. Generation of Coarse 3D Models of Urban Areas From High Resolution Stereo Satellite Images, ISPRS Congress, Beijing, China.

Krauß, T. and Reinartz, P., 2009. Refinement of Urban Digital Elevation Models From Very High Resolution Stereo Satellite Images, High-Resolution Earth Imaging for Geospatial Information, ISPRS Workshop, Hanover, Germany.

Krauß, T., Reinartz, P., Lehner, M., Schroeder, M. and Stilla, U., 2005. DEM Generation from Very High Resolution Stereo Satellite Data in Urban Areas Using Dynamic Programming., International Archives of the Photogrammetry, Remote Sensing and Spatial Information Sciences.

Kressler, F.P. and Steinnocher, K., 2006. Image Data and LIDAR – An Ideal Combination Matched by by Object Oriented Analysis, 1st International Conference on Object-based Image Analysis (OBIA 2006), Salzburg University, Austria.

Lehner, M., Müller, R. and Reinartz, P., 2005. DSM and Orthoimages from Quickbird and Ikonos Data Using Rational Polynomial Functions, ISPRS workshop, Hannover, Germany.

Lhomme, S., He, D.-C., Weber, C. and Morin, D., 2009. A new approach to building identification from very-high-spatial-resolution images. International Journal of Remote Sensing, 30(5): 1341-1354.

Li, Z. and Gruen, A., 2004. Automatic DSM Generation from Linear Array Imagery Data, XXth ISPRS congress, International Archives of the Photogrammetry, Remote Sensing and Spatial Information Science, Istanbul, Turkey, pp. 128-133.

Liu, Y., Li, M., Mao, L., Xu, F. and Huang, S., 2006. Review of remotely sensed imagery classification patterns based on object-oriented image analysis. Chinese Geographical Science, 16(3): 282-288.

Maune, D.F., 2007. Digital Elevation Model Technologies and Applications: The DEM Users Manual. The American Society for Photogrammetry and Remote Sensing, Behesda, Maryland,.

Miliaresis, G. and Kokkas, N., 2007. Segmentation and object-based classification for the extraction of the building class from LIDAR DEMs. Computers & Geosciences, 33(8): 1076-1087.

Okeke, F.I., 2009. Review of Digital Image Orthorectification Techniques, GIS Development: Geospatial Resource Portal. GIS Development, Noida, India, URL: http://www.gisdevelopment.net/technology/ip/fiopf.htm, Accessed on 02-01-2010.

Poon, J., Fraser, C.S., Zhang, C.S., Li, Z. and Gruen, A., 2005. Quality assessment of digital surface models generated from IKONOS imagery. Photogrammetric Record, 20(110): 162-171.

Prudhviraju, K., Kumar, S., Mohan, K. and Pandey, M., 2008. Urban cadastral mapping using very high resolution remote sensing data. Journal of the Indian Society of Remote Sensing, 36(3): 283-288.

Radhadevi, P.V. et al., 2009. Potential of High-Resolution Indian Remote Sensing Satellite Imagery for Large Scale Mapping, ISPRS Conference Hannover, Germany.

Rau, J.Y. and Chen, L.C., 2005. DSM Generation from IKONOS Stereo Imagery. Journal of Photogrammetry and Remote Sensing, 10(3): 265-274.

Rekik, A., Zribi, M., Hamida, A.B. and Benjelloun, M., 2007. Review of satellite image segmentation for an optimal fusion system based on the edge and region approaches. IJCSNS International Journal of Computer Science and Network Security, 7(10): 242-250.

Reulke, R., Becker, S., Haala, N. and Tempelmann, U., 2006. Determination and improvement of spatial resolution of the CCD-line-scanner system ADS40. ISPRS Journal of Photogrammetry and Remote Sensing, 60(2): 81-90.

Rottensteiner, F. and Briese, C., 2003. Automatic Generation of Building Models from LIDAR Data and the Integration of Aerial Images, ISPRS Workshop on 3-D Reconstruction from Airborne Laser Scanner and InSAR Data, Dresden, Germany, pp. 174-180.

Schenk, T., 1999. Digital Photogrammetry I. TerraScience, Laurelville 422 pp.

Schiewe, J., 2003. Integration of multi-sensor data for landscape modeling using a region-based approach. ISPRS Journal of Photogrammetry and Remote Sensing, 57(5-6): 371-379.

Scholten, F., Gwinner, K., Tauch, R. and Boulgakova, O., 2003. HRSC-AX - High-Resolution Orthoimages and Digital Surface Models for Urban Regions, 2nd GRSS/ISPRS Joint Workshop on Data Fusion and Remote Sensing over Urban Areas, Berlin, Germany, pp. 225-229.

Shamaoma, H., 2005. Extraction of Flood Risk - Related base - Data from Multi Source Remote Sensing Imagery, ITC, Enschede, 92 pp.

Sithole, G. and Vosselman, G., 2004. Experimental comparison of filter algorithms for bare-Earth extraction from airborne laser scanning point clouds. ISPRS Journal of Photogrammetry and Remote Sensing, 59(1-2): 85-101.

Sohn, G. and Dowman, I., 2007. Data fusion of high-resolution satellite imagery and LiDAR data for automatic building extraction. ISPRS Journal of Photogrammetry and Remote Sensing, 62(1): 43-63.

Suga, Y., Ogawa, H. and Sugimura, T., 2003. Generation of digital terrain model and image interpretation by using EROS-Al stereo pair images observed from multiple directions. Advances in Space Research, 32(11): 2247-2252.

Syed, S., Dare, P. and Jones, S., 2005. Semi-Automatic 3D Building Model Generation from LIDAR and High Resolution Imagery, Spatial Intelligence, Innovation and Praxis: The national biennial Conference of the Spatial Sciences Institute,, Spatial Sciences Institute, Melbourne, Australia

Teo, T.A. and Chen, L.C., 2004. Object -Based Building Detection from LIDAR Data and High Resolution Satellite Imagery, 25th Asia Conference on Remote Sensing, Chiang Mai, Thailand, pp. 1614 -1619.

Tian, J. and Chen, D.-M., 2007. Optimization in multi-scale segmentation of high-resolution satellite images for artificial feature recognition. Int. J. Remote Sens., 28(20): 4625-4644.

Toutin, T., 2004. Geometric processing of remote sensing images: models, algorithms and methods. International Journal of Remote Sensing, 25: 1893-1924.

Toutin, T., 2006. Generation of DSMs from SPOT-5 in-track HRS and across-track HRG stereo data using spatiotriangulation and autocalibration. ISPRS Journal of Photogrammetry and Remote Sensing, 60(3): 170-181.

University of Vanderbilt, Webpage of University of Vanderbilt, quality library, What is quality? University of Vanderbilt, Nashville, Tennessee , USA URL: http://mot.vuse.vanderbilt.edu/mt322/Whatis.htm, accessed on 27-12-2009.

Vosselman, G., Sester, M. and Mayer, H., 2004. Basic Computer Vision Techniques. In: J.C. McGlone, E.M. Mikhail and J. Bethel (Editors), Manual of Photogrammetry. American Society for Photogrammetry and Remote Sensing, Bethesda Maryland.

Vu, T.T., Yamazaki, F. and Matsuoka, M., 2009. Multi-scale solution for building extraction from LiDAR and image data. International Journal of Applied Earth Observation and Geoinformation, 11(4): 281-289.

Weidner, U. and Förstner, W., 1995. Towards automatic building reconstruction from high-resolution digital elevation models. ISPRS Journal of Photogrammetry and Remote Sensing, 50(4): 38-49.

Wolff, K. and Gruen, A., 2007. DSM Generation from Early ALOS/PRISM Data Using SAT-PP High-Resolution Earth Imaging for Geospatial Information, ISPRS Workshop Hanover , Germany.

Wolff, K. and Gruen, A., 2008. Up to Date DSM Generation Using High Resolution Satellite Image Data, The International Archives of the Photogrammetry, Remote Sensing and Spatial Information Sciences, Beijing.

Zhang, C. and Fraser, C., 2008. Generation of Digital Surface Model from High Resolution Satellite Imagery, The International Archives of the Photogrammetry, Remote Sensing and Spatial Information Sciences. , Beijing

Zhang, C.S. and Fraser, C.S., 2007. Automated Registration of High-Resolution Satellite Images. Photogrammetric Record, 22(117): 75-87.

Zhang, L. and Gruen, A., 2006. Multi-Image Matching for DSM Generation from IKONOS Imagery. ISPRS Journal of Photogrammetry and Remote Sensing, 60(3): 195-211.

Zhou, G. et al., 2004. True orthoimage generation in urban areas with very tall buildings International Journal of Remote Sensing 25(22): 5163 - 5180.

Annexes

Annex 1: Spatial profile along different objects for bands 4(NIR), 3 (R), 2(G) and 1(B)

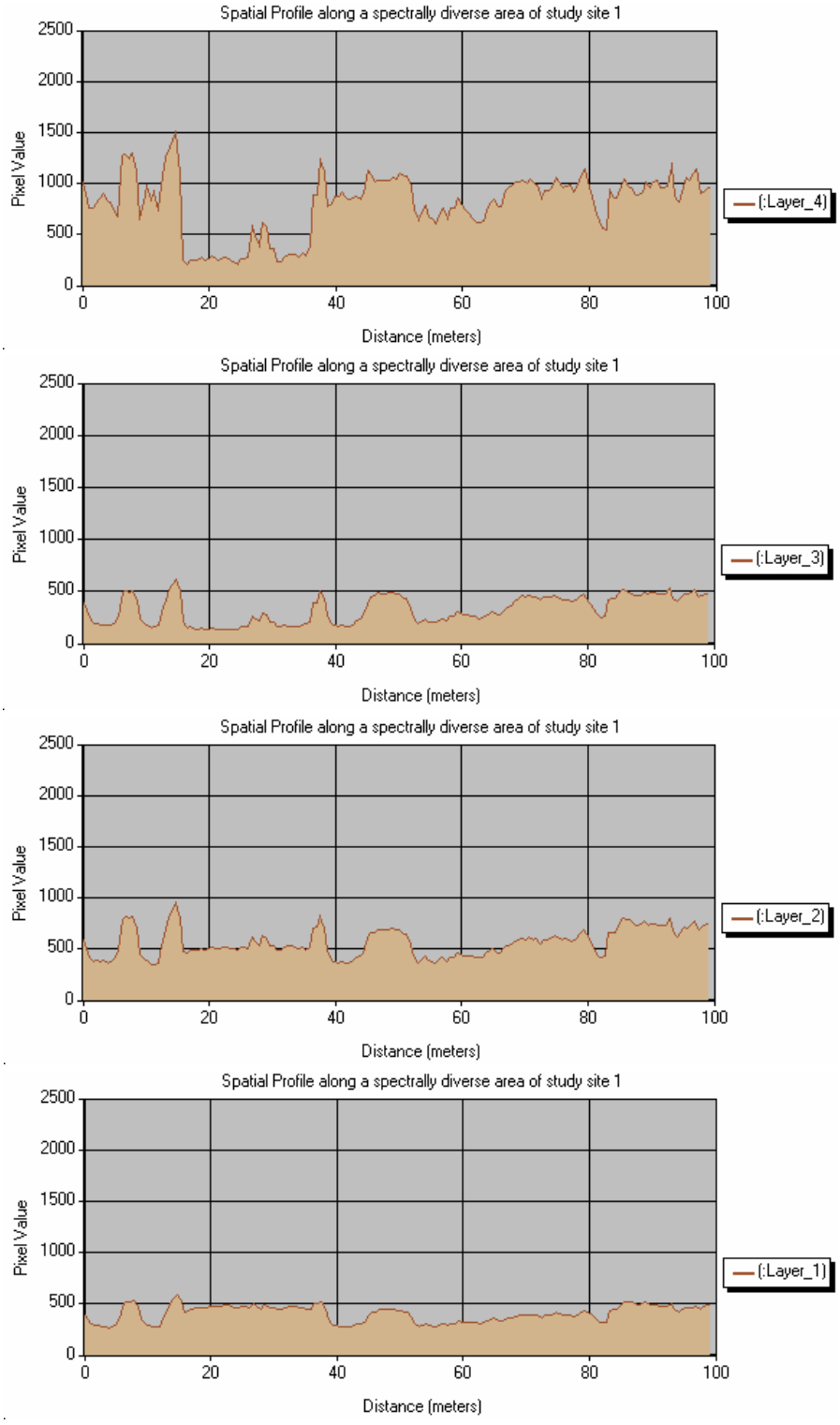

Annex 2: Spectral profile of different object class in 4 bands

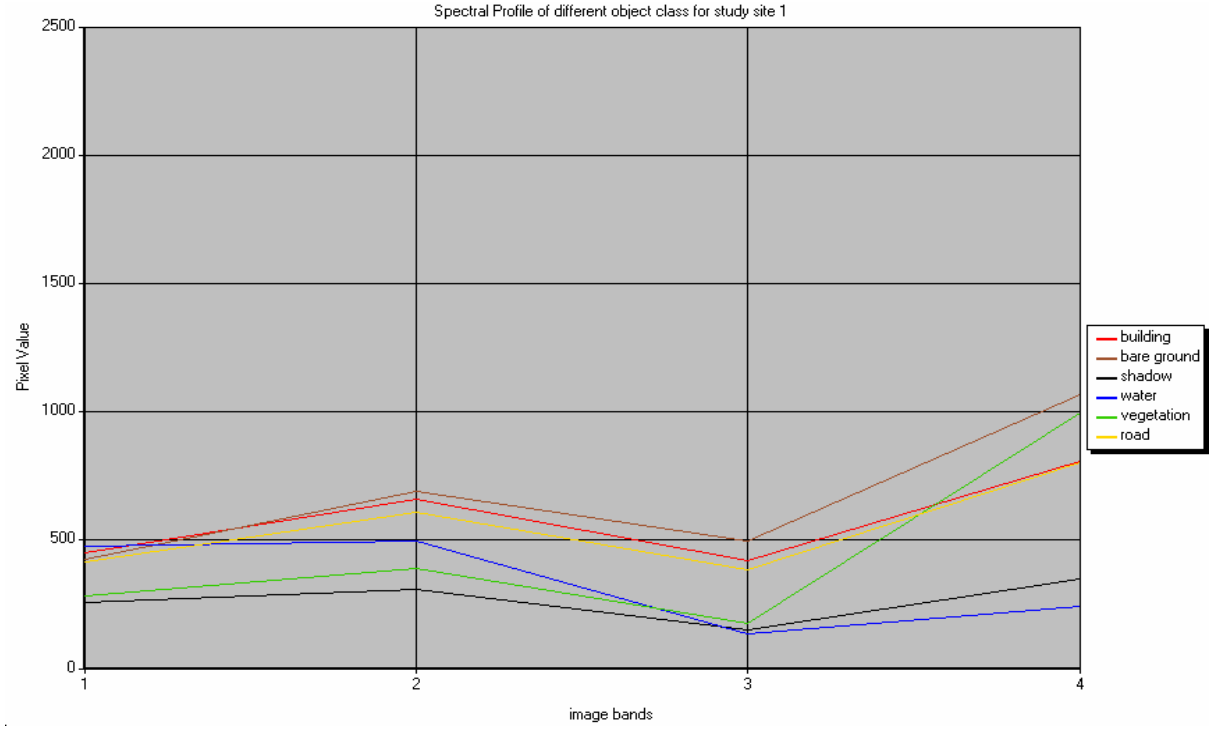

Annex 3: 3D shape file generated from a) band 1, b) band 2, c) band 3 and d) band 4 of the study site 1 (inconsistency in matching 16 bit image)

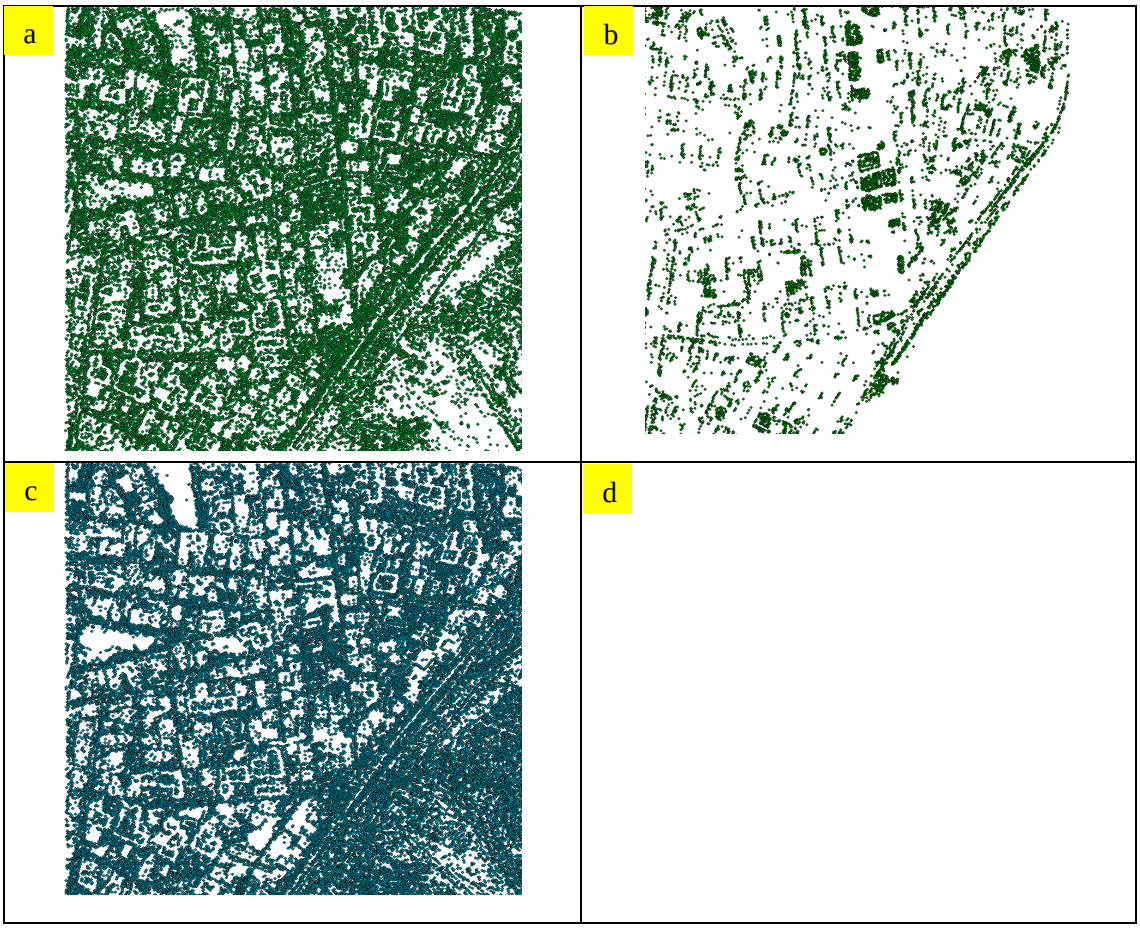

Annex 4: Raster DEM generated from a) band 1, b) band 2, c) band 3 and d) band 4 (Left) and 4 band orthoimage of the study site 1 (Right) (inconsistency in matching 16 bit image)

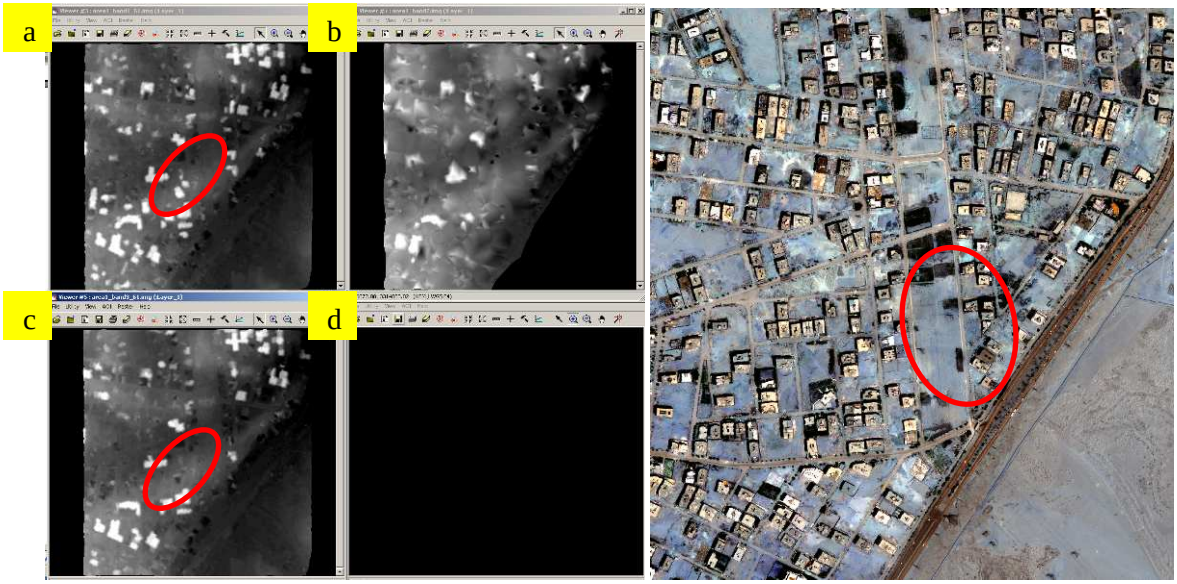

Annex 5: Missing buildings in DSM, a zoomed in area encircled in figure 3-8 (Inconsistency in matching 16 bit image)

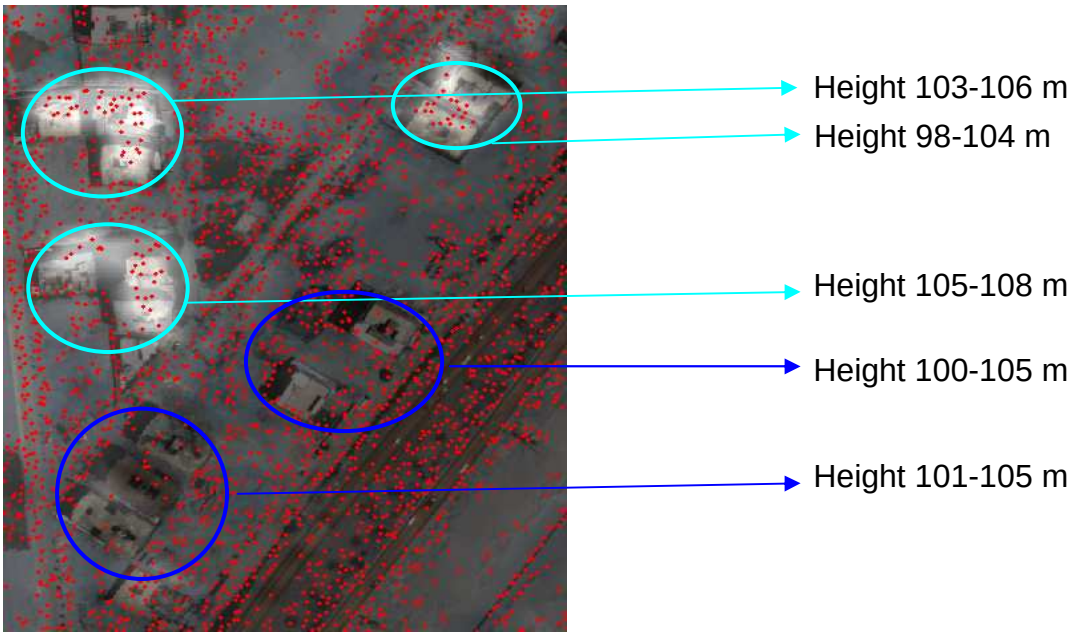

Annex 6: Accuracy analysis and comparison of orthoimage

Stereo		ownDTM		const95		difference		dist	difference		dist
X	Y	X1	Y1	X2	Y2	X-X1	Y-Y1		X-X2	Y-Y2	
316436.59	3315150.38	316437.98	3315145.11	316437.50	3315145.93	-1.39	5.27	5.45	-0.91	4.45	4.54
316444.76	3315381.78	316445.90	3315377.37	316445.32	3315379.42	-1.13	4.41	4.55	-0.55	2.36	2.42
316452.07	3315264.74	316452.91	3315260.56	316452.60	3315262.22	-0.84	4.19	4.27	-0.53	2.52	2.58
316456.76	3315217.90	316458.01	3315213.02	316458.04	3315214.03	-1.25	4.89	5.04	-1.28	3.87	4.08
316464.46	3315156.25	316465.38	3315151.89	316464.99	3315152.58	-0.93	4.36	4.46	-0.53	3.68	3.71
316490.18	3315313.91	316491.47	3315309.73	316490.94	3315310.86	-1.29	4.18	4.38	-0.76	3.05	3.15
316491.44	3315149.71	316492.47	3315146.03	316492.49	3315147.19	-1.03	3.68	3.82	-1.05	2.52	2.73
316493.32	3315290.96	316494.86	3315285.37	316493.98	3315287.13	-1.54	5.59	5.80	-0.66	3.84	3.89
316517.09	3315151.78	316518.53	3315147.24	316517.94	3315148.79	-1.44	4.54	4.76	-0.85	2.99	3.11
316551.30	3315226.76	316552.67	3315221.04	316552.02	3315222.26	-1.37	5.72	5.88	-0.72	4.49	4.55
316551.54	3315251.73	316551.82	3315249.04	316551.03	3315250.26	-0.28	2.69	2.70	0.51	1.46	1.55
316553.83	3315201.75	316555.32	3315196.89	316554.64	3315197.90	-1.50	4.86	5.08	-0.81	3.85	3.93
316559.23	3315369.93	316560.78	3315364.56	316559.95	3315366.85	-1.55	5.36	5.58	-0.72	3.08	3.16
316581.60	3315411.50	316582.83	3315406.43	316582.30	3315408.77	-1.24	5.07	5.22	-0.70	2.73	2.82
316584.87	3315302.05	316586.05	3315296.97	316584.97	3315298.58	-1.19	5.07	5.21	-0.10	3.46	3.46
316585.18	3315371.38	316586.26	3315366.82	316585.72	3315368.99	-1.09	4.56	4.68	-0.54	2.39	2.45
316592.06	3315157.16	316593.45	3315151.90	316592.87	3315153.82	-1.39	5.26	5.44	-0.82	3.33	3.43
316611.45	3315370.16	316612.44	3315365.62	316611.81	3315367.21	-0.99	4.54	4.65	-0.36	2.95	2.97
316636.40	3315375.08	316637.53	3315370.40	316636.98	3315371.85	-1.12	4.68	4.81	-0.57	3.23	3.28
316640.30	3315173.40	316640.69	3315170.10	316640.64	3315171.80	-0.40	3.30	3.32	-0.34	1.60	1.64
316661.90	3315379.32	316663.09	3315374.10	316662.44	3315376.09	-1.20	5.22	5.36	-0.54	3.23	3.27
316665.82	3315164.86	316667.32	3315159.54	316667.01	3315160.90	-1.49	5.32	5.52	-1.18	3.96	4.13
316680.38	3315223.87	316680.89	3315221.30	316680.40	3315222.59	-0.51	2.57	2.62	-0.01	1.29	1.29
316683.27	3315416.25	316684.44	3315411.63	316683.65	3315413.50	-1.17	4.62	4.77	-0.38	2.75	2.77
316691.03	3315165.98	316692.17	3315161.15	316691.86	3315162.57	-1.14	4.83	4.96	-0.83	3.41	3.51
316723.48	3315308.19	316725.27	3315303.74	316724.88	3315305.39	-1.79	4.45	4.80	-1.39	2.81	3.13
316729.87	3315281.42	316731.59	3315276.27	316730.85	3315277.59	-1.73	5.15	5.43	-0.99	3.83	3.96
316735.39	3315198.72	316736.20	3315194.35	316735.62	3315195.27	-0.80	4.37	4.45	-0.22	3.45	3.46
316735.53	3315425.74	316736.37	3315420.67	316735.69	3315423.30	-0.84	5.06	5.13	-0.16	2.44	2.44
316736.81	3315171.30	316737.89	3315166.58	316737.45	3315167.75	-1.08	4.72	4.84	-0.63	3.55	3.61
316739.04	3315384.75	316740.68	3315379.40	316739.83	3315381.78	-1.64	5.34	5.59	-0.79	2.97	3.07
316760.80	3315339.69	316762.34	3315334.83	316762.00	3315336.26	-1.54	4.86	5.10	-1.20	3.43	3.63
316770.64	3315229.21	316771.91	3315225.15	316771.58	3315226.32	-1.27	4.06	4.25	-0.94	2.90	3.04
316773.70	3315202.46	316774.69	3315197.62	316774.11	3315199.50	-0.98	4.84	4.94	-0.41	2.96	2.99
316776.87	3315174.94	316778.47	3315169.85	316777.74	3315171.89	-1.60	5.09	5.33	-0.87	3.05	3.17
316799.39	3315451.80	316800.43	3315446.91	316799.47	3315449.39	-1.04	4.89	5.00	-0.08	2.41	2.41
316805.04	3315399.07	316805.67	3315394.57	316805.11	3315396.34	-0.63	4.50	4.54	-0.07	2.72	2.73
316812.17	3315313.86	316812.40	3315314.46	316812.04	3315316.05	-0.23	-0.60	0.65	0.12	-2.19	2.19
316821.21	3315240.40	316822.33	3315235.07	316821.68	3315236.69	-1.12	5.34	5.45	-0.46	3.71	3.74
316826.73	3315484.03	316828.85	3315478.59	316827.89	3315481.05	-2.12	5.44	5.84	-1.15	2.98	3.19
316837.63	3315377.56	316838.67	3315372.83	316838.51	3315374.85	-1.04	4.74	4.85	-0.88	2.71	2.85
316851.98	3315217.81	316853.81	3315212.09	316853.63	3315214.30	-1.84	5.72	6.01	-1.66	3.51	3.88
316857.10	3315163.66	316857.79	3315160.87	316856.91	3315163.37	-0.70	2.79	2.88	0.19	0.30	0.35
					Mean	**-1.17**	**4.55**	**4.73**	**-0.62**	**2.88**	**3.08**
					SD	**0.41**	**1.10**	**1.02**	**0.45**	**1.13**	**0.84**

Annex 7: Spectral variation within one (top), among different buildings (middle) and spectral similarity among different class- bare ground, road and building (bottom)

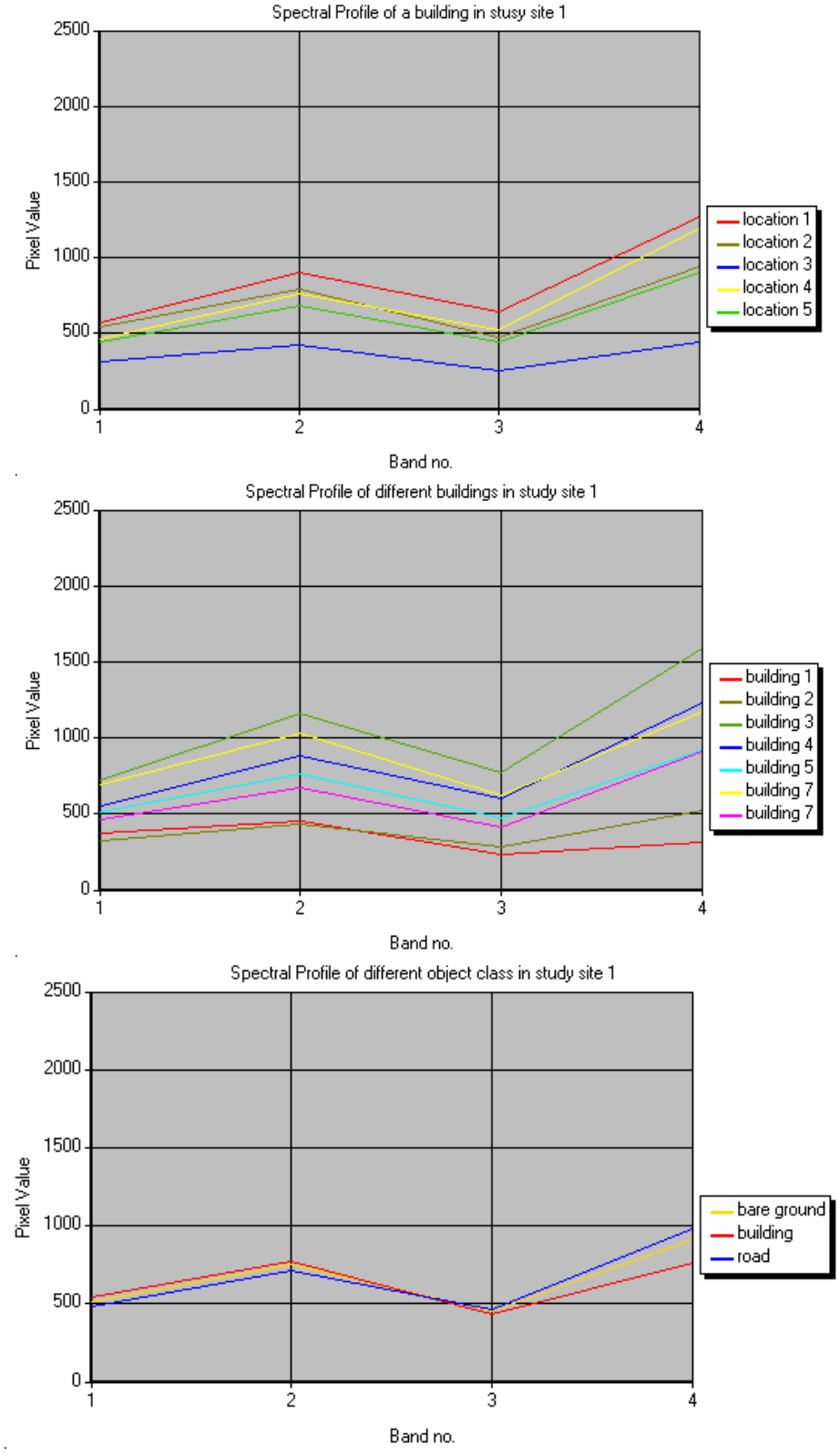

Annex 8: Halcon Script for improving quality of DSM in study site 1

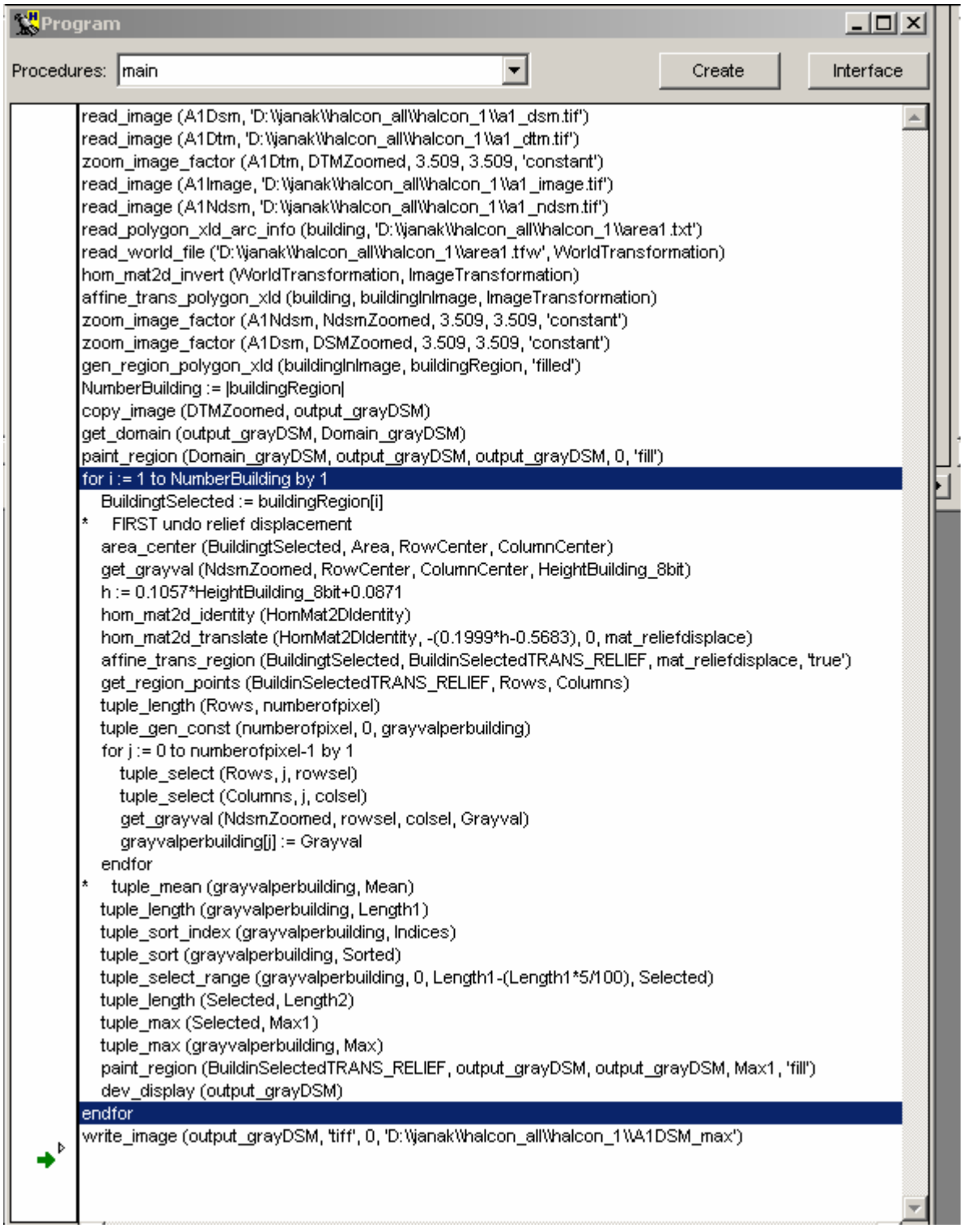

Annex 9: Detailed process of implementation and result in halcon for DSM improving

Implementation process	Result
The nDSM was produced in Erdas imagine and was in .img file format. As Halcon doesn't accept .imag format, the nDSM was converted in .tiff format. This nDSM file was with 8 bit continuous gray values ranging from 0-255, which represent the height of the building. During later processing, these gray values were converted in floats which represent absolute building height by using linear transformation.	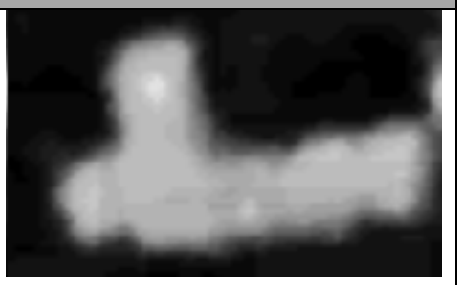
The building outline extracted by OOA were converted to text file in python and entered in Halcon. Halcon accepts this dataset as polygon XLD. Later this file was converted to image by affine transformation of a homogeneous matrix prepared by inverting a world coordinate system (.tfw) file. The building image was later converted to region as we need building regions for further processing.	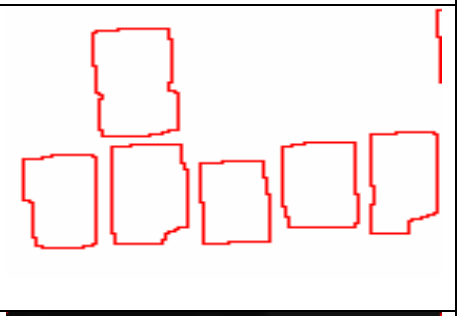
Since nDSM and building outline are in image coordinate system and they have different pixel size, they do not fit on top of each other. Buildings were extracted from image of 0.57 m cell size whereas nDSM has 2 m cell size. So rescaling was done by a factor of 3.51. Further, the building outlines were suffered from a relief displacement. So they need to be corrected in the later stage.	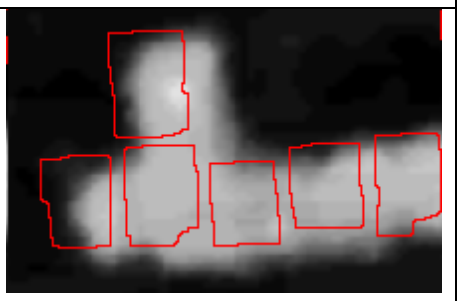
A correspondence between rows and columns of building regions and nDSM was established. Gray values were converted to height and assigned to the building centre. The building region was then translated to correct the relief displacement by a distance which was a function of building height. Finally, gray values were extracted from nDSM and mean gray values were assigned to each building.	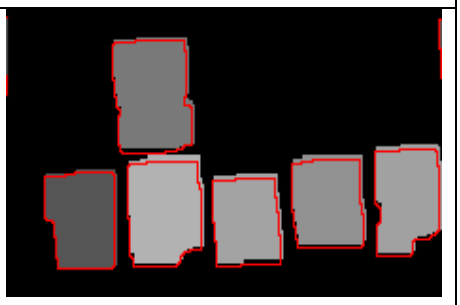

After processing in Halcon, an improved nDSM image file was obtained. This file has image coordinate system and continuous 8 bit gray values to represent the building height and image background with a value 0. So, raster addition of this nDSM with a similar format DTM gives final improved DSM.

Table 1 gives a brief procedure of implementation and results obtained from it. To make the whole process clear and comparable, the DSM, DTM and nDSM produced in earlier steps (chapter 3) are repeated and brief explanation and results is given in each row and column.

Table 1: Implementation processes in Erdas imagine and results obtained

Implementation process	Result
The DSM generated from Geoeye-1 stereo image by image matching technique in LPS (see chapter 3)	
The DTM produced by filtering the above DSM. It was produced by applying mathematical morphological operation, erosion and dilation. Some peak gray values, which cannot be removed were smoothed by using raster interpolation and low pass filtering.	
The nDSM produced by subtracting the DTM from the DSM.	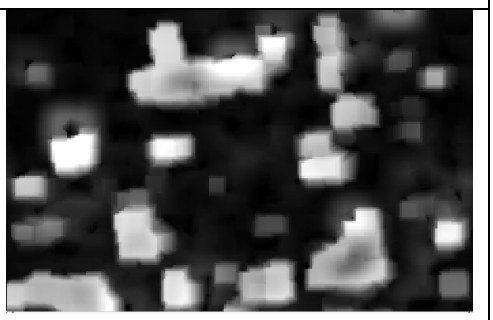
nDSM improved in Halcon was exported as image and transformed back to world coordinate system. The gray values were also transformed to actual height values by applying linear transformation.	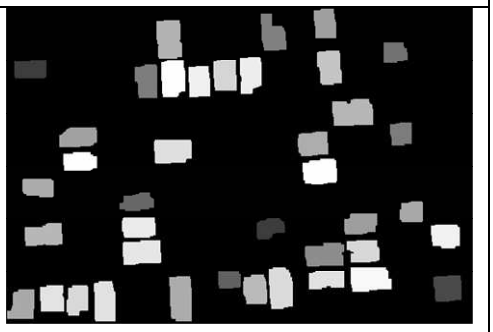
The improved nDSM and DTM were added to get a DSM. The Both of the datasets have same coordinate system, grid cell size and gray value scale to represent the actual terrain height. The pixel wise addition adds building height value to the pixels of ground height at building location to give the height of building above ground and other background 0 values in nDSM were added to the bare terrain height value without any influence in the final DSM.	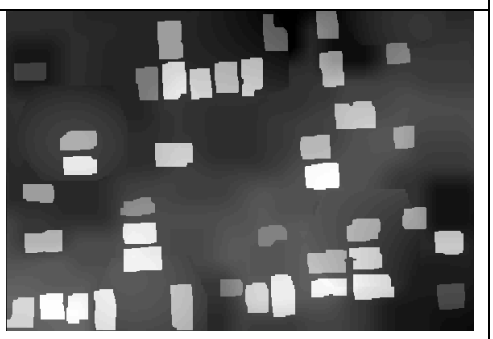

Annex 10: Accuracy analysis of improved DSM (position)

Stereo		buil_DSM		difference		dist
X	Y	X1	Y1	X-X1	Y-Y1	
316436.59	3315150.38	316436.53	3315148.41	-0.06	-1.96	1.97
316444.76	3315381.78	316444.63	3315380.82	-0.13	-0.96	0.97
316452.07	3315264.74	316452.62	3315264.09	0.55	-0.65	0.85
316456.76	3315217.90	316458.26	3315216.37	1.50	-1.53	2.15
316464.46	3315156.25	316465.98	3315154.34	1.52	-1.91	2.45
316491.44	3315313.91	316491.94	3315313.96	0.50	0.04	0.50
316493.32	3315290.96	316493.22	3315290.00	-0.11	-0.96	0.96
316517.09	3315151.78	316518.03	3315151.50	0.94	-0.28	0.98
316551.30	3315251.73	316550.54	3315249.67	-0.75	-2.06	2.19
316551.54	3315226.76	316551.73	3315224.66	0.19	-2.10	2.11
316553.83	3315201.75	316554.77	3315199.95	0.95	-1.80	2.04
316559.23	3315369.93	316559.61	3315369.24	0.38	-0.69	0.79
316581.60	3315411.50	316581.62	3315410.17	0.02	-1.33	1.33
316584.87	3315302.05	316585.17	3315300.59	0.30	-1.46	1.49
316585.18	3315371.38	316585.38	3315371.95	0.20	0.58	0.61
316592.06	3315157.16	316593.03	3315154.76	0.97	-2.39	2.58
316611.45	3315370.16	316611.37	3315368.72	-0.08	-1.44	1.45
316636.40	3315375.08	316637.01	3315374.59	0.61	-0.49	0.79
316640.30	3315173.40	316641.02	3315172.53	0.72	-0.87	1.13
316665.82	3315164.86	316666.66	3315162.86	0.84	-2.00	2.17
316680.38	3315223.87	316680.94	3315223.46	0.56	-0.42	0.70
316683.27	3315416.25	316683.33	3315415.12	0.06	-1.12	1.12
316691.03	3315165.98	316691.78	3315164.66	0.75	-1.32	1.52
316723.48	3315308.19	316723.89	3315307.45	0.41	-0.75	0.85
316729.87	3315281.42	316730.78	3315279.90	0.91	-1.52	1.77
316735.39	3315198.72	316735.61	3315197.31	0.21	-1.41	1.43
316735.53	3315425.74	316735.72	3315425.43	0.19	-0.30	0.36
316736.81	3315171.30	316736.34	3315172.72	-0.47	1.42	1.50
316739.04	3315384.75	316740.24	3315382.75	1.20	-1.99	2.33
316760.80	3315339.69	316762.98	3315337.94	2.18	-1.75	2.79
316770.64	3315229.21	316771.18	3315228.13	0.54	-1.09	1.21
316773.70	3315202.46	316773.75	3315201.22	0.05	-1.24	1.24
316776.87	3315174.94	316779.82	3315173.76	2.94	-1.18	3.17
316799.39	3315451.80	316799.80	3315451.30	0.42	-0.49	0.65
316805.04	3315399.07	316804.51	3315397.33	-0.54	-1.74	1.82
316821.21	3315240.40	316821.02	3315239.46	-0.19	-0.94	0.96
316826.73	3315484.03	316827.31	3315483.43	0.57	-0.60	0.83
316851.98	3315217.81	316854.82	3315215.82	2.84	-2.00	3.47
316857.10	3315163.66	316857.00	3315164.34	-0.10	0.67	0.68
			Mean	**0.55**	**-1.08**	**1.48**
			SD	**0.81**	**0.84**	**0.77**

Annex 11: Accuracy analysis of improved DSM (Height)

ht_stereo(h)	ht_before(h1)	ht_after_mean(h2)	ht_after_5%max(h3)	h-h1	h-h2	h-h3
123.22	124.20	116.10	126.90	-0.98	7.12	-3.68
121.35	122.41	112.36	124.08	-1.06	8.99	-2.73
122.62	123.52	123.89	123.88	-0.90	-1.27	-1.26
122.50	121.63	121.50	124.63	0.87	1.00	-2.13
122.08	122.75	119.24	124.06	-0.67	2.84	-1.98
122.35	123.32	120.42	123.43	-0.97	1.93	-1.08
121.95	123.01	110.34	123.26	-1.06	11.61	-1.31
128.64	129.45	121.54	131.40	-0.81	7.10	-2.76
116.00	116.24	114.61	117.18	-0.24	1.39	-1.18
128.70	130.12	124.79	130.76	-1.42	3.91	-2.06
127.78	128.55	125.02	129.85	-0.77	2.76	-2.07
126.72	127.39	120.20	128.92	-0.67	6.52	-2.20
127.39	128.16	124.41	129.31	-0.77	2.98	-1.92
126.99	128.07	126.19	129.26	-1.08	0.80	-2.27
127.46	127.70	126.75	129.70	-0.24	0.71	-2.24
128.92	130.39	122.20	131.26	-1.47	6.72	-2.34
125.67	126.02	118.20	125.31	-0.35	7.47	0.36
121.69	122.63	115.98	124.65	-0.94	5.71	-2.96
127.85	127.75	124.09	130.26	0.10	3.76	-2.41
123.69	122.41	117.78	125.83	1.28	5.91	-2.14
119.43	121.72	106.11	117.42	-2.29	13.32	2.01
113.75	114.27	110.27	115.23	-0.52	3.48	-1.48
116.87	117.48	114.02	117.04	-0.61	2.85	-0.17
126.17	127.16	122.10	128.16	-0.99	4.07	-1.99
128.12	130.73	124.80	130.36	-2.61	3.32	-2.24
115.83	116.10	113.11	117.52	-0.27	2.72	-1.69
126.95	127.68	119.07	128.05	-0.73	7.88	-1.10
125.56	126.28	125.62	128.30	-0.72	-0.06	-2.74
123.99	124.67	123.71	126.09	-0.68	0.28	-2.10
123.82	124.18	122.13	124.25	-0.36	1.69	-0.43
124.69	125.66	117.99	125.70	-0.97	6.70	-1.01
125.38	120.37	116.77	127.12	5.01	8.61	-1.74
126.25	127.17	120.62	127.59	-0.92	5.63	-1.34
110.80	111.40	107.18	111.53	-0.60	3.62	-0.73
129.19	130.10	126.44	131.56	-0.91	2.75	-2.37
124.33	125.26	119.32	127.14	-0.93	5.01	-2.81
124.16	125.09	120.52	125.55	-0.93	3.64	-1.39
124.16	123.99	117.04	125.24	0.17	7.12	-1.08
121.03	121.08	112.83	122.05	-0.05	8.20	-1.02
122.24	122.78	117.52	123.06	-0.54	4.72	-0.82
118.94	120.11	112.54	120.19	-1.17	6.40	-1.25
			Mean	**-0.58**	**4.63**	**-1.65**
			SD	**1.11**	**3.16**	**1.00**